Conformational Analysis of 4-Azidoproline Derivatives

and their Application in Molecular Recognition

Inauguraldissertation

zur

Erlangung der Würde eines

Doktors der Philosophie

vorgelegt der

Philosophisch-Naturwissenschaftlichen Fakultät

der Universität Basel

von

Diplom-Chemiker

Louis-Sebastian Sonntag

aus Frankfurt am Main (Deutschland)

Basel 2005

Genehmigt von der Philosophisch-Naturwissenschaftlichen Fakultät der Universität Basel auf Antrag der Professoren:

Prof. Dr. Helma Wennemers

Prof. Dr. Bernd Giese

Prof. Dr. Urs Séquin

Basel, den 10. Mai 2005

Prof. Dr. Hans-Jakon Wirz

(Dekan)

Edel sei der Mensch,
Hilfreich und gut!
Denn das allein
Unterscheidet ihn
Von allen Wesen,
Die wir kennen.

- Johann Wolfgang von Goethe, *Das Göttliche*

"William James describes a man who got the experience from laughing gas:
whenever he was under its influence, he knew the secret of the universe,
but when he came to, he had forgotten it.

At last with immense effort, he wrote down the secret before the vision faded.
When completely recovered he rushed to see what he had written.
It was "A smell of petroleum prevails throughout."

- Bertrand Russell, *A History of Western Philosophy*

ABSTRACT

Conformational Analysis of 4-Azidoproline Derivatives

and their Application in Molecular Recognition

Louis-Sebastian Sonntag

This thesis presents studies on the influence of 4-azido-substitutents in azidoproline on the conformation of the pyrrolidine ring system as well as the conformation around the peptide bond in acetylated monomers and dimers. The azido-group may be reduced to an amine, which allows for further modifications. The insights gained were applied to the synthesis of a tripodal molecular scaffold. This scaffold was used as a backbone for a synthetic receptor, which binds peptides in aqueous solution.

In the first part of this thesis the effect of the azido-substituent on the conformation of 4-azidoproline is described. By NMR-spectroscopy, X-ray diffraction, FT-IR spectroscopy and *ab initio* calculations, the conformation of 4-azidoproline derivatives was analyzed. Particular focus was laid on the *s-cis*:*s-trans* ratio and the factors influencing it. Furthermore, the kinetics of the interconversion of the *s-cis* and *s-trans* conformation of diastereomeric 4-azidoproline derivatives were determined by EXSY-NMR.

The second part of this thesis describes the synthesis and structural analysis of the azido-functionalized cyclotriproline and its application as a molecular scaffold for a peptide receptor. The binding properties were analyzed in on-bead screenings against an encoded tripeptide library in different buffer solutions. The binding affinity to a selected peptide was measured by isothermal titration calorimetry (ITC).

Acknowledgements

First and foremost I would like to thank my supervisor, Prof. Dr. Helma Wennemers for her support and guidance, her contagious enthusiasm and for stimulating her co-workers to strive for their highest potential. I am grateful to Prof. Dr. Bernd Giese for accepting to co-referee this thesis.

Furthermore, I would like to thank my colleagues and friends with whom I had the pleasure to share the lab in the last years, Dr. Matteo Conza, Dr. Philipp Krattiger, Dipl. Chem. Michael Kümin, Dr. Matthias Nold and Dr. Jefferson Revell for the good times in- and outside the lab. I would like to thank Dipl. Chems. Jessica Grun and Kristen Koch for ESI measurements and Dipl. Chem Jana Lubkoll for help with the HPLC.

I would like to thank Dr. Daniel Häussinger and Dr. Klaus Kulicke for NMR measurements, Markus Neuburger, Dr. Silvia Schaffner for X-ray diffraction and Dr. Werner Kirsch and Dr. Heinz Nadig for elemental analysis and MS. Furthermore, I would like to thank all the members of the technical staff, from the "Werkstatt" and the "Materialausgabe" as well as the secretaries for their highly efficient and friendly service, without which the chemical institute would not run smoothly.

Special thanks to Dr. Jefferson Revell and Dr. Valérie Jullien for their invaluable help in revising the manuscript.

Finally, but not less heartfelt, I would like to thank my family and friends, for their support, their love and their friendship.

1 Introduction

In nature, the function of a molecule depends largely upon its conformation. This holds true for nature's largest molecules such as DNA and proteins, as well as for its relatively small molecules, such as peptides (both linear and cyclic) or polyketides among many others. As these molecules are typically only active in a specific conformation, understanding the factors that control the conformation of relatively small molecules is of great importance. While proteins have secondary, tertiary and even quaternary structural elements controlling their conformation, the conformation of small molecules is controlled by more elementary, structure-inherent effects.

A basic principle nature applies to control the conformation of small molecules is by covalently restricting the conformation, for instance by cyclization. Cyclization to cyclic or even polycyclic systems, restricts the conformational flexibility of molecules, leading to more rigid, conformationally defined structures. A well-known example illustrating this principle is Vancomycin, a glycopeptidic antibiotic isolated from *Amycolatopsis orientalis*.[1]
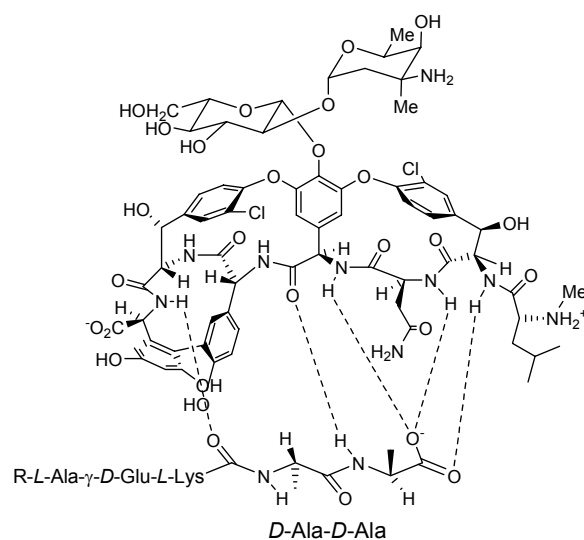
Figure 1: Vancomycin and its target sequence.

The efficiency of Vancomycin is highly dependent upon its conformation. The vancomycin skeleton (figure 1) consists of three interlocked cyclic tripeptides which collectively afford a conformationally rigid cup-shaped structure.[2] Small changes in

the structure of Vancomycin lead to less active or even inactive compounds. Due to the perfect alignment of hydrogen donor and acceptor sites on the molecule, Vancomycin binds its target sequence UDP-*N*-acetylmuramyl-L-Ala-D-Glu-L-Lys-D-Ala-D-Ala-OH with a binding constant of 1.6×10^{-5} M^{-1} (or a dissociation constant of $62.5 \mu M$).[3]

In the realm of the polyketides, nature uses two major principles to destabilize undesired conformations: one is to avoid 1,3-allylic strain and the other is to avoid *syn*-pentane interactions.[4,5,6]
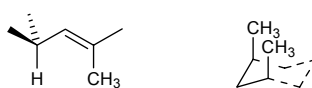
Figure 2: Preferred conformation of a 1,1-disubstituted allylic system (left) and of a pentane destabilized by a syn-pentane interaction (right).

The destabilizing *syn*-pentane interaction is created when a hydrocarbon chain is folded in such a way that the terminal methyl groups are in *gauche* conformations to the backbone. This brings the methyl groups into close proximity, similar to the 1,3-diaxial arrangement in substituted cyclohexanes. Thus, the conformation shown in figure 2 on the right is energetically unfavorable and will be avoided if possible. In contrast, the 1,1-disubtituted allylic system shown in figure 2 on the left is a low energy conformation and will be adopted if possible. Using these basic principles, nature controls the conformation of seemingly flexible molecules. One example is Zincophorin **1**, an ionophore antibiotic isolated from a strain of *Streptomyces griseus*.[7,8]
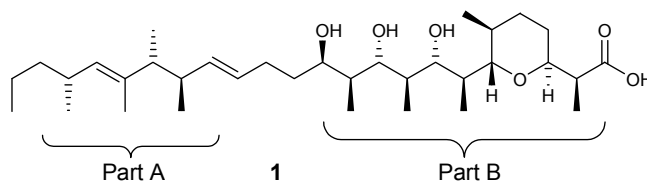
Figure 3: The ionophore antibiotic Zincophorin.

The conformation of Zincophorin is governed by avoidance of 1,3 allylic strain (in the part of the molecule marked "Part A" in figure 3) and *syn*-pentane interactions (in the part of the molecule marked "Part B" in figure 3). Hoffmann and coworkers have shown

that the careful placement of the methyl groups along the backbone of hydrocarbon and polyketide natural products renders them "flexible molecules with a defined shape".[9]

These examples illustrate some of the ways in which nature controls the conformation of small molecules. These conformation-directing elements have been applied to control the stereochemical outcome of organic reactions,[10a-c] in the total synthesis of natural products,[10d] as well as in the design of structurally defined small molecules.[10e] Hoffmann and coworkers have demonstrated, that with the principles of the allylic strain and the *syn*-pentane interaction, a mimic for the β^{II}-hairpin can be designed (figure 4).[10e]
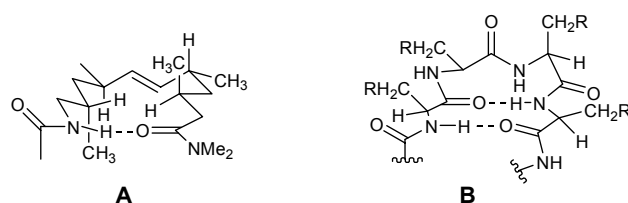
Figure 4: β^{II}-hairpin-mimic A and natural β^{II}-hairpin B.

Using the same principles, Still and coworkers designed podand ionophores (figure 5).[11] Even though the molecule shown in figure 5 could principally form many conformers, by careful placement of methyl groups, the undesired conformations are destabilized through *syn*-pentane interactions. Thus, only one low energy conformation is found.[11f]
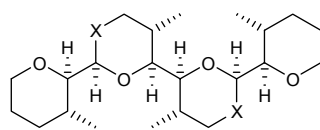
Figure 5: General structure of podand ionophores, $X=CH_2$, O, S or SO_2.

Still and coworkers showed that podands of this type are chiral analogs of 18-crown-6 and allow for highly enantioselective binding of the protonated N-terminus of amides and esters of amino acids, due to their highly defined structure. For example, a podand of the class shown in figure 5, in which $X=SO_2$ binds amides and esters of α-amino acids with enantioselectivities as high as 80% ee.[11]

Peptides can adopt secondary structure motifs such as α-helices, β-sheets and turn conformations. Furthermore, there are polyproline helices as found in collagen. With the exception of the polyproline helices, the stabilization of these secondary structure elements relies upon hydrogen bonding interactions and the number of residues needed to form these structures is typically larger than 5.[12] At a more basic level, the conformation of peptides is also governed by the principles shown above: *Syn*-pentane interactions and 1,3-allylic strain.
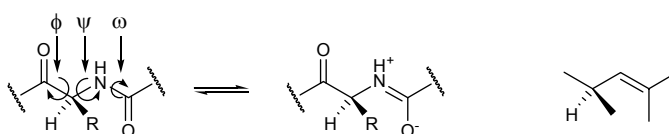
Figure 6: Mesomeric structures of an amide bond (left) and analogous allylic system (right).

The amide bond has two mesomeric structures, shown in figure 6 on the left. By comparison to 2,4-dimethylpent-2-ene shown on the right, it can be seen that the ionic mesomeric structure is analogous to the allylic systems discussed earlier. Likewise, the conformational preference is similar to the allylic systems discussed. The conformation of the peptide backbone is described by three dihedral angles, ϕ, ψ and ω (see figure 6). Taking the 1,3-allylic strain and the *syn*-pentane interactions into account, a peptide is ideally arranged when its backbone dihedral angles ϕ and ψ alternate between +120° and -120°.[12]

Due to the mesomeric structures shown in figure 6, ω can only take the value of 0 or 180°, which are referred to as *s-cis* and *s-trans*, respectively (figure 7). In most peptide bonds, the *s-trans* conformer is greatly favored over the *s-cis* conformer.
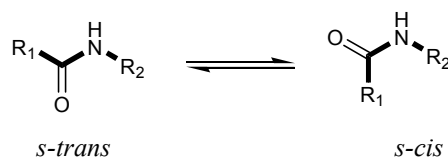
Figure 7: s-trans versus s-cis conformation in a peptide bond.

Among the natural amino acids, proline is special. It is the only cyclic proteinogenic amino acid and the only one with a secondary amine. Furthermore, it differs from the other amino acids in its conformational preference. In all other amino acids for steric reasons, the amide bond is found almost exclusively in the *s-trans* (ω = 180°)

conformation. A survey of 571 protein structures found 0.03% of Xaa_{i-1}-$nonPro_i$ peptide bonds to be in the *s-cis*. In contrast, the Xaa_{i-1}-Pro_i bond was found to be in the *s-cis* conformation ($\omega = 0$) in 5.2% of the peptide bonds of the proteins studied.[13, 14]

The *cis*-proline conformation plays an important role in the folding and the activity of proteins. An example, in which a *cis*-proline is an important for the folding of enzymes, is the class of the glutathione S-transferases. In this class of enzymes, a *cis*-proline unit mediates a sharp turn between an α-helical part of the protein and a β-strand, essential for its conformational stability and activity.[15] Bovine prothrombine is an example, in which the change from a *trans*-proline to a *cis*-proline is a switch for the activity of the protein. The binding of calcium leads to isomerization of a *trans*-proline to a *cis*-proline bond, inducing bovine prothrombine to assume its active, membrane-binding conformation.[16] Furthermore, proline *cis/trans* isomerizations have been identified as the rate-limiting step in the folding of many proteins.[17] For some proteins the correct conformation is achieved with the help of peptidylproline *cis/trans* isomerases (PPIases), a class of enzymes, which also plays an important role in the immune response.[18]

Apart from proline itself, a variety of proline derivatives are found in nature. Both dehydrogenated, as well as mono- and polysubstituted proline derivatives have been found (figure 8).[19] In many cases, the proline derivatives themselves, or peptides containing them, display antibiotic, neurotoxic or anti-tumor activity. The most common proline derivative is (4*R*)-hydroxyproline **3**, which is a major component of collagen and was first discovered in gelatin hydrolysates in 1902.[20] Collagen is an abundant triple-helical structure protein. In collagen, free hydroxyproline is not incorporated directly, instead proline is converted to hydroxyproline after its incorporation into the peptide chain.[21] 3-Hydroxyproline **4** was first isolated from hydrolysates of mediterranean sponge,[22] and was later also found in human urine, resulting from collagen metabolism.[23] Moreover, many members of the class of the actinomycin antibiotics[24] also contain (4*R*)-hydroxyproline **3**,[25] as well as 4-ketoproline **6**,[26,27] 3-hydroxy-5-methylproline **5**[28,29] or 5-methylproline **2**.[27,30]
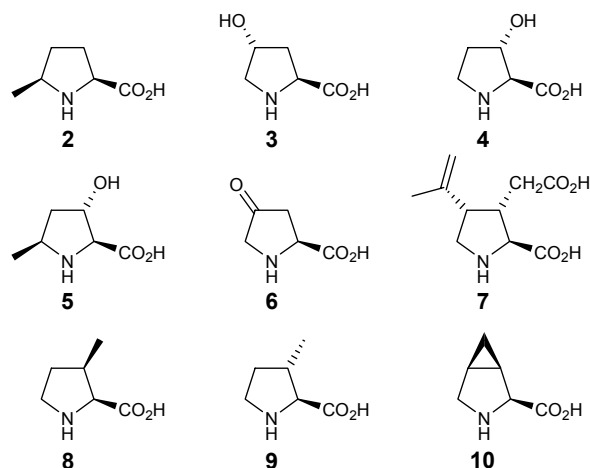
Figure 8: Natural proline derivatives.

Both diastereoisomers of 3-methylproline **8**[31] and **9**[32,33] are known, both as part of cyclic peptides, and even *cis*-3,4-methano-L-proline **10**[34] has been isolated. Another noteworthy member of the proline derivatives is kainic acid **7**,[35] which is a neurotoxin,[36] by a neurotransmitting effect mediated through glutamate receptors. It is a conformationally restricted analog of glutamic acid, which has been found to be the molecular basis for its activity.[37] By administration of kainic acid **7**, an animal model of Huntington's chorea in rats was generated.[38]

Non-natural proline derivatives have been developed as mimics of proline and hydroxyproline. It would be interesting to lock the Xaa$_{i-1}$-Pro$_i$ bond in an *s-cis* conformation to analyze its influence on the folding process. For example, 5,5'-dimethylproline (dmP) **11**[39,40] (figure 9) was developed as a proline mimic, which locks the *s-cis* conformation of the peptide bond N-terminal to it.
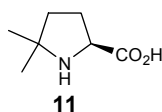
Figure 9: 5,5'-dimethylproline (dmP) 11.

This was studied with the tripeptide sequences Tyr-Pro-Asn and Asn-Pro-Tyr, of Bovine pancreatic nulclease A, in which the Xaa$_{i-1}$-Pro$_i$ bond is in the *s-cis* conformation in the native form. 5,5'-dimethylproline was incorporated into these two tripeptide fragments and it was shown that for the Tyr-dmP-Asn peptide, the *s-cis* conformation of the Tyr-dmP bond was stable over a temperature range of 6 to 60°C.[41]
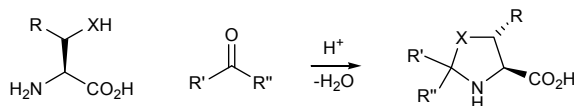
Scheme 1: Synthesis of ΨPro; X = O or S, R = H or CH₃, R', R'' = aryl, alky.

Another type of proline mimics are the pseudo-prolines (ΨPro). These analogs derive from serine, threonine and cysteine, which can be converted to (4S)-oxazolidine- and (4R)-thiazolidine-carboxylic acid, respectively (scheme 1).[42] They can be used as protected forms of the amino acids they derive from, as the oxazolidine- and thiazolidine rings can be cleaved after peptide synthesis.[42a] In peptide synthesis, the use of pseudo-prolines helps to facilitate the synthesis by their capability to break aggregates, self-association, and β-sheet-like structures, thus improving the solubility of the growing in peptide chain.[43] Furthermore, depending on the steric demand of the substituents R' and R'', the population of the *s-cis* conformation can be increased up to >99%.[44]
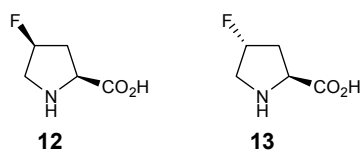
Figure 10: (4S)- and (4R)-fluoroproline 12 and 13 (left and right, respectively).

Another approach to modify proline to control the local conformation is the introduction of a fluoro-substituent at the 4-position (figure 10). Unlike 5,5'-dimethylproline **11** or the pseudo-prolines, the conformation of the 4-fluoroprolines **12** and **13** is not mainly influenced by steric effects, but by stereoelectronic effects.[45] The inductive effect of the electronegative substituent at the 4-position influences the equilibrium between the *s-cis* and *s-trans* conformation in dependence of the configuration at C(4).[46, 47]

This thesis presents studies on the influence of 4-azido-substitutents in azidoproline on the conformation of the pyrrolidine ring system as well as the conformation around the peptide bond in acetylated monomers and dimers. The azido-group may be reduced to an amine, which allows for further modifications. The insights gained were applied to the synthesis of a tripodal molecular scaffold. This scaffold was used as a backbone for a synthetic receptor, which binds peptides in aqueous solution.

In the first part the effect of a 4-azido-substituent on the conformation of azidoproline is described. By NMR-spectroscopy, X-ray diffraction, FT-IR spectroscopy and *ab initio* calculations, the conformation of 4-azidoproline derivatives was analyzed. Particular focus was laid on the *s-cis*:*s-trans* ratio and the factors influencing it. Furthermore, the kinetics of the interconversion of the *s-cis* and *s-trans* conformation of diastereomeric 4-azidoproline derivatives were determined by EXSY-NMR.

The second part of this thesis describes the synthesis and structural analysis of the azido-functionalized cyclotriproline and its application as a molecular scaffold for a peptide receptor. The binding properties were analyzed in on-bead screenings against an encoded tripeptide library in different buffer solutions. The binding affinity to a selected peptide was measured by isothermal titration calorimetry (ITC).

2   Conformational Analysis of Azidoproline Derivatives

2.1 Introduction

Previous studies have shown that the tendency for the formation of a diketopiperazine of 4-azidoproline is dependent on the configuration at the C(4)-position, on which the azide resides.[48] When the configuration is (4*S*), an activated ester of azidoproline reacts to form the diketopiperazine in a one-pot reaction in 47% yield (scheme 2a). However, when the configuration is (4*R*), the same reaction conditions yield less than 5% of the desired product (scheme 2b).[49]
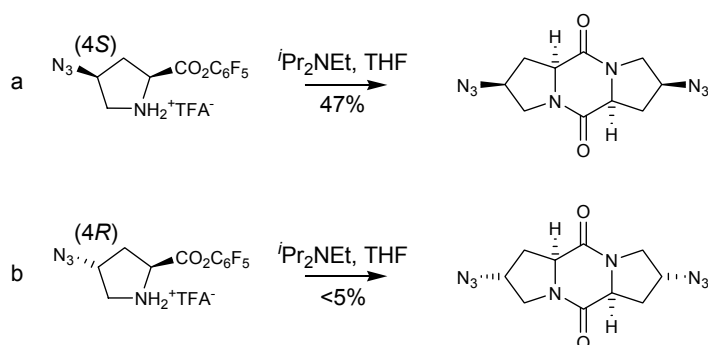
Scheme 2: Diketopiperazine formation in dependence of the configuration at C-4.

The diketopiperazine of (4*R*)-configured azidoproline can be formed; however, the linear dipeptide precursor needs to be formed first (scheme 3).[50]
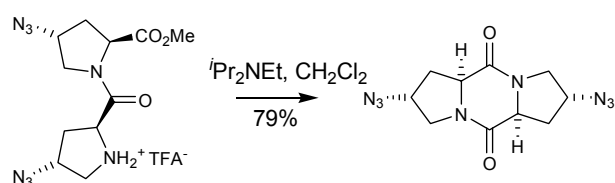
Scheme 3: Diketopiperazine formation of di[(4R)-azidoproline] methyl ester.

NMR studies revealed that the diketopiperazine derived from (4*R*)-configured azidoproline is rigid and possesses a single favorable conformation, with the azido-group occupying the pseudo-axial conformation. In contrast, the diketopiperazine derived from (4*S*)-azidoproline is more flexible and shows a fast equilibrium between conformations with azido-substituent in the pseudo-axial and pseudo-equatorial

positions.[51] These results indicate that the configuration of the C(4)-position of azidoproline influences the conformation of the pyrrolidine ring system. Furthermore, the different cyclization tendencies indicate that the *s-cis*:*s-trans* equilibrium is also influenced by the configuration at C(4).

Therefore, the influence of the azido-substituent and the configuration at C(4) on the conformation of 4-azidoproline was studied. The 4-azidoproline derivatives **14-21** (figure 11) were prepared for this study.
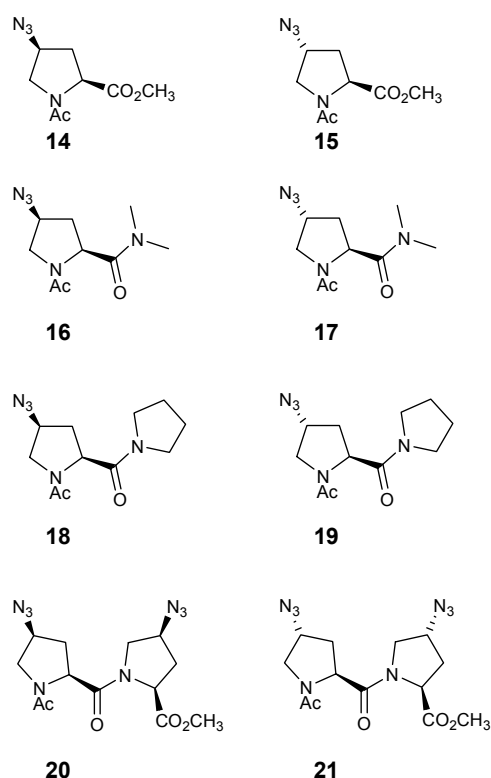
Figure 11: Acetylated 4-azidoproline derivatives studied.

Initially, the *s-cis*:*s-trans* ratio of the methyl ester derivatives **14** and **15** were determined by ^{1}H-NMR (chapter 2.3.1). Consequently, the influence of the C-terminal modification was analyzed by comparison with the amide derivatives **16-19** (chapter 2.3.2). Furthermore, the influence of the N-terminal modification was analyzed by comparison of the acetyl-derivatives **14-19** with the dipeptides **20** and **21** (chapter 2.3.3). To further probe the influence of the azido-substituent, the conformation of the pyrrolidine ring systems, **14** and **15** were analyzed by interpretation of the $^3J_{(H-H)}$ coupling constants, as well as COSY, TOCSY and NOESY experiments in various solvents (chapter 2.4.). Furthermore, crystal structure analysis, IR-spectroscopy and *ab*

inito calculations were performed (chapter 2.5). Finally, the kinetics of the *s-cis*:*s-trans* isomerization in **14** and **15** were determined by 2D EXSY NMR (chapter 2.6).

2.2 Synthesis of acetylated 4-azidoproline derivatives

a) i) Cs_2CO_3 (0.55 eq), MeOH, H_2O, r.t., 10 min.; ii) MeI (2 eq), DMF, r.t., 60 min., quant.; b) i) CH_3SO_2Cl (1.5 eq), NEt_3 (3 eq), CH_2Cl_2, 0°C, 30 min.; ii) NaN_3 (5 eq), DMF, 80°C, 3h, quant.; c) i) 4M HCl in dioxane, r.t., 30 min.; ii) Ac_2O (2 eq), NEt_3 (3 eq), CH_2Cl_2, r.t., 95%; d) i) CH_3SO_3H, PPh_3, DIAD, NEt_3, Toluene, 35°-70°C, 3h; ii) NaN_3, DMF, 80°C, 3h, 80%; e) i) 4M HCl in dioxane, r.t., 30 min.; ii) Ac_2O (2 eq), NEt_3 (3 eq), CH_2Cl_2, r.t., 95%.
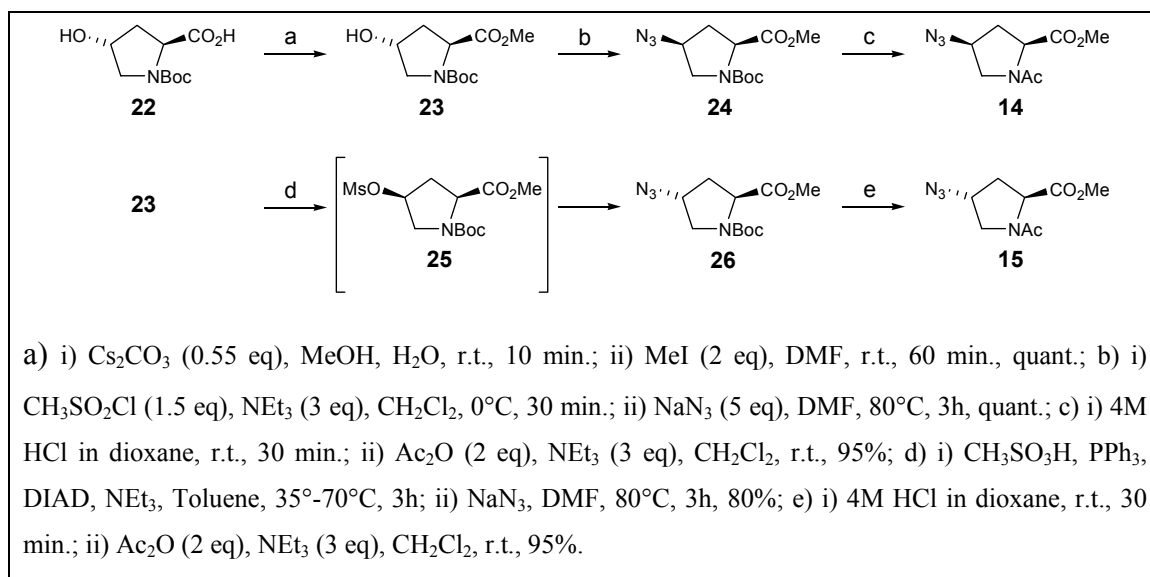
*Scheme 4: Synthesis of acetyl-(4S)-azidoproline methyl ester **14** and acetyl-(4R)-azidoproline methyl ester **15**.*

The synthesis started from commercially available N-α-Boc-(4*R*)-hydroxyproline **22**, which was converted into its methyl ester **23**. The hydoxy-group of N-α-Boc-(4*R*)-hydroxyproline methyl ester **23** was activated as the mesylate and reacted in an S_N2-reaction with sodium azide under inversion of configuration at C(4) to yield the N-α-Boc-(4*S*)-azidoproline methyl ester **24**. Boc-deprotection and acetylation led to acetyl-(4*S*)-azidoproline methyl ester **14**. To obtain the acetylated methyl ester with opposite stereochemistry at C(4), N-α-Boc-(4*R*)-hydroxyproline methyl ester **23** was converted in a Mitsunobu reaction to the mesylate **25** under inversion of configuration at C(4). The mesylate **25** was reacted without further purification under inversion of configuration with sodium azide, yielding N-α-Boc-(4*R*)-azidoproline methyl ester **26**. Boc-deprotection and acetylation led to acetyl-(4*R*)-azidoproline methyl ester **15** (scheme 4).
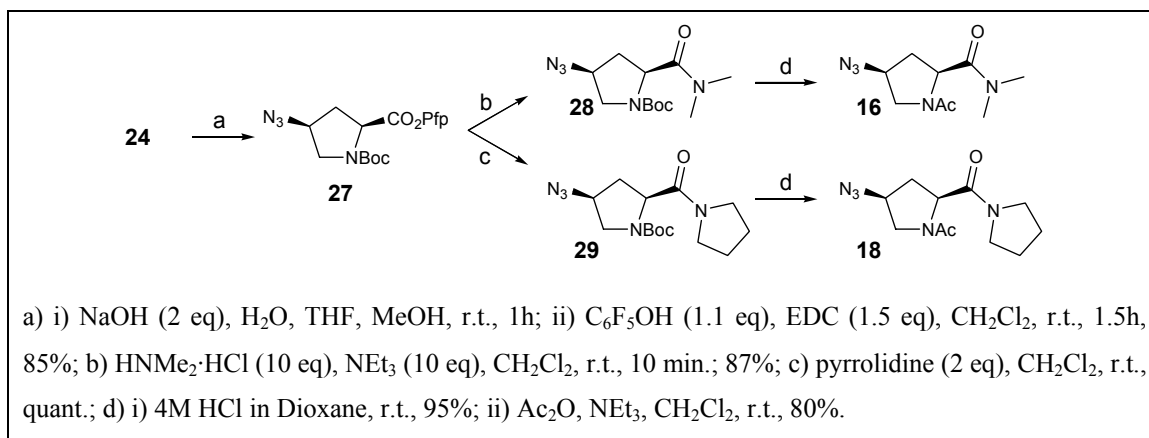
Scheme 5: Synthesis of acetylated 4-azidoproline amide derivatives.

The amide modified acetylated proline derivatives **16** and **18** were synthesized (scheme 5) starting from Boc[Pro-(4S)-N$_3$]OCH$_3$ **24**, which was converted into the pentafluorophenol ester **27**, which in turn was either reacted with dimethylamine hydrochloride yielding the dimethyl amide **28** or with pyrrolidine yielding the pyrrolidine amide **29**. The Boc-protected amide derivatives **28** and **29** were converted to their acetyl derivatives **16** and **18**, respectively, by Boc-deprotection followed by acetylation with acetic anhydride in the presence of triethylamine. The diastereomeric acetylated (4R)-azidoproline amide derivatives **17** and **19** (figure 11) were synthesized analogously starting from the (4R)-configured methyl ester **26**.
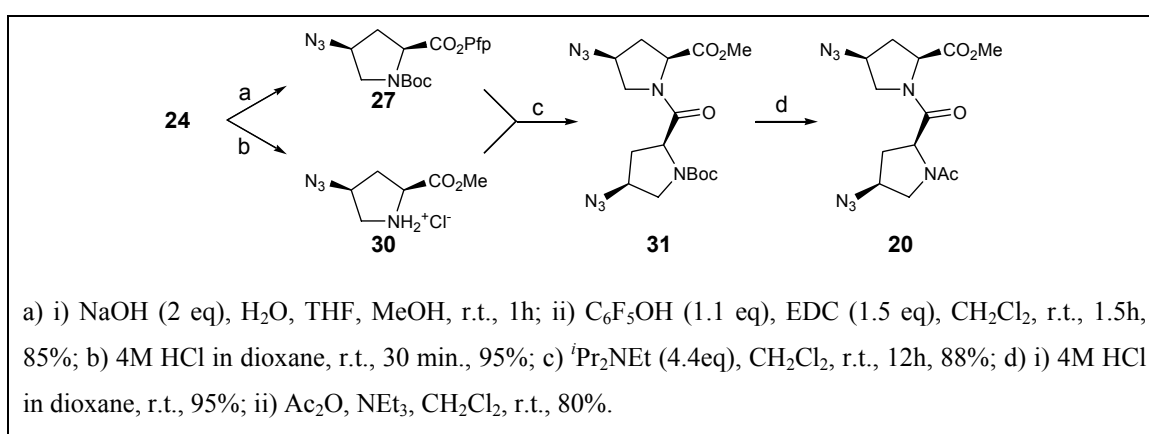
*Scheme 6: Synthesis of acetyl-di[(4S)-azidoproline]OCH$_3$ **20**.*

The synthesis of acetyl-di[(4S)-azidoproline]OCH$_3$ **20** (scheme 6) commences from N-α-Boc-(4S)-azidoproline methyl ester **24** which was on the one hand converted into

the pentafluorophenyl ester **27**, and on the other hand, Boc-deprotected to the hydrochloride salt **30**. The pentafluorophenyl ester **27** and the hydrochloride salt **30** were reacted with each other to form the dipeptide **31**. Boc-deprotection and acetylation lead to acetyl-di[(4*S*)-azidoproline]OCH$_3$ **20**. The diastereomeric acetyl-di[(4*R*)-azidoproline]OCH$_3$ **21** was synthesized analogously.

2.3 Analysis of the *s-cis*:*s-trans* ratio of 14-21

To study the dependence of the *s-cis*:*s-trans* equilibrium on the configuration of the C(4)-position of the 4-azidoproline derivatives, the relative populations of the *s-cis* and *s-trans* conformers of the (4*S*)-derivatives **14**, **16**, **18** and **20** and the (4*R*)-derivatives **15**, **17**, **19** and **21** (figure 11) were determined by ^{1}H-NMR. The ^{1}H-NMR spectra of all derivatives show two seperate six-spin systems corresponding to the protons of the pyrrolidine ring in the *s-cis* and the *s-trans* conformation. 2D NOE spectroscopy was used to assign the conformation of the two spin systems. Integration of the peaks in the ^{1}H-NMR yielded the relative populations.

2.3.1 Analysis of the *s-cis*:*s-trans* ratio in the methyl ester derivatives 14 and 15

Initially, the relative population of the *s-trans* and the *s-cis* conformation of the methyl ester derivatives **14** and **15** was determined in various solvents (table 1).

*Table 1: s-cis:s-trans ratios of **14** and **15** compared to Ac-Pro-OCH$_3$ as determined by ^{1}H-NMR.*

		14	**15**	Ac-Pro-OCH$_3$
Entry	Solvent	*s-cis*:*s-trans*	*s-cis*:*s-trans*	*s-cis*:*s-trans*
1	D$_2$O	1:2.5	1:6	1:5
2	DMF-d$_7$	1:1.5	1:4.5	1:3.6
3	pyridine-d$_6$	1:2	1:4.5	n.d.[a]
4	acetone-d$_6$	1:2	1:4	1:3.5
5	CDCl$_3$	1:2	1:4	1:3.7
6	dioxane-d$_8$	1:2	1:4	n.d.[a]

All samples were measured at 295K and 80 mM concentration. a) "n.d.": not determined.

As expected, in both diastereoisomers **14** and **15**, the *s-trans* conformation is favored (table 1). The comparison of the *s-cis*:*s-trans* ratio shows that the (4*R*)-configured diastereoisomer **15** displays a higher preference for the *s-trans* conformation than the (4*S*)-configured diastereoisomer **14**. Generally, the acetyl-(4*R*)-azidoproline methyl ester **15** favors the *s-trans* conformation by a factor of 2-3 compared its (4*S*)-diastereoisomer **14**. Furthermore the largest difference between **14** and **15** is observed in water and DMF (table 2, entries 1 and 2). The typical ratio found for **15** is 1:4; for **14** the typical ratio is 1:2. For **14**, in DMF an almost even distribution of the two conformations is observed (table 1, entry 2). The comparison to acetylated proline methyl ester demonstrates that the *s-cis*:*s-trans* ratio of (4*S*)-azidoproline **14** lies further to the side of the *s-cis* conformer, while it lies more to the side of the *s-trans* conformation for (4*R*)-azidoproline **15**. This shows that the configuration at C(4) has a distinct influence on the *s-cis*:*s-trans* ratio of acetyl 4-azidoproline methyl ester.

2.3.2 Analysis of the *s-cis*:*s-trans* ratio in the amide derivatives 16-19

The studies presented thus far have all been performed with 4-azidoproline methyl ester derivatives. To test the influence of the methyl ester, the amide derivatives **16-19** (figure 11) were analyzed. As the studies described in chapter 2.3.1 found the largest influence on the *s-cis*:*s-trans* ratio in DMF-d$_7$, this solvent was used for the NMR-spectroscopical analysis of the amide derivatives **16-19** (table 2).

Table 2: s-cis:s-trans ratio of acetylated 4-azidoproline amide derivatives in DMF-d$_7$, 80 mM.

Entry	Compound	*s-cis* to *s-trans* ratio
1	**16**	1:2
2	**17**	1:2
3	**18**	1:2
4	**19**	1:2

Intriguingly, in DMF both diastereoisomers of the dimethyl amide derivatives **16** and **17** as well as both diastereoisomers of the pyrrolidine amide derivatives **18** and **19**, show the same *s-cis* to *s-trans* ratio (table 2). This clearly indicates that the higher preference

for the *s-trans* conformation found in acetyl-(4*R*)-azidoproline methyl ester **15** is dependent on the C-terminal ester function.

2.3.3 Analysis of the *s-cis*:*s-trans* ratio in the dipeptides 20 and 21

To test whether the preferences for the ratio of *s-cis*:*s-trans* described in the previous chapters are dependent on the acetyl group, the acetylated diproline derivatives **20** and **21** were studied by NMR spectroscopy in DMF-d$_7$.

The ^{1}H-NMR spectra of **20** and **21** show four sets of signals, indicating the presence of four different conformers. Based on NOESY experiments, these conformers were assigned as the *s-trans*/*s-trans*, *s-trans*/*s-cis*, *s-cis*/*s-trans* and *s-cis*/*s-cis* conformations (scheme 7).
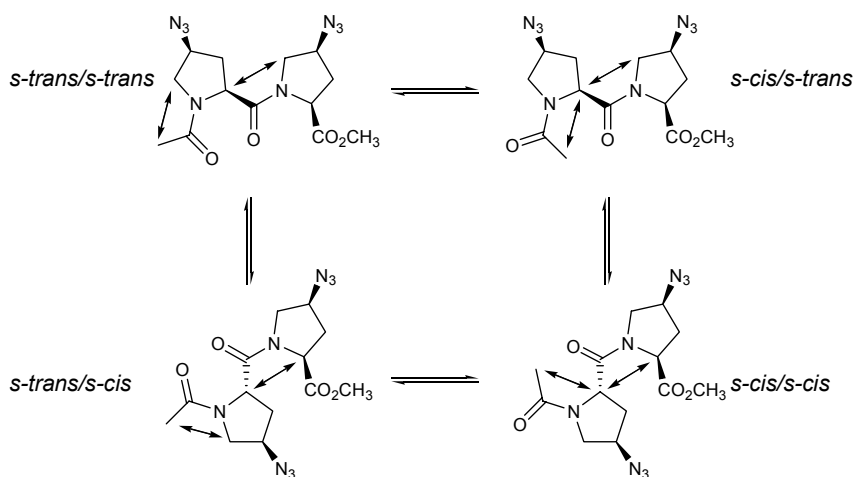
Scheme 7: The four possible conformers of acetyl-di[(4S)-azidoproline]OCH$_3$. The arrows indicate the positions of protons that show an NOE with each other, indicative of the conformation.

An NOE between the protons of the acetyl group and the protons at C(δ) is indicative of an *s-trans* conformation of the N-terminal amide bond (scheme 7, left). Conversely, an NOE between the protons of the acetyl group and the proton at C(α) indicates an *s-cis* conformation (scheme 7, right). The *s-trans* conformation of the central amide bond was assigned based on an NOE between the proton at C(α) of the N-terminal 4-azidoproline and the proton at C(δ) of the C-terminal 4-azidoproline (scheme 7, top). In the *s-cis* conformation of the central amide bond, an NOE between the two protons at the C(α) positions of the two 4-azidoprolines was observed (scheme 7, bottom).

Table 3: Population of conformations in 20 and 21, listed for each amide bond.

Entry	N-terminal	Central	**20**	**21**
1	*s-trans*	*s-trans*	21	22
2	*s-cis*	*s-trans*	8	8
3	*s-trans*	*s-cis*	1	1
4	*s-cis*	*s-cis*	4	1

Measurements at 80 mM concentration in DMF-d_7, 295K.

By integration of the ^{1}H-NMR signals corresponding to the different conformers, the relative population of each of the conformers was determined. The relative populations of the *s-trans/s-trans*, *s-trans/s-cis* and *s-cis/s-trans* conformations were found to be equal in both diastereoisomers, **20** and **21** (table 3, entries 1-3). However, **20** shows a 4-fold higher population of the *s-cis/s-cis* conformation (table 3, entry 4).

*Table 4: s-cis:s-trans ratio for the amide bonds of **20** and **21**.*

Entry	Amide Bond	**20** *s-cis:s-trans*	**21** *s-cis:s-trans*
1	N-terminal	1:2	1:2
2	Central	1:6	1:15

Measurements at 80 mM concentration in DMF-d_7, 295K.

Looking at each amide bond separately, the influence of the configuration at C(4) and of the C-terminal residue becomes apparent (table 4). For the conformation around the N-terminal amide bond, no difference between the diastereoisomers is found (table 4, entry 1). This is in accordance with the results presented in chapter 2.3.2, which indicated that 4-azidoproline derivatives with a C-terminal amide show the same *s-cis*:*s-trans* ratio, regardless of the configuration at C(4). The conformation around the central amide bond, however, shows a dependence on the configuration at C(4) (table 4, entry 2). While (4*S*)-derivative **20** shows a 1:6 ratio of the population of the *s-cis*:*s-trans* conformer, (4*R*)-derivative **21** shows a 1:15 ratio. Thus, **21** shows a 2.5-fold higher preference for the *s-trans* conformation than **20**. This is in accordance with the findings described in chapter 2.3.1, which indicated that acetyl-(4*R*)-azidoproline methyl ester **15**

has a 2- to 3-fold higher preference for the *s-trans* conformation than its diastereoisomer **14**.

2.4 Conformational analysis

To understand the basis of the higher preference for the *s-trans* conformation in *N*-α-acetyl-(4*R*)-azidoproline methyl ester **15** compared to its diastereoisomer **14**, the conformations of the diastereoisomers were further analyzed by interpretation of the $^3J_{(H-H)}$ coupling constants, as well as by COSY, TOCSY and NOESY experiments in various solvents.

The pyrrolidine ring of proline can occupy a variety of conformations, which are in fast equilibrium with each other.[52] For the analysis of the 4-azidoproline derivatives, two main conformations are of importance: An *endo*-conformation, shown in scheme 8 on the top, and an *exo*-conformation shown on the bottom. For reasons of clarity, scheme 8 shows idealized depictions of only one of each of the many *endo*- and *exo*-conformations.

endo-conformation   **14**: X = N₃, Y = Hγ   **15**: X = Hγ', Y = N₃

exo-conformation   **14**: X = N₃, Y = Hγ   **15**: X = Hγ', Y = N₃
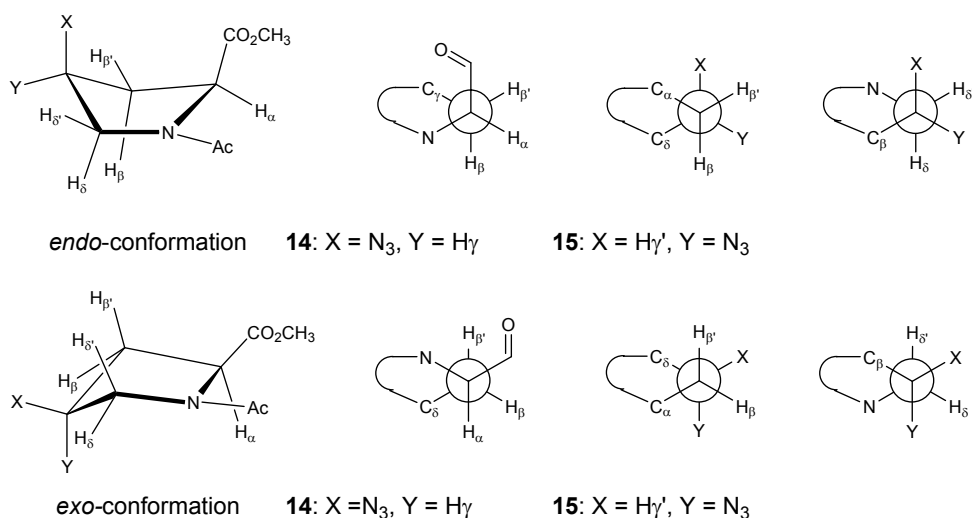
Scheme 8: Possible conformations of the pyrrolidine ring system in azidoprolines and Newman projections of these conformations (idealized).

The *endo*-conformation results in a pseudo-axial position of the azido-substituent in the case of acetyl-(4*S*)-azidoproline derivatives such as **14**, whereas for acetyl-(4*R*)-azidoproline derivatives, such as **15**, the azido-substituent is in a pseudo-equatorial position. Conversely, in a *exo*-conformation, the azide in **14** is in a pseudo-equatorial position, while in **15** it is in a pseudo-equatorial position. The

Newman projections in scheme 8 show, how the dihedral angles of these two conformations differ. The magnitude of the vicinal proton coupling constant, $^3J_{(H,H)}$, is dependent on the dihedral angle between the protons. This dependency can be fitted by the Karplus curve,[53] which enables conclusions about the dihedral angles based upon the magnitude of $^3J_{(H,H)}$ to be drawn. The Karplus curve is described by the following equation:

$$^3J_{H,H} = A\cos^2\Theta + B\cos\Theta + C$$

In this equation Θ is the dihedral angle between the vicinal protons and the factors A, B and C are parameters used to fit the curve to specific types of molecules.[54] In the following discussion, the parameters used are: A = 9.5, B = -1, C = 1.4. These parameters were developed for cyclotriproline.[55]

2.4.1 Conformational analysis of the pyrrolidine ring of 14

Table 5: $^3J_{H,H}$ Coupling constants of N-α-acetyl-(4S)-azidoproline methyl ester 14.

entry	$^3J_{(H,H)}$	D$_2$O		DMF-d$_7$		CD$_3$OD		CDCl$_3$	
		s-trans	s-cis	s-trans	s-cis	s-trans	s-cis	s-trans	s-cis
1	H$^\alpha$-H$^\beta$	9.6	7.2	9.1	9.0	9.2	8.5	8.9	6.1
2	H$^\alpha$-H$^{\beta'}$	2.5	3.1	4.2	1.5	3.7	1.5	4.3	4.1
3	H$^\beta$-H$^\gamma$	5.2	nd^a	6.0	5.2	5.7	4.8	nd^a	nd^a
4	H$^{\beta'}$-H$^\gamma$	2.4	nd^a	4.7	3.0	3.8	1.6	4.4	nd^a
5	H$^\gamma$-H$^\delta$	5.3	5.3	6.1	5.4	5.9	5.5	6.1	nd^a
6	H$^\gamma$-H$^{\delta'}$	1.6	<1	4.0	1.5	3.5	<1	4.2	1.3
7	H$^{\beta'}$-H$^{\delta'b}$	1.5	nd^a	<1	<1	0.7	1.6	nd^a	nd^a

All measurements were performed at 80 mM concentration at 295K. a) "nd" coupling constants could not be determined due to signal overlap; b) ^4J "W" coupling indicating the pseudo-equatorial protons at C(β) and C(δ).

Table 5 shows the vicinal coupling constants of **14** in various solvents. For the analysis of conformation of the pyrrolidine ring, three coupling constants are of particular interest, the H$^\alpha$-H$^{\beta'}$ coupling, the H$^{\beta'}$-H$^\gamma$ coupling and the H$^\gamma$-H$^{\delta'}$ coupling (table 5, entries 2, 4 and 6, respectively). From the magnitude of these couplings, and the

dihedral angles associated with them by the Karplus curve,[53,55] the conformation of the pyrrolidine ring was determined.

Based on the Karplus curve and the parameters used, coupling constants close to 1.4 Hz are indicative of dihedral angles close to 90°. For the *s-cis* conformer, the vicinal coupling constants found for the H^α-$H^{\beta'}$ coupling, the $H^{\beta'}$-H^γ coupling and the H^γ-$H^{\delta'}$ coupling (table 5, entries 2, 4 and 6, respectively) are almost all smaller than 3 Hz, in most cases even smaller than 1.5 Hz. This indicates that the dihedral angles of these protons are close to 90°. It is clear from the Newman projections in scheme 8 that these dihedral angles are in good agreement with the *endo*-conformation.

The somewhat larger values found for these coupling constants in the *s-trans* conformer indicate that the pyrrolidine ring is more flexible and that a higher population of the *exo*-conformation, with the azido-substituent in the pseudo-equatorial position, is present. This leads to an averaging of these coupling constants, however, the magnitude of the coupling constants found show that the weight of this equilibrium is largely on the side of the *endo*-conformation. This is further supported by the $^4J_{(H,H)}$ "W" coupling found between $H^{\beta'}$ and $H^{\delta'}$ (table 5, entry 7), which indicates that these protons occupy the pseudo-equatorial positions. Thus, for both the *s-cis* and the *s-trans* conformation, the pyrrolidine ring of *N*-α-acetyl-(4*S*)-azidoproline methyl ester **14** favors the *endo*-conformation. This leads to the azido-group being in the pseudo-axial position.

2.4.2 Conformational analysis of the pyrrolidine ring of 15

*Table 6: $^3J_{H,H}$ Coupling constants of N-α-acetyl-(4R)-azidoproline methyl ester **15**.*

entry	$^3J_{(H,H)}$	D$_2$O		DMF-d$_7$		CD$_3$OD		CDCl$_3$	
		s-trans	s-cis	s-trans	s-cis	s-trans	s-cis	s-trans	s-cis
1	H$^\alpha$-H$^\beta$	8.0	8.6	8.2	7.5	8.2	8.5	8.2	8.3
2	H$^\alpha$-H$^{\beta'}$	8.3	nd^a	7.1	6.7	7.5	6.0	6.4	5.8
3	H$^\beta$-H$^{\gamma'}$	3.3	4.7	4.4	nd^a	4.1	5.0	5.0	5.1
4	H$^{\beta'}$-H$^{\gamma'}$	5.3	nd^a	5.6	nd^a	5.5	5.9	6.1	6.1
5	H$^{\gamma'}$-H$^\delta$	2.3	nd^a	3.5	nd^a	3.2	1.5	3.8	4.8
6	H$^{\gamma'}$-H$^{\delta'}$	5.9	5.5	5.4	5.7	5.2	5.7	5.6	5.8
7	H$^\beta$-H$^{\delta b}$	1.5	nd^a	1.2	nd^a	1.4	1.4	1.0	1.2

a) "nd" coupling constants could not be determined due to signal overlap, b) ^4J "W" coupling indicating the pseudo-equatorial protons at C(β) and C(δ).

Analogously to the (4*S*)-diastereoisomer **14**, the coupling constants of the (4*R*)-diastereoisomer **15** were analyzed. At the first glance, the coupling constants observed for **15** differ significantly from the ones observed for **14** and are not in agreement with an *endo*-conformation. The H$^\alpha$-H$^{\beta'}$ coupling constant found (table 6, entry 2) is much larger than in the case of **14**, while the H$^{\gamma'}$-H$^\delta$ coupling constant (table 6, entry 5) is much smaller than in the case of **14**. The H$^{\gamma'}$-H$^\delta$ coupling constant is in the range of 1.5-4 Hz, indicating an angle close to 60 and 90°. Furthermore, the $^4J_{(H,H)}$ "W" coupling found between H$^\beta$ and H$^\delta$ (table 6, entry 7), indicates that now these protons occupy the pseudo-equatorial positions. The coupling constants found match the dihedral angles predicted for an *exo*-conformation, as shown in scheme 8. The pseudo-equatorial positions of H$^\beta$ and H$^\delta$ further support this analysis. Thus, the pyrrolidine ring of **15** is in an *exo*-conformation, with the azido-group in the pseudo-axial position.

It is intriguing that in both diastereoisomers the azide occupies the pseudo-axial position. This suggests that the conformation of the pyrrolidine ring is determined by the azido-substituent. In both diastereoisomers, the main conformers show a *gauche* arrangement between the azide and the amide. This suggests that the conformation of

the pyrrolidine ring is controlled by a *gauche* interaction of the azido-group analogous to the known *gauche* effect found for fluoride.[56]

2.5 Further studies using crystal structure analysis, IR-spectroscopy and *ab initio* calculations

The studies in the previous chapters have revealed a higher preference for the *s-trans* conformation of the N-terminal peptide bond of (4*R*)-azidoproline methyl ester derivatives (see chapters 2.3.1 and 2.3.3). Thus far, no indications why this preference exits have been found. Therefore, further studies to understand this preference were undertaken.

2.5.1 X-Ray analysis

Single crystals of **15**, suitable for X-ray diffraction were obtained by crystallization from acetone. Unfortunately, **14** is an oil, which could not be crystallized.
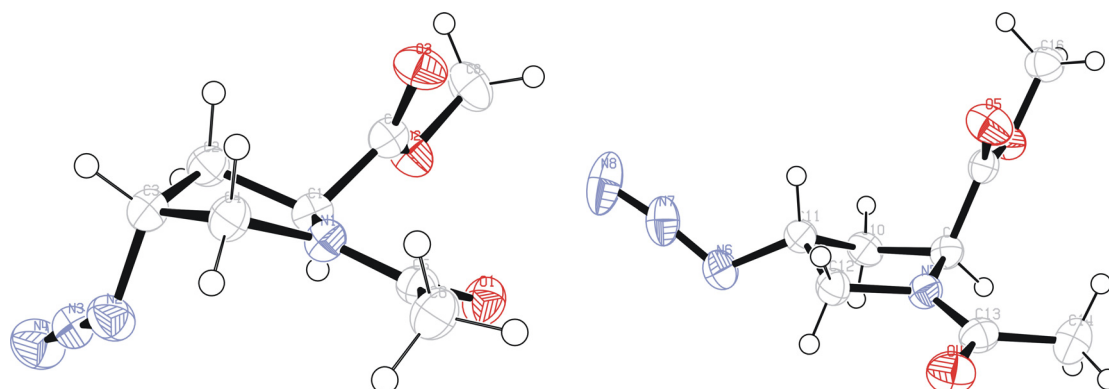
*Figure12: X-ray structure of N-α-acetyl-(4R)-azidoproline methyl ester **15***.

15 crystallized in a monoclinic system with four molecules per unit cell, with two different conformations. Figure 12 on the left, shows the *s-trans* Cγ-*exo*-conformation found in the crystal structure. This conformation is in good agreement with the conformations suggested by the anaylsis of the NMR-spectroscopical data (see chapter 2.4.2). The second structure found (figure 12, right) shows a twisted *s-cis* Cγ-*endo*-conformation, which is not in agreement with the analysis of the NMR spectra (see chapter 2.4.2). Probably this conformation is stabilized by interactions in the crystal lattice and thus does not represent an overall favorable conformation.

The analysis of the crystal structure reveals an element of the conformation which could not be analyzed by the NMR studies presented in the previous chapters: The orientation of the methyl ester. Its orientation is such that the oxygen of the acetyl group is at an angle of 98° and at a distance of 2.8 Å to the carbonyl carbon of the methyl ester (figure 13). This angle is close to the ideal 103° angle of the Bürgi-Dunitz-trajectory,[57] upon which a nucleophile attacks a carbonyl.
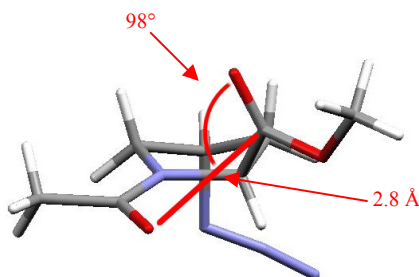
Figure 13: Bürgi-Dunitz-trajectory of the acetyl oxygen on the carbonyl group (X-ray structure).

The orientation of the methyl ester relative to the acetyl oxygen suggests a possible explanation for the higher *s-trans* preference of acetyl-(4*R*)-azidoproline methyl ester **15**. The *s-trans* conformation might be stabilized by an interaction of the non-bonding electrons of the acetyl group with the π*-orbital of the carbonyl bond of the methyl ester. Both the angle of 98° and the distance of 2.8 Å, which is well within the van-der-Waals distances, support this hypothesis. The existence of such an interaction is further supported by a slight pyramidalization of the carbonyl of the methyl ester, which is bent 3.7° out of its optimal plane. A similar observation was made in 4-fluroprolines, and has been referred to as an "n-π*" interaction.[58,59]

This hypothesis is furthermore supported by the results presented in the previous chapters. It was shown that the higher preference for the *s-trans* conformation is observed in *N*-α-acetyl-(4*R*)-azidoproline methyl ester **15**, but not in its amide derivatives **17** and **19** (see chapters 2.3.1 and 2.3.2, respectively). This is in agreement with the hypothesis of an "n-π*"-interaction between the acetyl group and the carbonyl carbon. The non-bonding electrons of the oxygen of the acetyl group may be seen as a nucleophile, the carbonyl carbon is the electrophile; it is interacting with the electrophilic carbonyl carbon. In the case of the amide derivatives **17** and **19**, the eletrophilicity of the carbonyl carbon is greatly reduced due to the mesomeric

stabilization from the nitrogen of the amide, which makes the nucleophilic interaction less favorable. The carbonyl carbon of the methyl ester is more electrophilic and thus, the nucleophilic interaction may take place.[60]

2.5.2 IR studies

To further test the hypothesis that an interaction between the oxygen of the acetyl group and the carbonyl group of the methyl ester, stabilizes the *s-trans* conformation in (4*R*)-azidoproline derivatives, the vibrational stretching frequency of the ester carbonyl was determined by FT-IR spectroscopy in solution. The vibrational stretching frequency of carbonyl bonds is indicative of the bond length and bond order. A lower wave number corresponds to a lower bond order and longer bond length. An electron donation into the π^*-orbital, as suggested by the "n-π^*-interaction, should lead to a weakening of the double bond, the single bond character should be increased, which should lead to a lowering of the bond order, which should reflected in a shorter wave number.

Table 7: Vibrational stretching frequencies of the ester carbonyl group of 14 and 15.

Entry	Compound	CHCl$_3$ [cm^{-1}]	Dioxane [cm^{-1}]
1	Ac-[Pro(4R)N$_3$]-OCH$_3$ **15**	1745.3	1747.9
2	Ac-[Pro(4S)N$_3$]-OCH$_3$ **14**	1749.0	1752.0

All measurements were performed at 100 mM concentration in a NaCl cell.

In chloroform the carbonyl stretching band of the (4*R*)-configured acetylated azidoproline methyl ester **15** is 4.7 cm^{-1} shorter (table 7, entry 1) than the carbonyl stretching band of the (4*S*)-configured diastereoisomer **14** (table 7, entry 2). In dioxane, the difference is 4.1 cm^{-1}.

Table 8: Vibrational stretching frequencies of the ester carbonyl group of 20 and 21.

Entry	Compound	CHCl$_3$ [cm^{-1}]
1	Ac-[Pro(4R)N$_3$]$_2$-OCH$_3$ **21**	1744.9
2	Ac-[Pro(4S)N$_3$]$_2$-OCH$_3$ **20**	1748.1

All measurements were performed at 100 mM concentration in a NaCl cell.

Similarly, FT-IR spectroscopy of the acetylated dipeptides **20** and **21** in solution show that the vibrational stretching frequency of the ester carbonyl of Ac-[Pro(4*R*)N$_3$]$_2$-OCH$_3$ **21** (table 8, entry 1) is 3.2 cm^{-1} shorter than that of the diastereomeric acetylated dipeptides **20** (table 8, entry 2).
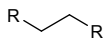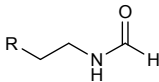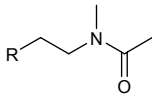
The shifts of the vibrational stretching frequencies of the diastereomeric methyl ester derivatives **14** and **15** and **20** and **21** support the hypothesis, that in the (4*R*)-configured methyl esters, the *s-trans* conformation is stabilized by an "n-π*"-interaction.

2.5.3 *Ab Initio* Calculations

The analysis of the data obtained by NMR spectroscopy, X-Ray diffraction and FT-IR spectroscopy suggests that the conformation of the pyrrolidine ring systems of the 4-azidoproline derivatives is governed by a *gauche* effect of the azide with the N-terminal amide, and that the *s-trans* conformation of the methyl ester derivatives of (4*R*)-azidoproline is stabilized by an "n-π*"-interaction between the non-bonding electrons of the oxygen of the acetyl group with the carbonyl carbon of the methyl ester. To further investigate the *gauche* effect found and to gain insight into why the (4*S*)-azidoproline methyl ester derivatives do not stabilize the *s-trans* conformation, *ab initio* calculations were performed in collaboration.[61] Conformational searches with Spartan'02[62] were performed using molecular mechanic calculations with the force field MMFF (Merck Molecular Force Field). The structures of the conformers were optimized at the B3LYP/6-31G** level using the *ab inito* program QChem.[63] RI-MP2/TZVP energetics were computed with Turbomole.[64] These calculations are models for the gas phase and do not take solvent effects into account.

The preference for a *gauche* conformation over an eclipsed or *anti* conformation of 1,2-difluoroethane has been termed the *gauche* effect.[56] In 1,2-difluoroethane, the *gauche* effect has been studied intensively in computational studies[65] and by spectroscopy.[66] The *gauche* effect has also been observed in amide derivatives, such as N-(2-fluoroethyl)benzamide derivatives, where it has been observed in the solid state.[67] Thus, as a benchmark for the accuracy of the *ab inito* calculations and to see if the azide *gauche* effect found in the pyrrolidine systems is also present in conformationally less restricted molecules, disubstituted ethane derivatives were initially studied by *ab initio* calculations.

Table 9: Energy differences between the anti and the gauche conformation, calculated for ethane derivatives.

| Entry | Compound | $\Delta E = E_{anti}-E_{gauche}$ [kcal mol^{-1}] | |
		$R = F$	$R = N_3$
1		0.9	1.3
2		1.4	1.3
3		1.7	3.3

For each ethane derivative the energy of the two conformations, *anti* and *gauche* was calculated. Table 9 lists the difference between the energies calculated; positive values indicate a preference for the *gauche* conformation. The energy difference calculated for 1,2-difluoroethane (table 9, entry 1) of 0.9 kcal mol^{-1} is in good agreement with the experimental value of 0.8 kcal mol^{-1}.[66a] Thus, it can be assumed that the methods used are able to detect a *gauche* effect, not only in 1,2-difluoroethane, but also in other compounds. It is intriguing that the azidoethane derivatives all show an equal or higher preference for the *gauche* conformation than the fluoroethane derivatives (table 9, entries 1-3).

After these basic studies, the energy difference between the pseudo-axial (*gauche*) and the pseudo-equatorial (*anti*) conformation of the substituent in the 4-position of azidoproline and fluoroproline was studied (table 10).

Table 10: Energy differences between the gauche and the anti conformation calculated for acetylated 4-azido- and 4-fluoroproline methyl ester.

			$\Delta E = E_{anti}\text{-}E_{gauche}$ [kcal mol^{-1}]	
Entry	Configuration	Conformation	Ac[Pro(4N$_3$)]OCH$_3$	Ac[Pro(4F)]OCH$_3$
1	(4*R*)	*s-trans*	0.7	0.5
2	(4*R*)	*s-cis*	1.8	1.5
3	(4*S*)	*s-trans*	0.8	0.7
4	(4*S*)	*s-cis*	3.2	3.0

Table 10 lists the calculated energy differences between the *anti* and the *gauche* conformations of 4-azidoproline methyl ester and 4-fluoroproline methyl ester, positive values indicate a *gauche* preference. The *ab initio* calculations suggest a preference for the *gauche* conformation in all diastereoisomers of both 4-azidoproline and 4-fluoroproline. In the *s-cis* conformers this preference is more pronounced than in the *s-trans* conformers. This finding is in agreement with the analysis of the NMR data as discussed in chapter 2.4 and the crystal structure analysis discussed in chapter 2.5.1.

Furthermore, the energy difference between the *s-trans* and the *s-cis* conformers was calculated for both azido- as well as fluoroproline (table 11).

Table 11: Energy difference between s-trans and s-cis conformations calculated for acetylated 4-azido- and 4-fluoroproline methyl ester.

			$\Delta E = E_{s\text{-}trans}\text{-}E_{s\text{-}cis}$ [kcal mol^{-1}]	
Entry	Configuration	Conformation	Ac[Pro(4N$_3$)]OCH$_3$	Ac[Pro(4F)]OCH$_3$
1	(4*R*)	*gauche*	-1.6	-1.6
2	(4*R*)	*anti*	-2.7	-2.6
3	(4*S*)	*gauche*	0.1	0.02
4	(4*S*)	*anti*	-2.4	-2.2

In general, the calculations show, in accordance with the data obtained by NMR (see chapter 2.3.1), a preference for the *s-trans* conformer (indicated by negative values in table 11). The acetylated (4*S*)-azidoproline methyl ester in the *gauche* conformation, as

well as the acetylated (4*S*)-fluoroproline methyl ester in the *gauche* conformation (table 11, entry 3) shows no preference for the *s-trans* or the *s-cis* conformation.

To judge, why acetylated (4*S*)-azidoproline methyl ester **14**, does not seem to stabilize the *s-trans* conformation as much as acetylated (4*R*)-azidoproline methyl ester **15** does, a comparison of the lowest energy conformations was made (figure 14). The conformation calculated for **15** is very similar to the conformation found in the solid state by X-ray diffraction. Likewise, the conformation calculated for **14** is in good agreement with the conformation derived from the analysis of the NMR data.
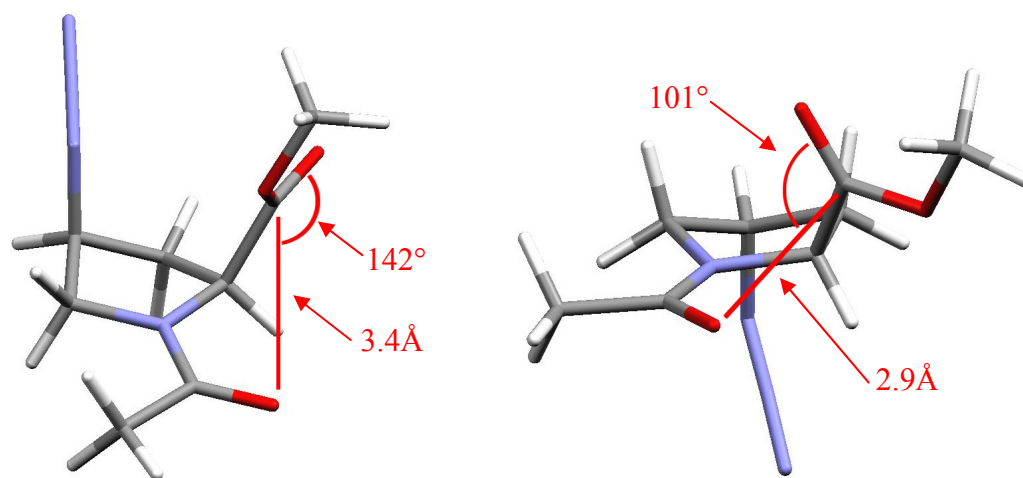
*Figure 14: Conformations calculated for Ac[Pro(4S)N₃]OCH₃ **14** (left) and Ac[Pro(4R)N₃-OCH₃ **15** (right).*

Figure 14 shows the lowest energy conformations found for the two diastereoisomers, **14** and **15**. In the conformation calculated for the (4*R*)-diastereoisomer **15** the angle of the oxygen of the acetyl group and the carbonyl group of the ester is close to 103° and the distance between the acetyl-oxygen and the carbonyl-carbon is calculated to be 2.9 Å. This is in complete agreement with the conformation found in the solid state and the proposed "n-π*"-interaction. The conformation of the diastereoisomer **14** shows an angle of 142° between the acetyl oxygen and the carbonyl group of the ester and the distance between the oxygen of the acetyl group and the carbon of the carbonyl group is calculated to be 3.4 Å. Thus, in the case of the (4*S*)-diastereoisomer, both the distance as well as the angle between the atoms involved, do not meet the requirements for an "n-π*" interaction. Therefore, a stabilization of the *s-trans* conformation by such an interaction is not feasible. This may explain why the (4*R*)-configured azidoproline

methyl ester derivatives show a higher pereference for the *s-trans* conformation than the (4*S*)-configured derivatives.

2.6 Kinetic studies using 2D EXSY NMR

The studies described so far, have all dealt with the thermodynamic stability of the different conformations of the diastereoisomers. To measure the kinetics of the interconversion between the conformers, two-dimensional EXSY NMR was performed.

EXSY NMR is a variant of NOESY NMR, making use of the fact that conformers, which are in chemical exchange on a millisecond time scale, have two distinct sets of signals. Cross-peaks with opposite phase to the regular NOE cross-peaks between the signals corresponding to the exchanging protons are observed. These peaks arise because the conformers interchange during the course of the measurement, and a proton, which at the beginning of the experiment is in one conformation, will be in another conformation at the end of the experiment. The value of the sum of the rate constants k_{ct} and k_{tc}, k can be determined by the following equation: [68]

$$k = \frac{1}{t_m} \ln \frac{r+1}{r-1} \quad (1)$$

The variable r is defined as follows:

$$r = \frac{4 X_A X_B (I_{AA} + I_{BB})}{(I_{AB} + I_{BA}) - (X_A - X_B)^2} \quad (2)$$

t_m is the mixing time of the EXSY experiment, *I* refers to the integrated intensity of the peak; the indices A and B refer to diagonal peaks of the *s-cis* and the *s-trans* conformer when they are equal and to cross peaks when they are different. *X* is the molar fraction of the conformers indicated in the index and k is equal to the sum of the isomerization rates k_{ct} and k_{tc}. From knowledge of k and the equilibrium constant K, which was determined by peak integration in the ^{1}H-NMR spectrum, the rates k_{ct} and k_{tc} were calculated.

EXSY experiments were performed with **14** and **15** in DMF-d_7. By measuring a series of experiments at different mixing times and temperatures, sets of k values were generated from which sets of k_{ct} and k_{tc} values were determined.

*Table 12: Isomerization rates and equilibrium constants of the s-cis:s-trans equilibrium of **14** and **15**.[a]*

	Ac[Pro(4*S*)N$_3$]OCH$_3$ **14**			Ac[Pro(4*R*)N$_3$]OCH$_3$ **15**		
T [K]	k$_{ct}$ [s^{-1}]	k$_{tc}$ [s^{-1}]	K[b]	k$_{ct}$ [s^{-1}]	k$_{tc}$ [s^{-1}]	K[b]
285.4	0.035	0.021	1.70	0.031	0.0075	4.11
298	0.14	0.07	1.7	0.11	0.028	3.81
303	0.30	0.16	1.68	n.d.[c]	n.d.[c]	n.d.[c]
308	0.44	0.18	1.70	0.36	0.10	3.58
313	n.d.[c]	n.d.[c]	n.d.[c]	0.64	0.18	3.47
325.3	3.5	2.1	1.70	2.6	0.83	3.10
336.4	9.2	5.7	1.70	7.2	2.4	2.96
348.5	28.5	16.5	1.68	21.1	7.1	2.87

a) All measurements were performed at 80mM concentration; b) as found by integration of the signals in the ^{1}H-NMR; c) " n.d." not determined.

The studies revealed that the rate of isomerization from the *s-cis* to the *s-trans* conformation (table 12, k$_{ct}$) is equally fast in both diastereoisomers, while the isomerization from *s-trans* to *s-cis* (table 12, k$_{tc}$) is significantly faster in the (4*S*)-derivative **14**. Thus, the higher population of the *s-trans* conformation in (4*R*)-configured azidoproline is not due to a faster isomerization from the *s-cis* to the *s-trans* conformer, but due to a slower isomerization from the *s-trans* to the *s-cis* conformer.
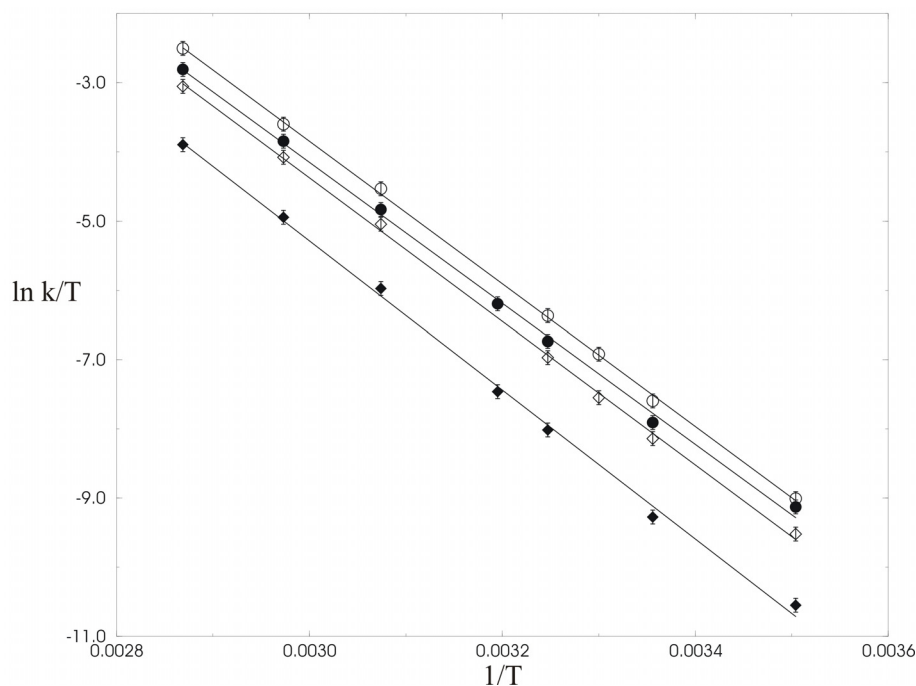
Figure 15: Eyring plots of the rate constants for the isomerization of the acetylated proline derivatives:
14 cis-to-trans (empty circles), 15 cis-to-trans (full circles), 14 trans-to-cis (empty diamonds),
15 trans-to-cis (full diamonds).

The activation enthalpy and entropy of the conversions from the *s-cis* to the *s-trans* conformation of the diastereomeric azidoproline derivatives were determined by analysis of the rate constants in Eyring plots (figure 15). The Eyring equation is defined as follows:

$$k = \frac{k_B T}{h} e^{-\frac{\Delta H^{\ddagger}}{RT}} e^{\frac{\Delta S^{\ddagger}}{R}} \quad (3)$$

Transformed:

$$\ln \frac{k}{T} = -\frac{\Delta H^{\ddagger}}{RT} + \ln \frac{k_B}{h} + \frac{\Delta S^{\ddagger}}{R} \quad (4)$$

Where k_B is the Boltzmann-constant, h is the Planck constant and R is the ideal gas constant. In the Eyring plot the natural logarithm of the rate constants per temperature is plotted against the reciprocal temperature. From the slopes of the lines defined by the data points the activation enthalpy of the conversion was determined. The axis intercept of the y-axis was used to calculate the activation entropy.

Table 13: Activation enthalpies and entropies of the s-cis to s-trans and s-trans to s-cis isomerization.[a]

Isomerization	Ac[Pro(4S)N$_3$]OCH$_3$ **14**		Ac[Pro(4R)N$_3$]OCH$_3$ **15**	
	$\Delta H^{\ddagger}$ [kcal mol^{-1}]	$\Delta S^{\ddagger}$ [cal mol^{-1}K^{-1}]	$\Delta H^{\ddagger}$ [kcal mol^{-1}]	$\Delta S^{\ddagger}$ [cal mol^{-1}K^{-1}]
s-cis to *s-trans*	20.5 ± 0.5	6.6 ± 2.6	20.2 ± 0.5	5.2 ± 2.8
s-trans to *s-cis*	20.6 ± 0.5	5.9 ± 2.6	21.4 ± 0.5	6.5 ± 2.8

a) Extracted from Eyring plots, errors were determined by least square fit analysis.

The analysis of the activation enthalpies and activation entropies extracted from the Eyring plots (table 13) shows that for both Ac[Pro(4S)N$_3$]OCH$_3$ **14** and Ac[Pro(4R)N$_3$]OCH$_3$ **15** the isomerization barrier is of enthalpic and not of entropic nature. Furthermore, for **14** the activation enthalpy (table 13, $\Delta H^{\ddagger}$) is equal for both the *trans*-to-*cis* and *cis*-to-*trans* isomerization. For **15** the *trans*-to-*cis* isomerization has a slightly higher activation energy than the *cis*-to-*trans* isomerization.
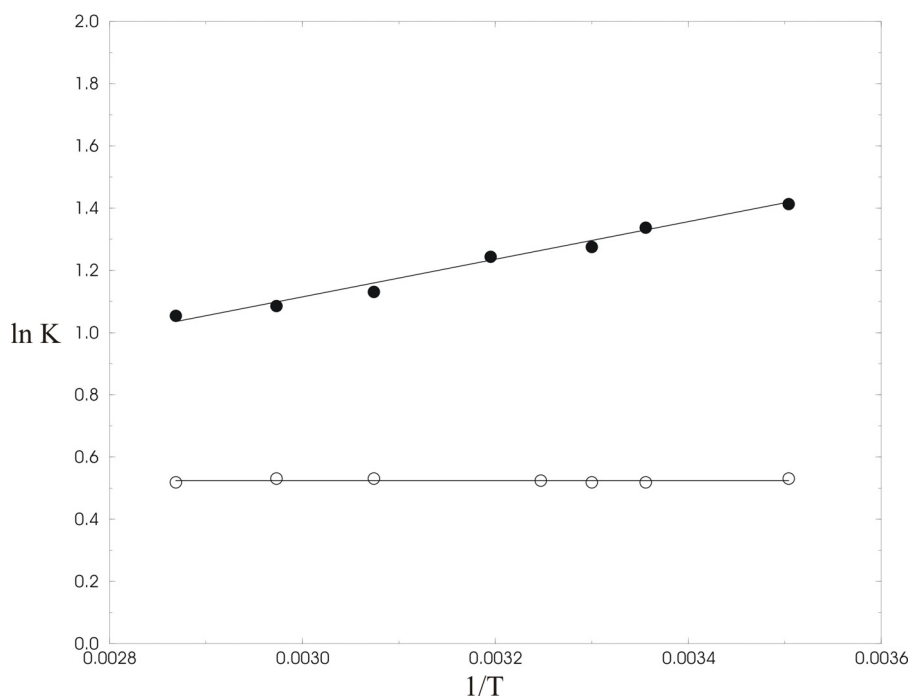
*Figure 16: Van't Hoff plot for Ac[Pro(4S)N$_3$]OCH$_3$ **14** (empty circles) and Ac[Pro(4R)N$_3$]OCH$_3$ **15** (full circles).*

Finally, the temperature dependence of the equilibrium constant K was determined. Figure 16 shows the van't Hoff plot of Ac[Pro(4S)N$_3$]OCH$_3$ **14** and

Ac[Pro(4R)N$_3$]OCH$_3$ **15**. The *s-trans*:*s-cis* equilibrium of **15** shows a slight dependence on temperature, approaching a 1:1 *s-cis*:*s-trans* ratio with increasing temperature (figure 16). Interestingly, the *s-trans*:*s-cis* equilibrium of **14** is independent of the temperature.

2.7 Summary

In conclusion, by analysis of a variety of acetylated 4-azidoproline derivatives using NMR spectroscopy, X-ray diffraction, FT-IR spectroscopy and *ab initio* calculations, it was shown that a *gauche* effect between the azido-group in the 4-position and the amide function dominates the conformation of acetylated azidoproline derivatives. This azide *gauche* effect was confirmed by *ab initio* calculations of 1,2 disubstituted ethanes and of 4-azidoproline derivatives. Furthermore, the *s-cis*:*s-trans* ratio of a variety of diastereomeric 4-azidoproline derivatives was determined and a higher preference for the *s-trans* conformation in (4R)-azidoproline methyl ester derivatives was found. By analysis of the conformation in the solid state, FT-IR measurements and *ab inito* calculations, it was shown that the reason for the preference is likely to be an "n-π*"-interaction between the oxygen of the N-terminal amide with the carbonyl carbon of the methyl ester. The kinetics of the interconversion between the *s-cis* and the *s-trans* conformation of the disastereomeric acetylated 4-azidoproline methyl esters were studied by EXSY NMR. These studies demonstrate that the isomerization from *s-cis* to *s-trans* is equally fast in both diastereoisomers, while the isomerization from *s-trans* to *s-cis* was slower in the case of the (4R)-configured acetylated azidoproline methyl ester.

3 The Cyclotriproline Scaffold

3.1 Background

Previous studies demonstrated that diketopiperazine-based two-armed receptors with tripeptides as recognition elements (scheme 9, top) are able to bind peptides with high affinity and sequence selectivity in organic and aqueous media.[50,51,69,70] A scaffold which allows for the attachment of three recognition elements, can be expected to lead to receptors with even higher binding affinities since the possible number of interactions with the guest molecules is increased. We therefore envisaged extending the diketopiperazine scaffold by another proline unit to a cyclotriproline derived scaffold. (scheme 9, bottom).
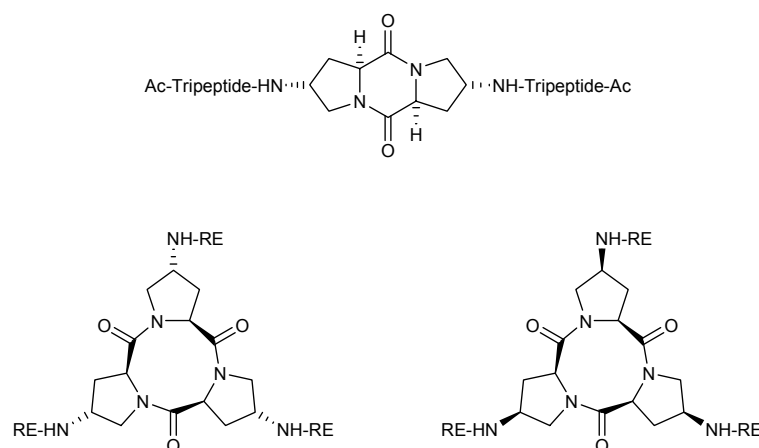
Scheme 9: Schematic drawings of the diketopiperazine receptor class (top) and the two possible diastereomeric cyclotriproline receptors (bottom); RE= recognition element.

Since the configuration at C(4) had proven to have a significant effect on the conformation and binding properties of the diketopiperazine receptors,[51] conformational searches were initially performed, using MacroModel 7.1[71,72] (figure 17). As the recognition elements will be attached by amide linkages (as in the case of the diketopiperazine based receptors), the two diastereoisomers cyclotri[(4S)-acetamidoproline] **33** and cyclotri[(4R)-acetamidoproline] **32** were used as minimal receptor models in these computational studies. The calculations used the

OPLS-AA[73] force field and the GB/SA[74] model for chloroform. Searching was performed using the MCMM method in blocks of 20'000 steps.
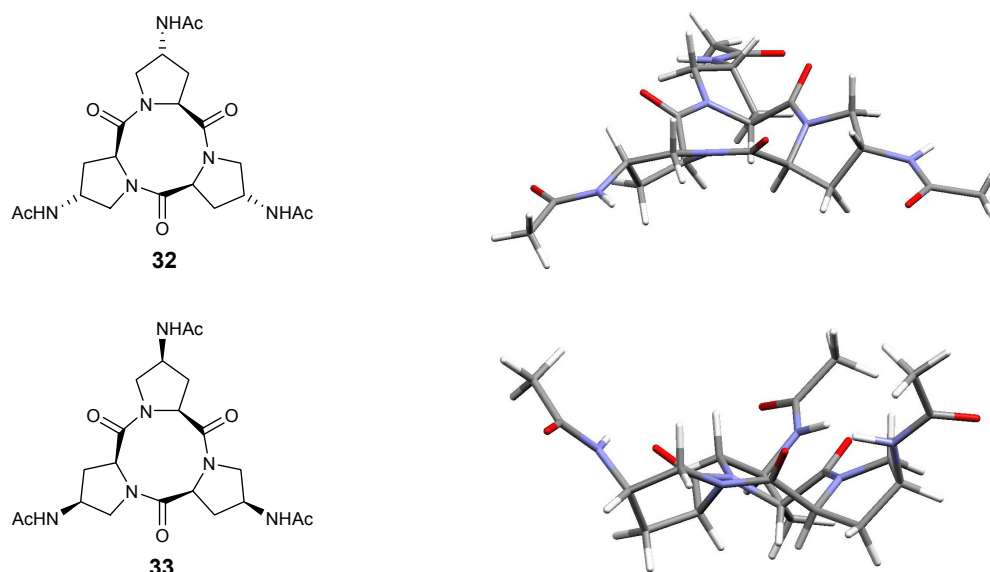
Figure 17: Lowest energy conformations of cyclotri[(4R)-acetamidoproline] (top) and cyclotri[(4S)-acetamidoproline] (bottom) as calculated by MacroModel 7.1.

In the case of the (4R)-derivative **32** (figure 17, top), the conformational searches yielded a flat, star-like arrangement of the acetamides, which occupy the pseudo-equatorial positions of the pyrrolidine rings as the lowest energy conformation. For a possible receptor, this arrangement is not favorable, as the recognition elements would be pointing away from each other. In the lowest energy conformation found for the (4S)-derivative **33** (figure 17, bottom), however, the acetamides occupy the pseudo-axial positions of the pyrrolidine rings, leading to a bowl-shaped structure. This creates a pocket which should be favorable for the enclosure of guest molecules.[51]
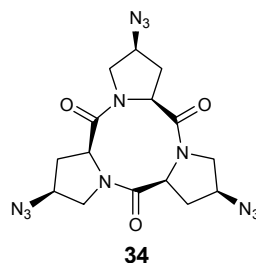
Figure 18: Cyclotri[(4S)-azidoproline] **34**.

Taking these considerations into account, cyclotri[(4S)-azidoproline] **34** (figure 18) was envisioned as a precursor for synthetic tripodal receptors.

3.2 Synthesis of the Cyclotriproline Scaffold

The logical precursor to cyclotri[(4S)-azidoproline] **34** is the linear tripeptide. The synthesis of linear tri[(4S)-azidoproline] **36** (scheme 10) commences from Boc[Pro(4S)N$_3$]$_2$OCH$_3$ **31**.

a) i) NaOH (2 eq), H$_2$O, THF, MeOH, r.t., 2h; ii) **30** (1.5 eq), HATU (3 eq), ^{i}Pr$_2$NEt (9 eq), DMF, r.t., 95%; e) i) NaOH (4 eq), H$_2$O, THF, MeOH, r.t., 2h; ii) 4M HCl in dioxane, r.t., 30 min., 90%.
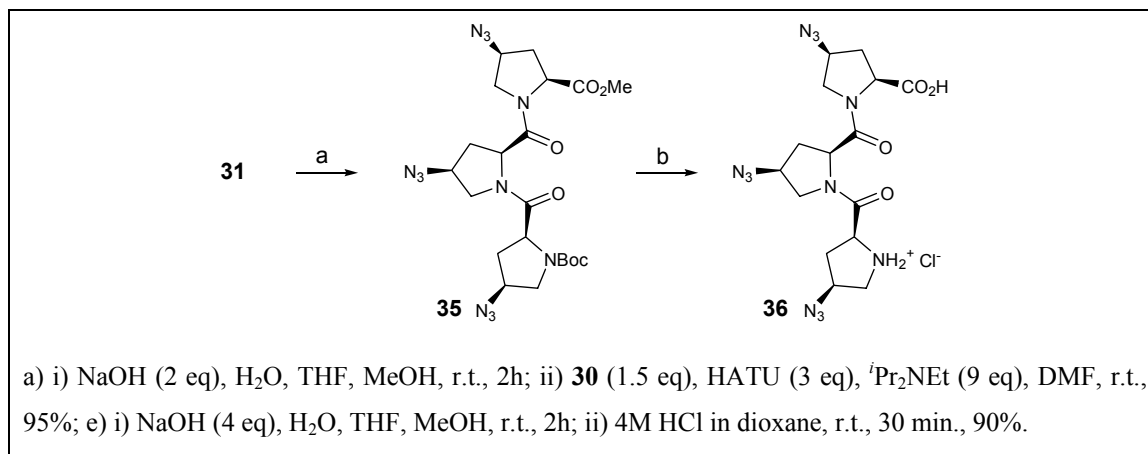
Scheme 10: Synthesis of tri[(4S)-azidoproline] 36.

The methyl ester **31** was saponified and the resulting acid coupled with the hydrochloride salt **30**, using HATU as the coupling reagent. The resulting methyl ester **35** was again saponified and the Boc-group was removed using 4M HCl in dioxane, which afforded the hydrochloride salt **36**.

a) pyridine, 1-4 days, 65°C; b) coupling reagent, ^{i}Pr$_2$NEt (9 eq), DMF, 2h, r.t.
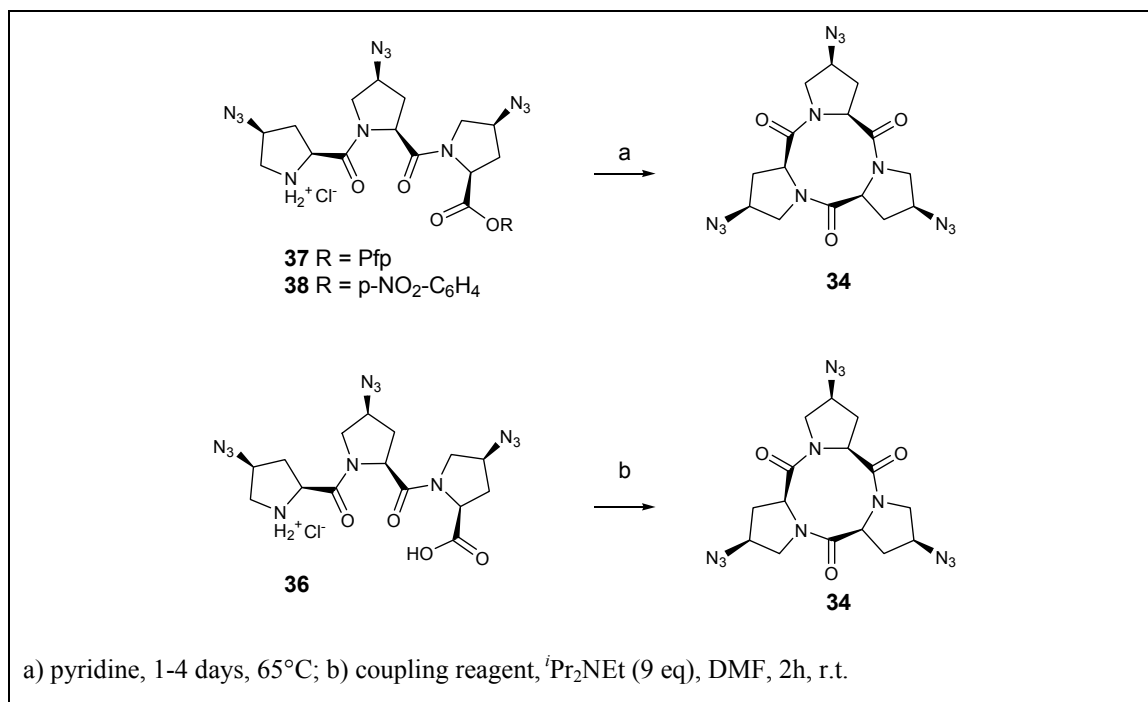
Scheme 11: Cyclization methods tested for cyclotriproline.

For the cyclization, a series of different reaction conditions were examined. Initially, the cyclization was attempted following the classical approach as used by Rothe (scheme 11, top);[75] an active ester derivative of the tripeptide was added to pyridine over the course of 16 hours by syringe-pump to a final peptide concentration of 1mM. Pyridine acted both as solvent and base. After 96 hours reaction time at 65°C, 40% of the cyclized product was isolated (table 14, entries 1 and 2).

Table 14: Cyclization conditions and yields for cyclotri[(4S)-azidoproline] 34.

Entry	Reactant	Conditions	Yield
1	**37**	pyridine, 1d, 65°C[a]	11 %
2	**38**	pyridine, 4d, 65°C	40 %
3	**36**	TBTU[b], 2h, r.t.,	31 %
4	**36**	PyBop, 2h, r.t.	38 %
5	**36**	HATU, 2h, r.t.	74 %

a: Final peptide concentration: 1mM; b: Final peptide concentration: 8 mM.

To optimize the reaction conditions, the cyclization was attempted by addition of a DMF solution of the hydrochloride salt **36** by syringe-pump during 1 hour to a solution of DMF with different coupling reagents and Hünig's base to a final peptide concentration of 8 mM (scheme 11, bottom). Under these conditions, the reaction was complete after 2 hours at room temperature. For TBTU and PyBOP, the yields were comparable to the yield obtained by addition of the C-terminally activated peptide to pyridine (table 14, entries 3 and 4). Using HATU as coupling reagent, the product was isolated in 74% yield even on a 1g scale.

a) coupling reagent (3 eq), ^{i}Pr$_2$NEt (9 eq), DMF, 2h, r.t.
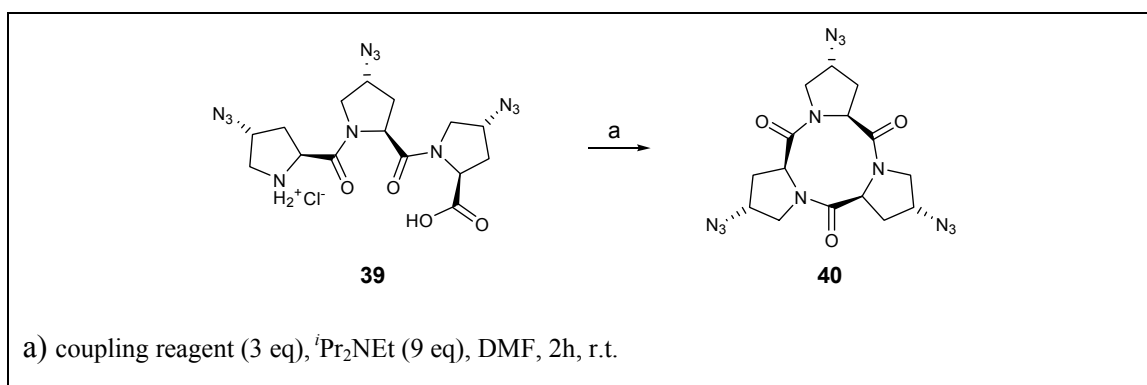
Scheme 12: Cyclization of tri[(4R)-azidoproline] 39.

The diastereomeric tripeptide, tri[(4R)-azidoproline] **39** was synthesized analogously to **36** and was also tested in cyclization experiments (scheme 12).

*Table 15: Cyclization conditions and yield for the cyclization of **16**.*

Entry	Conditions	Yield
1	TBTU, 2h, r.t.[a]	< 10 %
2	PyBop, 2h, r.t.[a]	< 15 %
3	HATU, 2h, r.t.[a]	< 15 %

a: Final peptide concentration: 8 mM.

Under identical conditions the cyclization yields of tri[(4R)-azidoproline] **39** were significantly lower than the yields obtained with the diastereomeric tripeptide **36** (table 15). Using HATU and PyBOP as coupling reagents (table 15, entries 2 and 3) less than 15% yield was obtained, using TBTU (table 15, entry 1) the yield was even less than 10%. The low yields obtained for the cyclization of **39** can be explained by the higher preference for the *s-trans* conformation in (4R)-azidoproline derivatives as described in the previous chapter.

3.3 Global reduction of the azides to amines followed by acetylation

To allow for the attachment of recognition elements to the cyclotriproline scaffold, the azides were reduced to amines. The reduction of the azides was achieved both through hydrogenation with palladium on activated charcoal as a heterogeneous catalyst, as well as by Staudinger reduction, using trimethyl phosphine and water (scheme 13).

a) Pd/C, H_2, MeOH/THF (3/1), r.t, 1h, quant.; b) $P(CH_3)_3$ in THF (2M), H_2O, 15 min., r.t., quant.; c) Ac_2O, NEt_3, CH_2Cl_2, 90%.
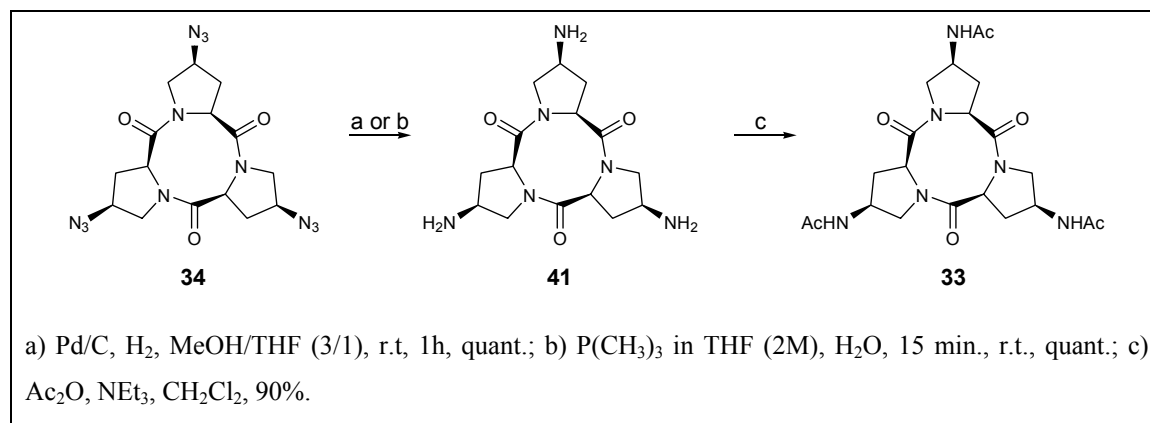
*Scheme 13: Reduction of the azide groups and acetylation of cyclotri [(4S)-azidoproline]**34**.*

Acetylation of the amines using acetic anhydride in the presence of triethylamine, yielded cyclotri[(4*S*)-acetamido proline] **33**, which served as a minimal receptor model for conformational analysis.

3.4 Structural analysis of cyclotri[(4*S*)-azidoproline] 34

Single crystals suitable for X-ray diffraction of cyclotri[(4*S*)-azidoproline] **34** were obtained by crystallization from chloroform.
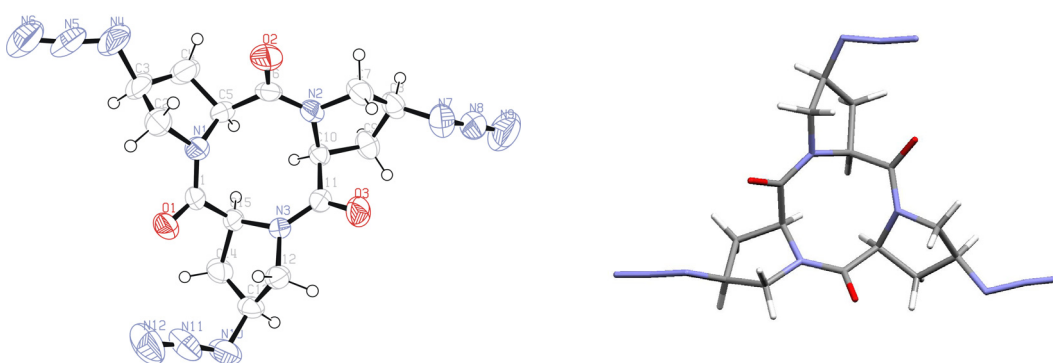
Figure 19: X-ray structure of cyclotri [(4S)-azidoproline] 34, ORTEP view (right) and capped stick view (left).

By X-ray diffraction, the unit cell was found to be orthorhombic, with four molecules per cell. Figure 19 shows the structure of cyclotri[(4*S*)-azidoproline] **34** in the crystalline state. The C_3-symmetry is only slightly distorted; one of the three pyrrolidine rings of the azidoprolines is in a perfect N-*exo*-conformation, the second shows a slightly distorted N-*exo*-conformation and the third is in a C^δ-*endo*-conformation. The azides are in a neutral position, which cannot be determined as pseudo-equatorial or pseudo-axial.

*Table 16: Comparison of coupling constants found for **34** and coupling constants calculated.*

Entry	Protons	Coupling constant found[a] [Hz ± 0.5]	Coupling constant expected for N-*exo*[b] [Hz ± 0.5]	Coupling constant exp. for distorted N-*exo*[b] [Hz ± 0.5]
1	H^α-H^β	8.2	8.7	8.9
2	H^α-$H^{\beta'}$	2.1	1.8	2.0
3	H^β-H^γ	10.0	9.9	9.8
4	$H^{\beta'}$-H^γ	5.2	4.1	5.7
5	H^γ-H^δ	8.1	9.0	8.0
6	H^γ-$H^{\delta'}$	8.1	7.8	9.4

a) Coupling constants as determined by ^{1}H-NMR spectroscopy in CDCl$_3$ at 295K. b) N-*exo* and distorted N-*exo* conformation as found in the crystal structure.

To analyze whether the conformation found in the crystalline state also occurs in solution, NMR studies were performed. The NMR spectrum of cyclotri[(4*S*)-azidoproline] in CDCl$_3$ shows a six-spin system for the pyrrolidine ring protons, indicating that on the average time scale of the NMR measurement, a C$_3$-symmetric conformation is present. The vicinal coupling constants of **34** in chloroform were compared to values expected for the torsion angles found in the crystal structure. These expected vicinal coupling constants were calculated based on the Karplus equation (see chapter 2.4),[53,54] using parameters developed for cyclotriproline[55] (table 16). The vicinal coupling constants found for the H^α-H^β, H^α-$H^{\beta'}$, and the H^β-H^γ coupling (table 16, entries 1-3) match the expected values within the margin of error. The values found for the $H^{\beta'}$-H^γ, the H^γ-H^δ and the H^γ-$H^{\delta'}$ coupling lie between the values expected for the N-*exo*-conformation and the distorted N-*exo*-conformation found in the crystal structure (table 16, entries 4-6). This indicates that the conformation in solution is likely to be a dynamic equilibrium between different forms of the N-*exo*-conformation found in the crystal structure.

In conclusion, the conformations determined by interpretation of the vicinal coupling constants of the ^{1}H-NMR in CDCl$_3$ and the conformation found in the crystal structure are in agreement. Furthermore, unlike in the acetylated monomers studied in chapter 2.4, in cyclotri[(4*S*)-azidoproline] **34** the azido-groups are not in the pseudo-axial conformation and assume an *anti*-conformation relative to the amide bond. This is probably due to the conformation of the nine-membered inner ring, which dominates the

conformation of the pyrrolidine rings, and thereby overrides the *gauche* effect observed for the linear 4-azidoproline derivatives (see chapters 2.4 and 2.5).

3.5 Structural analysis of cyclotri[(4*S*)-acetamidoproline] 33

Since receptors based on the cyclotriproline scaffold are designed to have amide linkages to the recognition elements, the conformation of the (4*S*)-acetamide derivative **33** was studied as a minimal receptor fragment. As in the case of the azide-derivative **34**, the NMR spectrum of **33** in CDCl$_3$ shows a six-spin system for the pyrrolidine ring protons, indicating that on the average time scale of the NMR measurement, a C$_3$-symmetric conformation is present.

Table 17: Coupling constants of cyclotri[(4S)-acetamido proline] 33.

Entry	^3J(H,H)	Coupling Constant [Hz ± 0.5]	Coupling Constant expected [Hz ± 0.5][a]
1	H$^\alpha$-H$^\beta$	7.4	7.6
2	H$^\alpha$-H$^{\beta'}$	< 1	1.4
3	H$^\beta$-H$^\gamma$	9.1	7.8
4	H$^{\beta'}$-H$^\gamma$	< 1	1.4
5	H$^\gamma$-H$^\delta$	8.7	9.3
6	H$^\gamma$-H$^{\delta'}$	4.1	2.3
7	H^N-H$^\gamma$	9.5	n.d.

a From calculating the vicinal coupling constant using the Karplus equation and the dihedral angles found in the MacroModel calculation described in chapter 3.1.

The vicinal coupling constants of the acetamide derivative **33** (table 17) differ from the vicinal coupling constants of azide derivative **34** (see table 16), indicating a change in conformation. The main difference lies in the coupling constants H$^\alpha$-H$^{\beta'}$ and especially H$^{\beta'}$-H$^\gamma$ (table 17, entries 2 and 4), which are less than 1 Hz, corresponding to a dihedral angle between these protons of approximately 90°. The two 90° torsion angles between H$^\alpha$ and H$^{\beta'}$, and H$^{\beta'}$ and H$^\gamma$ can only be realized in a conformation, in which the acetamide-groups are in the pseudo-axial positions. The vicinal coupling constants found for cyclotri[(4*S*)-acetamido proline] **33** are in agreement with both a

C^{β}-*exo*-conformation and a C^{α}-endo-conformation, as these conformations differ only slightly in the torsion angles.

The C^{β}-*exo*-conformation was also found to be the lowest energy conformation of cyclotri[(4*S*)-acetamido proline] **33** in the calculations using MacroModel (see figure 17, bottom). The coupling constants found for the H^{α}-$H^{\beta'}$ and the $H^{\beta'}$-H^{γ} coupling are in good agreement with the ones expected for the lowest energy conformation by the Karplus[53,54] equation using parameters optimized for cyclotriproline.[55] The values expected for the coupling constants of H^{α}-H^{β}, H^{α}-$H^{\beta'}$, $H^{\beta'}$-H^{γ} and H^{γ}-H^{δ} (table 17, entries 1, 2, 4 and 5) match the values found by ^{1}H-NMR within the margin of error. This indicates that the conformation found in the conformational searches is a good representation of the conformation in chloroform solution.

The lowest energy conformation found by conformational searches suggests a possible explanation for the difference in conformation found between cyclotri[(4*S*)-azidoproline] **34**, in which the C^{γ}-substituents (the azido-groups) are in neutral positions and the pyrrolidine ring is in a N-*exo*-conformation, and cyclotri[(4*S*)-acetamido proline] **33**, in which the C^{γ}-substituents (the acetamide-groups) are in a pseudo-axial conformation and the pyrrolidine ring systems are in a C^{β}-*exo*-conformation (figure 20).
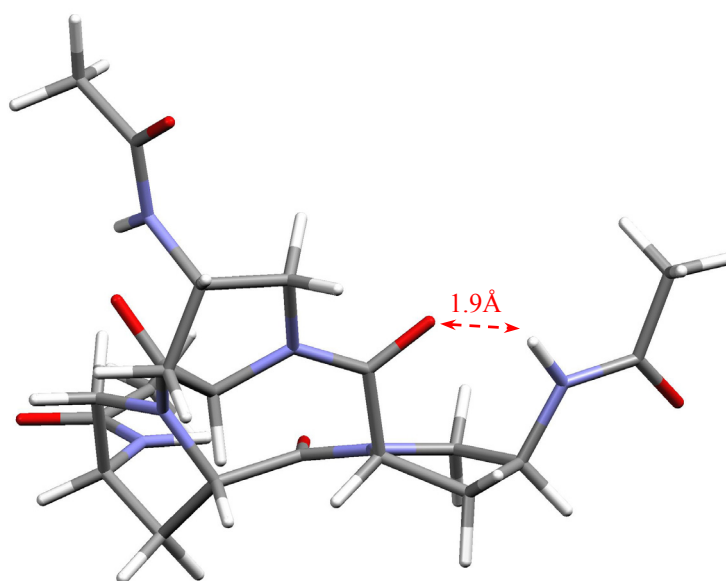

*Figure 20: Lowest energy conformation of [4S-acetamidoproline] **33** as calculated by MacroModel 7.1, possible hydrogen bond shown in red.*

The distance (1.9Å) and orientation of the N-H bonds of the acetamide relative to the carbonyl groups of the cyclic backbone found in the lowest energy conformation of cyclotri[(4*S*)-acetamido proline] **33**, suggest that the conformation of the pyrrolidine rings is stabilized by intramolecular hydrogen bonding (figure 20). This hydrogen bond could overrule the conformational preference induced by the nine-membered inner ring, leading to the conformation observed.

To test whether these hydrogen bonds are also present in the conformation found in solution by NMR spectroscopy, NOE spectroscopy was performed.
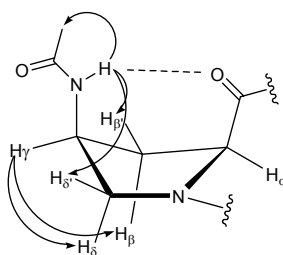
Scheme 14: NOE contacts in cyclotri [(4S)-acetamido proline] 33, shown for one of the pyrrolidine rings. The arrows indicate NOE contacts, while the dashed line indicates a possible hydrogen bridge.

Scheme 14 shows the intense NOE contacts found in 2D NOE spectroscopy of cyclotri[(4*S*)-acetamido proline] **33**. NOE contacts of the N-H to the δ'- and β'-protons are detected, while no NOE contacts to the δ and β protons and only a weak NOE contact to the γ-proton is found, suggesting that rotation around the C^γ-N^{Ac} bond is restricted and that the N-H bond is orientated towards the inner 9-membered ring. This is further supported by the H^N-H^γ coupling constant of 9.5 Hz (table 17, entry 7), indicating a *trans* geometry of the N-H and C^γ-H^γ bond. This leads to a conformation in which the N-H bond is orientated towards the carbonyl of the central, nine-membered ring, bringing them in a conformation, which supports the existence of a possible hydrogen bond.

In this conformation, the acetamides occupy the pseudo-axial conformation, giving the molecule a bowl-shaped form, opening a cavity in between the recognition elements in which host molecules can interact with the receptor. Such a conformation has been favorable in the case of the diketopiperazine receptors developed previously.[50,51,69,70]

3.6 Summary

Based on computational models of the two diastereoisomers of cyclotri[4-acetamido proline], cyclotri[(4*S*)-azidoproline] **34** was envisioned as the precursor to tripodal molecular receptors. **34** was synthesized and its conformation was analyzed using NMR spectroscopy. Cyclotri[(4*S*)-acetamidoproline] **33** was synthesized as a minimal receptor fragment to analyze the conformation of the pyrrolidine rings in a receptor. The conformational analysis suggests that a tripodal molecular scaffold based on cyclotri[(4*S*)-aminoproline] should be a good molecular template for synthetic receptors.

4 Binding Studies of a Cyclotriproline-Based Peptide Receptor

4.1 Synthesis of cyclotriproline based peptide receptors

Based on the finding that the conformation of the (4S)-amide-substituted cyclotriproline (see chapter 3.5) is likely to be suitable as a scaffold for a tripodal receptor, a model receptor was synthesized. Previous studies in the Wennemers group showed that diketopiperazine receptors functionalized with acid-rich peptides as recognition elements recognize arginine-rich sequences selectively in aqueous buffers.[70] Thus, an analogous three-armed receptor was designed. Dye-marked tyrosine[50] was chosen as the first amino acid of the tripeptidic recognition element, as it allows for visual detection of binding in on-bead combinatorial binding assays. Aspartates were chosen as second and third amino acid in the recognition elements, in order to introduce acidic functional groups.

The cyclotriproline based peptide receptors were synthesized by coupling the Disperse Red-marked Boc-Tyr(DR)-OH[50] to the primary amines of cyclotri[(4S)-aminoproline] **41**. HATU in DMF with Hünig's base was used as coupling reagent in the first coupling step. After removal of the Boc-protecting group by treatment with 4M HCl in dioxane, the resulting hydrochloride salt was coupled in CH_2Cl_2 with Fmoc-Asp(^{t}Bu)-OH using EDC as coupling reagent to yield the dipeptide modified cyclotriproline **43**. After Fmoc-deprotection using diethylamine, another Fmoc-Asp(^{t}Bu)-OH was coupled as the last amino acid of the receptor "arms".
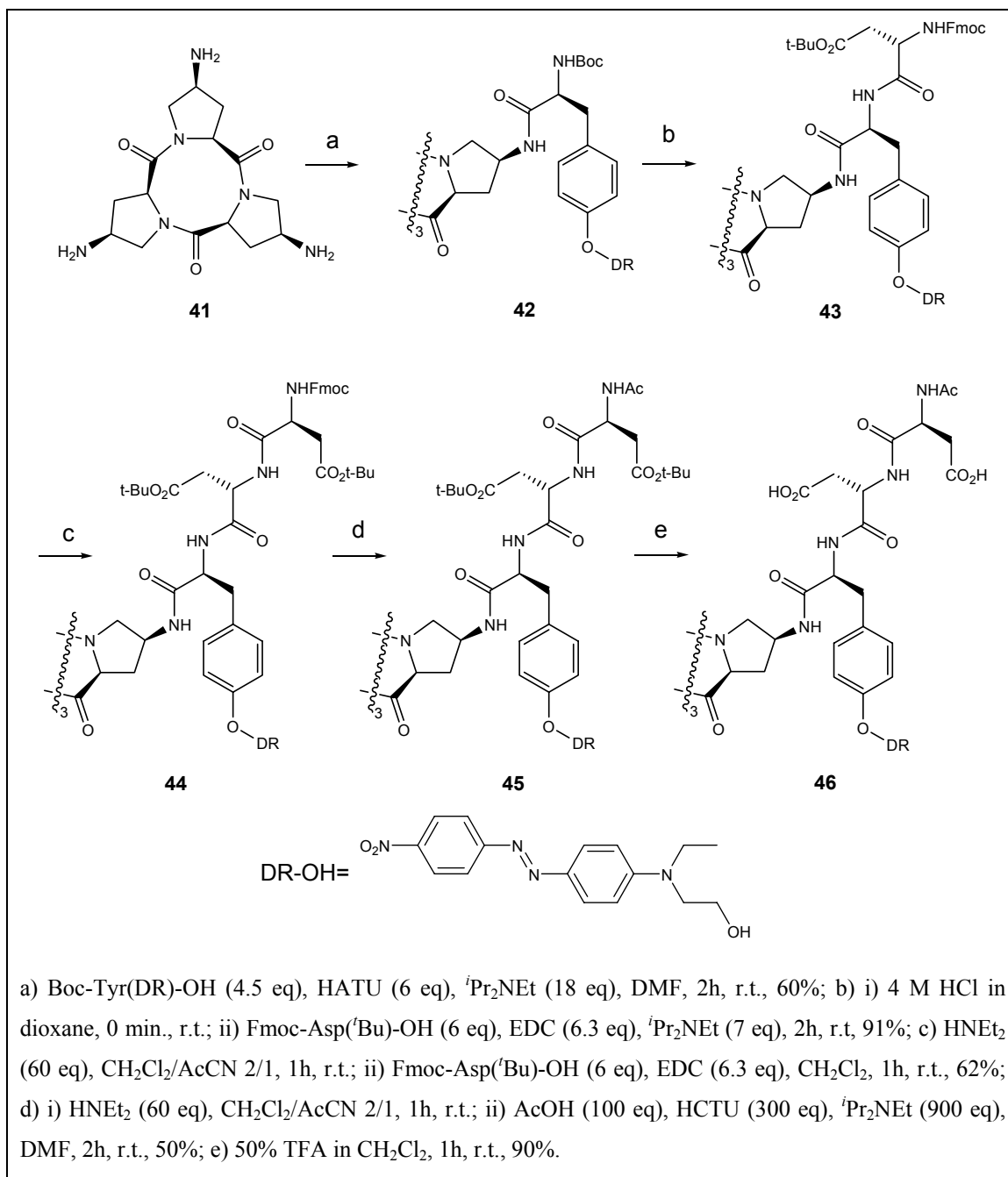
Scheme 15: Synthesis of the cyclotriproline based peptide receptors.

After removal of the Fmoc-group, the N-termini of the peptides were acetylated to yield **45**. The side-chain protecting groups were removed using 50% TFA in CH_2Cl_2 to yield the final receptor **46** (scheme 15).

4.2 Combinatorial Screenings

To test the binding properties of the cyclotriproline based peptide receptor **46**, combinatorial on-bead assays in aqueous buffer against an encoded [76,77] split-and-mix[78,79] library of tripeptides[80] were performed. In the library, 31 D- and L-amino acids were used in each position of the combinatorially varied tripeptide, leading to a maximum of 29'791 different tripeptide sequences. To allow for further cleavage studies the tripeptide was flanked by nitrotyrosine on the N-terminus and by an anthranilic acid functionalized lysine on the C-terminus (scheme 16).
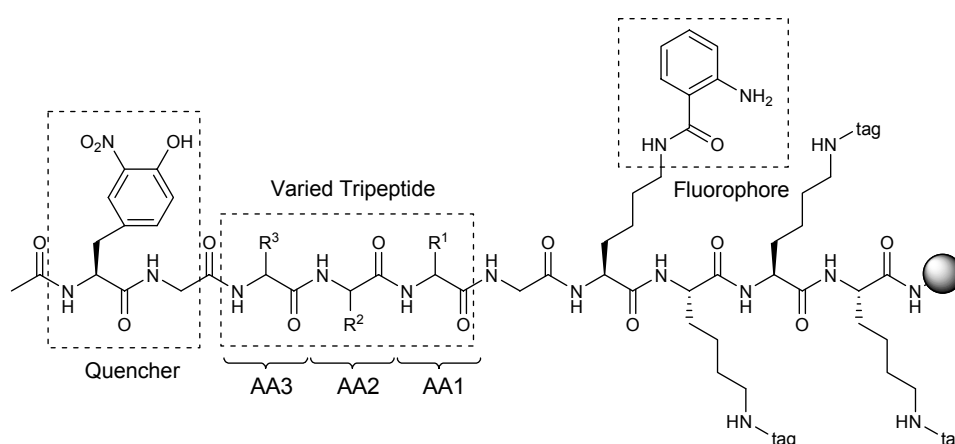
Scheme 16: General structure of the combinatorial tripeptide library used.

Each amino acid in the library was encoded with a set of "tags", which may later be used to identify the tripeptide sequence.[76,77] The "tags" of the library consist of chloro-phenol ethers of long chain diols, which can be detected in their silylated form using a gas chromatograph with an electron capture detector (ECD). The tags have different retention times, due to different chain lengths and substitution patterns. The amino acids are encoded in a binary fashion, with each tag representing one digit. Five tags together code for one position of the library.

For the screenings, 10 mM Tris·HCl buffer at pH 7.2, 10 mM NaHCO$_3$ buffer at pH 8.5 and 10 mM NaOH at pH 12 were used. Since the side chain carboxylic acid of aspartate has a pK$_a$ of 3.9, screenings at acidic pH were not performed, as the carboxylates of the aspartates in the receptor arms would become at least partially protonated. The interaction between the receptor and the peptide is assumed to be at least in part based

upon electrostatic interactions, thus protonated, and therefore neutral, aspartate residues would not be favorable.

After 24 hours at room temperature, inspection of the beads under a visual light microscope showed that in 10 mM Tris·HCl buffer at pH 7.2 none of the beads had picked up the red color of the receptor **46** (figure 21a). In 10 mM NaHCO$_3$ buffer at pH 8.5 some of the beads had picked up the red color (figure 21b) of the dye-marked receptor **46**, indicating a binding interaction. The screening in 10 mM NaOH at pH 12.0 (figure 21c) also showed red beads.

*Figure 21: Screenings of the dye-marked receptor **46** in different buffers; a) 10 mM Tris·HCl buffer at pH 7.2 (left); b) 10 mM NaHCO$_3$ buffer at pH 8.5 (middle); c) 10 mM NaOH at pH 12.0 (right).*

Comparing the results of the screenings at pH 8.5 and 12.0 under the microscope, it was found that for the screenings at pH 8.5 most of the beads remained colorless (the slight yellow coloring of the beads is inherent of the library at basic pH), some show a slight hue of orange and a few are slightly red (approximately 1 in 150). At pH 12, again most beads remained colorless, but here, the beads that did pick up the color of the receptor **46**, are dark red (approximately 1 in 150), rather than just orange. This indicates that the binding of receptor **46** at pH 12 is probably more specific than at pH 8.5.

To elucidate the tripeptide sequence on the beads which picked up the color of the receptor, several of the red beads were isolated and the "tags" of each bead were cleaved off separately and analyzed by ECD-GC.

*Table 18: Percentage of L- and D-arginine in the sequences found in the screenings of **46**.*

Entry	Position	10 mM NaHCO$_3$ buffer pH 8.5[a]			10 mM NaOH at pH 12.0[b]		
		L-Arg	D-Arg	Total	L-Arg	D-Arg	Total
1	AA1	28%	49%	77%	18%	15%	33%
2	AA2	23%	40%	63%	33%	39%	72%
3	AA3	28%	35%	63%	42%	36%	78%

a) a total of 43 sequences were analyzed; b) a total of 33 sequences were analyzed.

Previous results had shown that receptors based on the diketopiperazine scaffold with tripeptidic recognition elements bind arginine-rich sequences in basic aqueous buffer.[70] Based on these results it was expected that the cyclotriproline based receptor would also bind arginine-rich sequences, which it does indeed (table 18). Furthermore, depending on the buffer and pH used, slight differences in selectivity were found. In 10 mM NaOH at pH 12.0, receptor **46** binds mainly peptides with sequences containing an arginine as the second and third amino acid, indiscriminate of stereochemistry (table 18, entries 2 and 3). In 10 mM NaHCO$_3$ buffer pH at 8.5 on the other hand, receptor **46** binds peptides with sequences containing almost equal frequencies of arginine in all three positions (table 18, entries 1-3). Intriguingly, for positions 1 and 2 an almost 1:2 ratio between L-and D-arginine (table 18, entries 1 and 2) is found.

Table 19: Distribution of sequences containing at least two arginines.

Entry	Sequence[a]	NaHCO$_3$ buffer pH 8.5[b]	NaOH pH 12.0[c]
1	Arg-Arg-X	12 %	51 %[d]
2	X-Arg-Arg	28 %	18 %
3	Arg-X-Arg	37 %	21 %
4	Arg-Arg-Arg	12 %	3 %
		Total: 89%[e]	Total: 94%[e]

a) Arg stands for both L- and D-arginine, X stands for any other amino acid; b) a total of 43 sequences were analyzed; c) a total of 33 sequences were analyzed; d) 70% of the residues found in the X position were hydrophobic amino acids; e) the remaining sequences contained one arginine residue.

Most sequences found for receptor **46**, both in 10 mM NaHCO$_3$ buffer at pH 8.5 and in 10 mM NaOH at pH 12.0, contain at least two arginine residues (table 19, totals).

Nonetheless, the pH influences the distribution of sequences found. In 10 mM $NaHCO_3$ buffer at pH 8.5 receptor **46** selects for peptides with sequences with an Arg-X-Arg motif, in which the two arginines are flanking another, random, amino acid (table 19, entry 3). Likewise, with nearly equal selectivity, sequences with an X-Arg-Arg motif were found, in which a random amino acid is followed by two arginines (table 19, entry 2). In contrast, in 10 mM NaOH at pH 12.0, receptor **46** shows a preference for peptides with an Arg-Arg-X motif, in which two arginines are followed by a random amino acid. This sequence was not favored in 10 mM $NaHCO_3$ buffer at pH 8.5 (table 19, entry 1). While the overall selectivity for sequences with at least two arginines was equal for both screening conditions (table 19, totals), the selectivity for a triple arginine sequence was slightly higher in 10 mM $NaHCO_3$ buffer at pH 8.5 (table 19, entry 4). The differences in selectivity found for the different buffers and pH, indicate that small changes can influence the binding.

In summary, the combinatorial on-bead screenings show that receptor **46** binds to arginine-rich sequences, both in 10 mM NaOH at pH 12.0, as well as in 10 mM $NaHCO_3$ buffer at pH 8.5. In 10 mM NaOH at pH 12.0, the screenings indicate that receptor **46** has a preference for sequences containing an Arg-Arg-X motif, where X is a random amino acid. In 10 mM $NaHCO_3$ buffer at pH 8.5, receptor **46** displays selectivity for arginines in each of the three positions, and also shows binding to a triple arginine sequence.

4.3 Determination of Binding Affinities by Isothermal Titration Calorimetry

To analyze the binding affinity of receptor **46** to a specific target sequence, isothermal titration calorimetry (ITC) was performed. During ITC the enthalpy ΔH is measured while the ligand is titrated to the receptor. The enthalpy released per injection changes over the course of the titration, as the receptor molecules become saturated with peptidic guest molecules. From the change in enthalpy per injection in dependence of the molar ratio of receptor to ligand, the stoichiometry of the complex, the enthalpy ΔH, the binding constant K, and from it the free energy, ΔG, of the binding is determined.

The combinatorial screening indicated that receptor **46** is able to bind to arginine-rich sequences (see chapter 4.1). In 10mM $NaHCO_3$-buffer at pH 8.5, receptor **46** binds to sequences with at least two arginine residues, as well as to triple arginine. To get an estimate of the binding energy, the peptide Ac-Arg-Arg-Arg-NH-propyl was used as guest molecule. Previous studies with diketopiperazine-based receptors have shown that, even though other sequences were also found in the screening, the binding affinity was highest with a triple arginine sequence.[81] An N-acetylated peptide with a propylamide C-terminus was used since the tripeptides in the library used are part of longer peptides, and therefore do not bear a free N- or C-terminus either.

Two ITC measurements were performed, with receptor concentrations of 150 μM and 175 μM, respectively, at 25° C in 10mM $NaHCO_3$ buffer at pH 8.0. A solution of the target peptide in 10mM $NaHCO_3$ buffer at pH 8.0 was titrated to the receptor in aliquots of 5 μL. A total of 59 injections were made, at five minute intervals. As the peptide was titrated to the receptor, the ratio of receptor to peptide changed from 8:1 to 1:8 in the measurement performed with a 150 μM receptor concentration, and from 10:1 to 1:6.5 in the measurement performed with 175 μM receptor concentration.
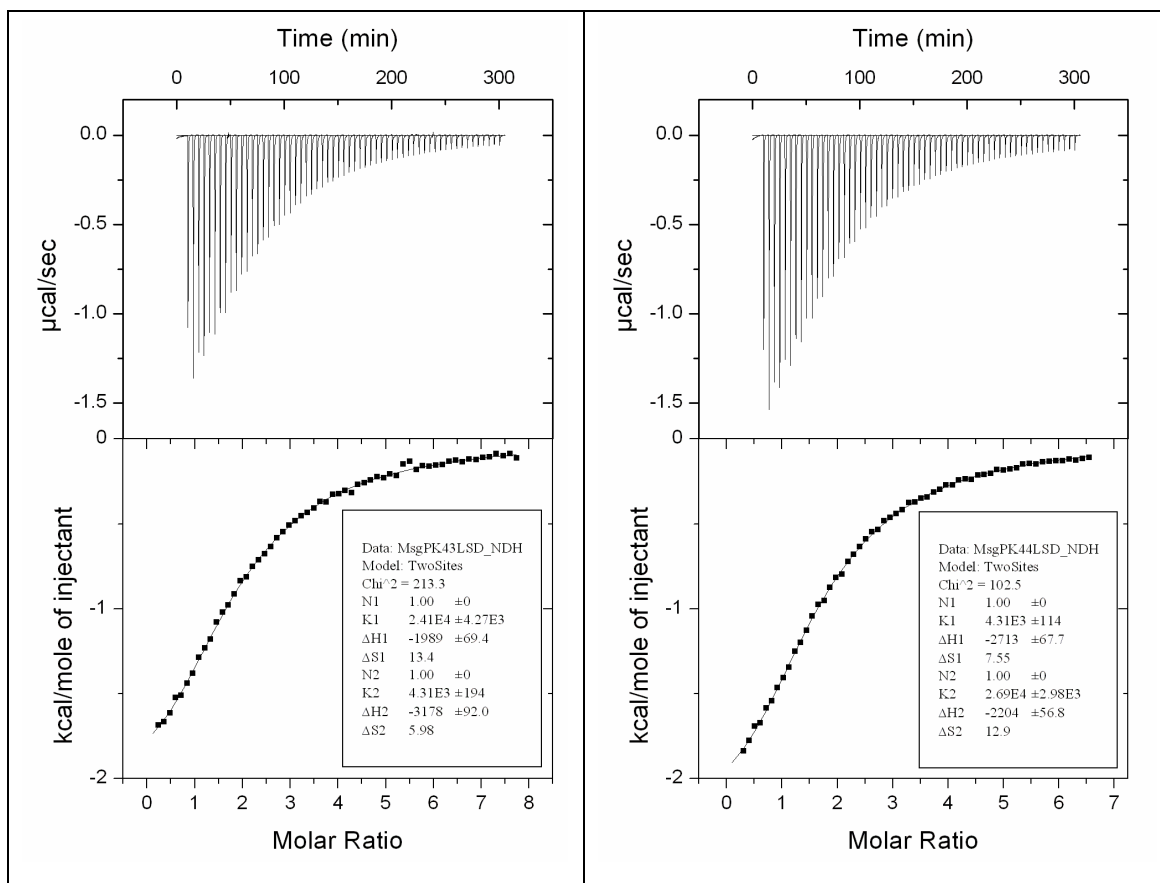
Figure 22: ITC titration curves and fits of the curves of the change of ΔH per injection. Left measurement 1, right measurement 2.

In an ITC measurement, the area underneath the curve recorded is equal to the ΔH per injection. For the interpretation of the data measured, ΔH per injection is plotted against the molar ratio of receptor to ligand (figure 22). The titration curve for ΔH recorded for the titration of the ligand to a buffer solution without receptor is subtracted, eliminating the heat of dilution of the peptide. The data is fitted using a method of least squares, in which the complex stoichiometry, ΔH of the complex formation and the binding constant are varied.[82]

The best fit for the data recorded showed a 2:1 receptor:peptide complex. The mathematical model used assumes a receptor with two independent binding sites, which bind one substrate per binding site. The fit therefore provides two different binding constants for the two different binding sites as well as ΔH and TΔS values for each complexation step.[82]

*Table   20:   Thermodynamic   data   determined   for   the   binding   of   **46**   with   the   peptide*
Ac-Arg-Arg-Arg-NH-propyl by ITC measurements.

Entry	Thermodynamic Parameter[a]	Value found[b]
1	ΔG_1 [kcal/mol]	-6.0 ± 0.1
2	ΔG_2 [kcal/mol]	-4.9 ± 0.1
3	ΔH_1 [kcal/mol]	-2.2 ± 0.1
4	ΔH_2 [kcal/mol]	-2.9 ± 0.1
5	$T\Delta S_1$ [kcal/mol]	3.9 ± 0.1
6	$T\Delta S_2$ [kcal/mol]	2.0 ± 0.1

a) The subscripts of the values denote the two different binding events, b) averaged values of two measurements, using 150μM and 175μM receptor solutions.

The two measurements are in close agreement, showing that the binding is a reproducible event. Table 20 shows the averaged values for the thermodynamic parameters determined. The binding energy for the first binding (table 20, entry 1), ΔG is averaged to be -6.0±0.1 kcal mol^{-1} (K_a = 25500±500 M^{-1}). The second binding energy (table 20, entry 2) is averaged to be -4.9±0.1 kcal mol^{-1} (K_a = 4300±500 M^{-1}). The other thermodynamic data indicate, that the binding is favored both enthalpically (table 20, entries 3 and 4) and entropically (table 20, entries 5 and 6). As the binding constants are relatively close to each other, the least square fit is equally good when the chronological order of binding is reversed, thus the first binding might be the second in time and vice versa.

4.4 Summary

The dye–marked tripodal receptor **46** was screened in combinatorial on-bead assays at different pH against an encoded split-and-mix library of approximately 29'000 different tripeptides. The acid-rich receptor **46** shows selectivity for arginine-rich sequences. ITC measurements show that receptor **46** binds peptides in a 2:1 peptide:receptor stoichiometry, with binding affinities, ΔG, averaging at -6.0±0.1 kcal mol^{-1} and -4.9±0.1 kcal mol^{-1}.

5 Conclusions and Outlook

This thesis presents studies on the influence of the azido-substituent on the conformation of 4-azidoproline. An azide *gauche* effect was observed in several diastereomeric 4-azidoproline derivatives by conformational analysis using a combination of NMR-spectroscopy, X-ray diffraction, FT-IR-spectroscopy and *ab initio* calculations. This *gauche* effect dominates the conformation of both, (4*R*)- and (4*S*)-configured azidoproline derivatives. As a result, the pyrrolidine ring adopts a C^{γ}-*endo*-conformation in the case of the (4*S*)-configured derivatives and a C^{γ}-*exo*-conformation in the case of the (4*R*)-configured derivatives. Furthermore, in the comparison of the *s-cis/s-trans* equilibrium of acetylated 4-azidoproline derivatives, the (4*R*)-azidoproline methyl ester derivatives show a higher preference for the *s-trans* conformation than the (4*S*)-diastereoisomers. This *s-trans* preference of the (4*R*)-derivatives was rationalized by a stabilization of the *s-trans* conformation by an "n-π*"-interaction of the non-bonding electrons of the acetyl oxygen with the carbonyl carbon of the methyl ester. The kinetics of this equilibrium were studied and the individual rate constants and activation enthalpy and entropy were determined by EXSY NMR.

(4*S*)-azidoproline was then employed in the synthesis of a tripodal molecular scaffold for synthetic receptors. A model receptor with tripeptidic, acid-rich recognition elements was prepared and showed selective binding properties to arginine-rich peptides in combinatorial on-bead screenings. Isothermal titration calorimetry (ITC) studies revealed binding affinities, ΔG, in the range of -5 to -6 kcal mol^{-1} for a 2:1 peptide:receptor complex with the tripeptide Arg-Arg-Arg in aqueous media.

The azide *gauche* effect in general and the effect of the 4-azido substituent on the conformation of proline in particular, can be applied to the design of conformationally defined molecules. For instance, the stability of secondary structure elements, such as the polyproline II (ppII) helix, which is found in collagen, is dependent on the conformation of the amide bond. All amide bonds in a ppII helix are in the *s-trans* conformation. Thus, introduction of (4*R*)-azidoproline should increase the stability of the ppII helix due to its higher preference for the *s-trans* conformation. Furthermore, 4-azidoproline can not only be used as a structure directing element, but also allows for further modifications, for example, by reaction with alkynes in a [3+2] cycloaddition (also referred to as "Click Chemistry"). Polyproline II helices containing 4-azidoproline are therefore going to be applied in the design of new materials and as inhibitors of helical peptide binding proteins.

6 Experimental Section

6.1 List of abbreviations

AA	amino acid
Ac	acetyl
Ac$_2$O	acetic anhydride
AcOH	acetic acid
Ala	alanine
anh.	anhydrous
aq.	aqueous
Arg	arginine
Asn	aspargine
Asp	aspartic acid
Bn	benzyl
Boc	*tert*-butyloxycarbonyl
Boc$_2$O	*tert*-butyloxycarbonyl anhydride
CAM	ceric ammonium molybdate
DEPBT	3-(diethoxyphosphoryloxy)-1,2,3-benzotriazin-4(3H)-one
DIAD	diisopropylazodicarboxylate
DIPEA	*N,N*-diisopropylethylamine
DMAP	*N,N*-dimethylamino pyridine
DMF	*N,N*-dimethylformamide
DMSO	dimethylsulfoxide

DNA	deoxyribonucleic acid
DR	disperse Red
EC-GC	electron capture gas chromatography
EDC	1-ethyl-3-(3-dimethylaminopropyl)-carbodiimide
eq	equivalent
Et_3N	triethylamine
EXSY	Exchange spectroscopy
Fmoc	9-fluorenylmethoxycarbonyl
Gln	glutamine
Glu	glutamic acid
Gly	glycine
h	hour(s)
HATU	*O*-(7-azabenzotriazol-1-yl)1,1,3,3-tetramethyluronium hexafluorophosphate
HCTU	2-(6-Chloro-1H-benzotriazole-1-yl)-1,1,3,3-tetramethlyuronium hexafluorophosphate
His	histidine
HOBt	*N*-hydroxybenzotriazole
Leu	leucine
Lys	lysine
min	minute(s)
MsCl	methansulfonylchloride
NaN_3	Sodium azide
NOE	nuclear overhauser enhancement
NOESY	nuclear overhauser enhancement spectroscopy

Pbf   2,4,6,7-Pentamethyldihydrobenzofurane-5-sulfanyl

PEG   polyethylene glycol

Pfp   pentafluorophenol

Phe   phenylalanine

Pmc   2,2,5,5,7,8-pentamethylchroman-6-sulfonyl

PPh$_3$ triphenylphosphine

Pro   proline

quant.   quantitative

r.t.   room temperature

sat.   saturated

Ser   serine

sol.   solution

TBTU   2-(1H-Benzotriazole-1-yl)-1,1,3,4-tetramethyluronium

                       tetrafluoroborate

TFA   trifluoro acetic acid

THF   tetrahydrofuran

Thr   threonine

TLC   thin layer chromatography

UDP   uridine 5'-diphosphate

Val   valine

6.2 General Methods

Materials and reagents were of the highest commercially available grade and used without further purification. Reactions were monitored by thin layer chromatography using Merck silica gel 60 F_{254} plates. Compounds were visualized by UV, ceric ammonium molybdate (CAM) and ninhydrin. Flash chromatographies were performed using Merck silica gel 60, particle size 40 - 63 μm. Gel filtrations were performed on Sephadex LH20 resin purchased from Sigma. ^{1}H and ^{13}C NMR spectra were recorded on a Varian Gemini 300, a Bruker DPX 400 or a Bruker DPX 500 spectrometer. Chemical shifts are reported in ppm using $CHCl_3$ and TMS as a reference. Infrared spectra were obtained on a Perkin-Elmer 1600 series; peaks are reported in cm^{-1}. Finnigan MAT LCQ and TSQ 700 instruments were used for electrospray ionization (ESI) mass spectrometry.

EXSY-NMR Spectroscopy. Experiments were performed on a Bruker DMX 600 instrument (600.13 MHz) using a 5 mm inverse broadband probe equipped with a shielded z-gradient. Samples of Ac[Pro(4S)-N$_3$]OMe and Ac[Pro(4R)-N$_3$]OMe were prepared in DMF-d$_7$ (99.5 % D) and were both 80 mM. Experiments were performed in the temperature range from 288 K to 345 K. Temperature calibrations were carried out using a glycerol standard and were reproducible within ±0.5 K. For each temperature setting, a one-dimensional ^{1}H-NMR spectrum was recorded with a recovery delay of 10 s, to allow for complete relaxation. The *trans*:*cis* ratio K was obtained from these spectra by simple peak integration. EXSY spectra were recorded using a standard pulse scheme[83,84]: 90^x-t$_1$-90^x-t$_{mixing}$/2-grad(z)-180^x-grad(-z)-t$_{mixing}$/2-90^x-aquisition.

2048 data points in the direct and 512 data points in the indirect dimension were collected using a TPPI phase cycle resulting in acquisition times of 170 ms and 85 ms respectively. After zero-filling in the indirect dimension to 1024 data points, shifted squared sine bell window functions were applied in both dimensions prior to Fourier transformation. For a given temperature at least five EXSY spectra were recorded with different mixing times in a range from 10 ms to 4s to obtain cross peak intensities that were smaller than the diagonal peak intensities for all temperatures. Linear baseline

corrections were carried out in both dimensions and peak volumes were determined manually. At least two resonances (O-CO-CH_3 and Hα or Hδ') were analyzed independently for each compound in order to minimize experimental errors.

Kinetics. Rate constants were calculated from peak volumes using the following equation:[68]

$$k = \frac{1}{t_m} \ln \frac{r+1}{r-1}$$

Where r is defined as follows:

$$r = \frac{4X_A X_B (I_{AA} + I_{BB})}{(I_{AB} + I_{BA}) - (X_A - X_B)^2}$$

t_m is the mixing time of the EXSY experiment, I refers to the integrated intensity of the peak; the indices A and B refer to diagonal peaks of the *s-cis* and the *s-trans* conformer when they are equal and to cross peaks when they are different. X is the molar fraction of the conformers indicated in the index and k is equal to the sum of the isomerization rates k_{AB} and k_{BA}.

For each temperature the ten (or fifteen) independent values for k were averaged and k_{AB} and k_{BA} were obtained thereof using the mole fraction obtained from the one-dimensional ^{1}H-NMR spectra. Thermodynamic parameters and their standard deviations were then obtained by linear least-squares fitting of k_{AB}, k_{BA} and K to the Eyring and Van't Hoff equation.

Isothemal Titration Calorimetry. Titrations were performed at 25°C using a Microcal VP-ITC titration microcalorimeter. Sample solutions were prepared using Milli-Q water. Titrations of Ac-Arg-Arg-Arg-NHPr were performed by adding aliquots of a 5 mM peptide solution to a 0.2 mM receptor solution. The titrations were analyzed using a least squares curve-fitting procedure (Origin® implemented with the calorimetric setup provided by Microcal).

6.3 General Procedures:

6.3.1   General procedure for the saponification of a methyl-ester (2 mmol scale):

The methyl ester was dissolved in a 1:1 mixture of THF and MeOH (20 mL) and a solution of NaOH (1.5 eq) in water (2 mL) was added. The reaction mixture was stirred for 2 h at room temperature and was then carefully acidified to pH 4 using 1M HCl. CH_2Cl_2 (100 mL) and water (20 mL) were added, and the mixture was extracted once with additional 1M HCl (20 mL). The aqueous layer was extracted with CH_2Cl_2 (2×50 mL), the organic layers were washed with brine and dried over Na_2SO_4. Filtration and evaporation of the solvent at reduced pressure yielded the acid that was used without further purification, unless otherwise stated.

6.3.2   General procedure for the formation of a Pentafluorophenyl ester (2 mmol scale):

Pentafluorophenol   (Pfp-OH)   (1.05   eq)   and   1-(3-Dimethylaminopropyl)-3-ethylcarbodiimide hydrochloride (EDC) (1.5 eq) were added to the solution of the carboxylic acid in CH_2Cl_2 (5 mL). The reaction mixture was stirred for 1 h, then extracted with CH_2Cl_2 (100 mL) and 0.5M HCl (50 mL). The aqueous layer was extracted with CH_2Cl_2 (2×50 mL) and the combined organic phases were dried over Na_2SO_4. Filtration and removal of all volatiles afforded the Pfp-ester.

6.3.3   General procedure for Boc-deprotection (2 mmol scale):

The Boc-protected amine was dissolved in 4M HCl in dioxane (5 mL) and stirred at room temperature for 1 hour. After removal of all volatiles at reduced pressure, the residue was triturated with Et_2O (3×10 mL) providing the HCl-salt.

6.3.4 General procedure for Fmoc-deprotection (2 mmol scale)

The Fmoc-protected amine was dissolved in CH_2Cl_2/AcCN 3/1 (4 mL). Diethylamine (200 eq) was added and the reaction mixture was stirred at room temperature for 1 hour. After removal of all volatiles at reduced pressure, the residue was triturated with pentanes (3×10 mL) providing the free amine.

6.3.5 General procedure for the coupling of a Pfp-ester with a HCl-salt (2 mmol scale):

The Pfp-ester (1.1 eq) was added to a solution of the HCl-salt (1 eq) in CH_2Cl_2 (2 mL) and Hünig's base (2.5 eq). After stirring over night, the reaction mixture was extracted with CH_2Cl_2 (100 mL) and 0.5M HCl (50 mL). The aqueous layer was extracted with CH_2Cl_2 (2×50 mL) and the combined organic layers were dried over Na_2SO_4. Filtration and removal of all volatiles at reduced pressure yielded the crude product.

6.4 Synthesis of the acetylated 4-azidoproline derivatives

6.4.1 Synthesis of the monomeric methyl ester derivatives.

6.4.1.1 Boc-(4*S*)-azidoproline methyl ester **24**
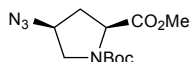
Boc-hydroxyproline methyl ester (16.28 g, 66.36 mmol) was cooled to 0°C in dry CH_2Cl_2 (30 mL). Triethylamine (11.08 mL, 79.63 mmol) and methanesulfonylchloride (6.2 mL, 79.63 mmol) were added. After 30 minutes, the reaction mixture was extracted with sat. $NaHCO_3$ solution (30 mL). The aqueous phase was washed twice with CH_2Cl_2 (15 mL). The combined organic layers were dried and the solvent was removed *in vacuo*. The residual oil was dissolved in dry DMF (50 mL). Sodium azide (21.57 g, 331.8 mmol) was added and the suspension was stirred for 3 hours at 80°C. The DMF was removed *in vacuo* and the residual slurry was taken up in diethyl ether (50 mL). Remaining sodium azide was filtered off and the filtrate was extracted with sat. $NaHCO_3$ solution (50 mL). The aqueous phase was washed with diethyl ether (3×30 mL). The combined organic layers were dried and the solvent was removed *in vacuo* to yield the desired Boc-(4*S*)-azidoproline methyl ester **24** (17.93 g, 66.36 mmol, quant.).

The NMR-spectra show a mixture of major and minor signals or two conformers.

^{1}H NMR (400 MHz, CDCl$_3$, 25°C): δ = 4.38 (dd, *J* = 8.8 Hz, 3.5 Hz, 1H; Hα minor), 4.27 (dd, *J* = 8.6 Hz, 4.0 Hz, 1H; Hα major), 4.11 (m, 1H; Hγ major + minor), 3.71 (s, 3H; OC*H*$_3$ major+ minor), 3.66 (m, 1H; Hδ major + minor), 3.43 (m, 1H; Hδ major + minor), 2.43 (m, 1H; Hβ major + minor) 2.12 (dt, *J*= 13.5, 4.4 1H; Hβ major + minor), 1.43 (s, 9H; *t*bu minor), 1.37 (s, 9H; *t*bu major).

^{13}C NMR (100 MHz, CDCl$_3$, 22°C): δ (major) = 172.1, 153.3, 80.4, 58.1, 57.6, 52.1, 35.9, 28.1.

^{13}C NMR (100 MHz, CDCl$_3$, 22°C): δ (minor) = 171.8, 153.8, 80.4, 59.1, 57.2, 51.1, 35.0, 28.2.

ESI-MS: *m/z*: calculated for $C_{11}H_{18}N_4O_4$ [*M*+Na]+ 293; found 293 (100%).

6.4.1.2 Acetyl-(4S)-azidoproline methyl ester 14
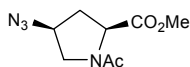
Boc-[Pro-(4S)-N$_3$]OCH$_3$ **24** (340 mg, 1.258 mmol) was Boc-deprotected following the general procedure. The crude product was reacted with acetic anhydride (238 µL, 2.517 mmol) and triethylamine (524 µL, 3.774 mmol) in dry CH$_2$Cl$_2$ (2 mL). The reaction was monitored by T.L.C., after completion, 1M HCl (1 mL) was added and the mixture was extracted twice with ethyl acetate (25 mL). The combined organic layers were dried and the solvent was removed *in vacuo*. After flash chromatography on silica gel (gradient of DCM:MeOH from 98:2 to 97:3) the acetylated methyl ester **14** (253 mg, 1.192 mmol, 95%) was isolated as a colorless oil.

^{1}H NMR (500 MHz, DMF-d$_7$, 25°C): δ (s-*trans*) = 4,53 (m, 1H; Hγ) , 4,49 (dd, *J* = 9.2, 4.3, 1H; Hα), 3,97 (dd, *J* = 11, 6.1, 1H; Hδ), 3,54 (dd, *J* = 11, 3.9, 1H; Hδ'), 2,62 (ddd, *J* = 13.5, 9.2, 6, 1H; Hβ), 2,03 (dt, *J* = 13.5, 4.3, 1H; Hβ');

^{1}H NMR (500 MHz, DMF-d$_7$, 25°C): δ (s-*cis*) = 4,84 (dd, *J* = 9.05, 1.5, 1H; Hα), 4,53 ppm (m, 1H; Hγ), 3,69 (dd, *J* = 13, 5.5, 1H; Hδ), 3,41 (dt, *J* = 13, 1.5, 1H; Hδ), 2,62 (m, *J* = 9.05, 5.2, 1H; Hβ), 2,38 (dddd, *J* = 13.7, 3.2, 1.5, 0.4, 1H; Hβ').
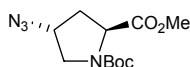
^{13}C NMR (125 MHz, DMF-d$_7$, 25°C): δ (s-*trans*) = 172.3, 169.4, 57.7, 60.2, 52.3, 52.7, 34.9, 22.1.

^{13}C NMR (125 MHz, DMF-d$_7$, 25°C): δ (s-*cis*) = 172.7, 170.1, 59.1, 59.1, 52.8, 51.7, 36.7, 22.1.

ESI-MS: *m/z*: calculated for C$_8$H$_{12}$N$_4$O$_3$ [*M*+Na]+ 235; found 235 (100%); [2*M*+Na]+ 447; found 447 (60%).

Elemental analysis calculated for C$_8$H$_{12}$N$_4$O$_3$ (212,09): C 45,28; H 5,70; N 26,40; found: C 45.26; H 5.63; N 26.28.

6.4.1.3 Boc-(4*R*)-azidoproline methyl ester 26

A solution of triphenylphosphine (9.5 g, 36.239 mmol, 1.8 eq) and methanesulfonic acid (1.57 mL, 24.160 mmol 1.2 eq) were stirred in dry toluene (20 mL). Following the addition of triethylamine (1.12 mL, 8.053 mmol, 0.4 eq) and boc-hydroxyproline methyl ester (5.232 g, 20.133 mmol, 1 eq) dissolved in dry toluene (2.5 mL), DIAD (7.8 mL, 40.266 mmol, 2 eq) was added drop-wise. The temperature of the reaction mixture was held below 35°C by cooling with an ice bath. After completion of the addition, the reaction mixture was heated to 70°C for 3 h. After cooling, the reaction mixture was poured in sat. NaHCO$_3$ (100 mL) solution and extracted three times with CH$_2$Cl$_2$ (100 mL). The combined organic layers were dried over Na$_2$SO$_4$ and evaporated. The crude mesylate was dissolved in DMF (15 mL) and NaN$_3$ (6.54 g, 100.665 mmol, 5 eq) was added. The reaction mixture was stirred at 80°C for 3 h. After cooling, the solvent was removed at reduced pressure. The residual oil was dissolved in Et$_2$O (100 mL) and poured onto sat. NaHCO$_3$ solution (100 mL). The aqueous phase was extracted with Et$_2$O (3×100 mL). The combined organic layers were dried with Na$_2$SO$_4$ and evaporated. After flash chromatography on silica gel (gradient of pentanes:ethyl acetate from 10:1 to 7.5:1) N-α-Boc-(4*R*)-azidoproline methyl ester 26 (4.327 g, 16.009 mmol, 80%) was isolated as a colorless oil.

^{1}H and ^{13}C NMR show a double set of peaks (≈ 1.5:1) due to the s-*trans* and s-*cis* conformers.

^{1}H NMR (400 MHz, CDCl$_3$, 25°C): δ (major) = 4.31 (dd, *J* = 8.8 Hz, 4.4 Hz, 1H; Hα), 4.15 (m, 1H; Hγ), 3.75 (s, 3H; OC*H*$_3$), 3.7 (m, 1H; Hδ), 3.45 (m, 1H; Hδ), 2.49 (m, 1H; Hβ) 2.16 (m, 1H; Hβ), 1.41 (s, 9H; C(C*H*$_3$)$_3$);

^{1}H NMR (400 MHz, CDCl$_3$, 25°C): δ (minor) = 4.42 (dd, *J* = 8.9Hz, 3.8 Hz, 1H; Hα), 4.15 (m, 1H; Hγ), 3.75 (s, 3H; OC*H*$_3$), 3.7 (m, 1H; Hδ), 3.45 (m, 1H; Hδ), 2.49 (m, 1H; Hβ) 2.16 (m, 1H; Hβ), 1.47 (s, 9H; C(C*H*$_3$)$_3$).

^{13}C NMR (100 MHz, CDCl$_3$, 22°C): δ (major) = 172.9, 153.3, 80.6, 58.7, 57.7, 52.1, 51.2, 36.2, 28.1.

^{13}C NMR (100 MHz, CDCl$_3$, 22°C): δ (minor) = 172.7, 153.9, 80.6, 59.2, 57.3, 52.3, 51.3, 35.3, 28.3.

ESI-MS: *m/z*: calculated for C$_{11}$H$_{18}$N$_4$O$_4$ [*M*+Na]+ 293; found 293 (100%).

N-α-acetyl-(4*R*)-Azidoproline methyl ester **15**
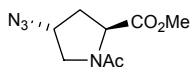
N-α-acetyl-(4*R*)-azidoproline methyl ester **15** was synthesized according to the same procedure as **14**.

^{1}H NMR (500 MHz, DMF-d$_7$, 25°C): δ (s-*trans*) = 4.53 (m, *J* = 9.3, 5.1, 3.9, 1H; Hγ) 4.38 (dt, *J* = 7.7, 1H; Hα), 3.89 (dd, *J* = 11.1, 5.3, 1H; Hδ'), 3.66 (m, 1H; Hδ), 2.38 (dddd, *J* = 12.0, 8.2, 4.4, 1.2, 1H; Hβ), 2.25 (dd, *J* = 7.1, 5.6, 1H; Hβ').

^{1}H NMR (500 MHz, DMF-d$_7$, 25°C): δ (s-*cis*) = 4.78 (dd, *J* = 8.0, 6.4, 1H; Hα), 4.43 (m, *J* = 9.2, 5.4, 1H; Hγ), 3.66 (m, 1H; Hδ), 3.56 (dd, *J* = 12.3, 5.7, 1H; Hδ'), 2.48 (m, 1H; Hβ'), 2.23 (dd, *J*= 7.1, 5.6, 1H; Hβ).

^{13}C NMR (125 MHz, DMF-d$_7$, 25°C): δ (s-*trans*) = 172.8, 169.3, 60.7, 57.9, 53.1, 52.3, 35.3, 22.1;
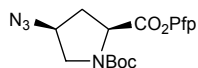
^{13}C NMR (125 MHz, DMF-d$_7$, 25°C): δ (s-*cis*) = 173.1, 169.8, 59.0, 58.9, 52.92, 51.2, 37.0, 21.6.

ESI-MS: *m/z*: calculated for C$_8$H$_{12}$N$_4$O$_3$ [*M*+Na]+ 235; found 235 (100%); [2*M*+Na]+ 447; found 447 (60%).

Elemental analysis calculated for C$_8$H$_{12}$N$_4$O$_3$ (212,09): C 45,28; H 5,70; N 26,40; found: C 45.27; H 5.64; N 26.36.

6.4.2 Synthesis of the monomeric amide derivatives.

6.4.2.1 Boc-(4*S*)-azidoproline pentafluorophenyl ester **27**

The methyl ester of Boc-(4*S*)-azidoproline methyl ester **24** (2.00 g, 7.40 mmol) was saponified with NaOH (0.44 g, 11.04 mmol) following the general procedure. The resulting acid was reacted with pentafluorophenol (1.43 g, 7.77 mmol) and EDC (2.13 g, 11.11 mmol) following the general procedure to provide the Pfp-ester **27** (2.90 g, 6.87 mmol, 93%) as a colorless oil.

^{1}H and ^{13}C NMR show a double set of peaks ($\approx$ 2:1) due to the s-*trans* and s-*cis* conformers.

^{1}H NMR (300 MHz, CDCl$_3$, 25°C): δ (major) = 4.70 (dd, 9.3 Hz, 2.8 Hz, 1H; Hα), 4.29 (m, 1H; Hγ), 3.76 (m, *J* = 11.9, 1H; Hδ), 3.63 (dd, *J* = 11.8 Hz, 2.5 Hz, 1H; Hδ′), 2.68 (m, 1H; Hβ), 2.37 (m, 1H; Hβ′), 1.46 (s, 9H; ^{t}bu); δ (minor) = 4.76 (dd, *J* = 9.2 Hz, 3.2 Hz, 1H; Hα), 4.29 (m, 1H; Hγ), 3.76 (m, *J* = 11.9, 1H; Hδ), 3.54 (dd, *J* = 11.3 Hz, 3.0 Hz, 1H; Hδ′), 2.68 (m, 1H; Hβ), 2.37 (m, 1H; Hβ′), 1.49 (s, 9H; ^{t}bu).

^{13}C NMR (100.5 MHz, CDCl$_3$, 25°C): δ (major) = 168.3, 153.6, 143.5, 138.8, 81.9, 59.8, 57.7, 51.5, 36.9, 28.5; δ (minor) = 168.0, 153.9, 143.5, 138.8, 81.6, 60.8, 57.5, 51.7, 35.8, 28.7.

FT-IR (NaCl, v/cm-1): 2980, 2118, 1798, 1713, 1518, 1260.

ESI-MS: *m/z*: calculated for C$_{16}$H$_{15}$F$_5$N$_4$O$_4$ [*M*+H]+ 423; found 423 (100%).

Elemental analysis calculated for C$_{16}$H$_{15}$F$_5$N$_4$O$_4$ (422.3): C 45.51, H 3.58, N 13.27; found C 45.27, H 3.56, N 13.14.

6.4.2.2 Boc-(4*S*)-azidoproline dimethyl amide **28**
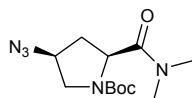
Boc-Pro[(4S)-N$_3$]-OPfp (147 mg, 0.348 mmol) was dissolved in dry CH$_2$Cl$_2$ (2.5 mL). Dimethlyamine hydrochloride (284 mg, 3.48 mmol) and triethylamine (540 µL, 3.83 mmol) were added and the reaction mixture was stirred at room temperature for 30 min. The reaction mixture was diluted with CH$_2$Cl$_2$ (10 mL) and extracted with 1N HCl (10 mL). The aqueous layer was extracted twice with CH$_2$Cl$_2$ (10 mL). The combined organic layers were dried using Na$_2$SO$_4$. After evaporation, the residual oil was purified by flash chromatography on silica gel (gradient, CH$_2$Cl$_2$:MeOH 100:0 to 96:4) to yield Boc-[Pro-(4*S*)-N$_3$]-N(CH$_3$)$_2$ (86 mg, 0.303 mmol, 87%) as a colorless oil.

^{1}H NMR (400 MHz, CDCl$_3$, 25°C): δ (major) = 4.65 (dd, *J* = 8.5 Hz, 6.4 Hz, 1H; Hα), 4.04 (m, 1H; Hγ), 3.85 (dd, *J* = 11.0 Hz, 7.1 Hz, 1H; Hδ), 3.42 (d, *J* = 11.0 Hz, 1H; Hδ), 3.05 (s, 3H; NC*H*$_3$), 2.96 (s, 3H; NC*H*$_3$), 2.53 (t, *J* = 7.7 Hz, 1H; Hβ), 1.89 (m, 1H; Hβ), 1.43 (s, 9H; ^{t}bu).

^{1}H NMR (400 MHz, CDCl$_3$, 25°C): δ (minor) = 4.55 (t, *J* = 7.8 Hz, 1H; Hα), 4.02 (m, 1H; Hγ), 3.90 (dd, *J* = 10.7 Hz, 7.3 Hz, 1H; Hδ), 3.40 (d, *J* = 10.9 Hz, 1H; Hδ), 3.03 (s, 3H; NC*H*$_3$), 2.72 (s, 3H; NC*H*$_3$), 2.55 (t, *J* = 7.9 Hz, 1H; Hβ), 1.87 (m, 1H; Hβ), 1.37 (s, 9H; ^{t}bu).

^{13}C NMR (100 MHz, CDCl$_3$, 22°C): δ (major) = 170.9, 153.9, 80.3, 58.3, 55.0, 53.4 51.0, 36.8, 34.6, 28.3.

^{13}C NMR (100 MHz, CDCl$_3$, 22°C): δ (minor) = 171.3, 153.2, 80.2, 57.6, 55.2, 55.0, 50.4, 36.1, 35.3, 28.2.

ESI-MS: *m/z*: calcd for C$_{12}$H$_{21}$N$_5$O$_3$ [*M*+Na]+ 306; found 306 (100%).

6.4.2.3 Boc-(4*S*)-azidoproline pyrrolidine amide **29**
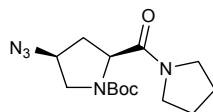
Boc-[Pro(4*S*)-N₃]OPfp **27** (50 mg, 0.118 mmol) was dissolved in dry CH₂Cl₂ (1 mL). Pyrrolidine (20 μL, 0.236 mmol) was added and the reaction mixture was stirred at room temperature for 30 min. The reaction mixture was diluted with CH₂Cl₂ (10 mL) and extracted with 1N HCl (10 mL). The aqueous layer was extracted twice with CH₂Cl₂ (10 mL). The combined organic layers were dried using Na₂SO₄. Evaporation of the solvent yielded Boc-(4*S*)-azidoproline pyrrolidineamide (36 mg, 0.118 mmol, quant.) as a colorless solid.

¹H NMR (400 MHz, CDCl₃, 25°C): δ = 4.32-4.49 (m, 2H; Hα), 4.01 (m, 1H), 3.37 (1H), 3.29-3-71 (m, 5H), 2.52 (m, 1H), 1.75-2.01 (m, 5H), 1.35-1.44 (9H, *t*bu).

The carbon spectrum shows a 1:1 mixture of signals.

¹³C NMR (100 MHz, CDCl₃, 22°C): δ = 169.7, 169.4, 153.9, 153.2, 80.2, 58.3, 57.6, 56.7, 56.4, 51.0, 50.4, 46.2, 46.1, 35.2, 34.5, 28.4, 28.2, 26.3, 26.2, 24.0, 23.9.

ESI-MS: *m/z*: calcd for C₉H₁₅N₅O₂ [*M*+Na]+ 332; found 332 (100%).

6.4.2.4 Acetyl-(4S)-azidoproline dimethyl amide 16
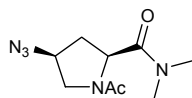
Boc-Pro[(4S)-N$_3$]-N(CH$_3$)$_2$ (106 mg, 0.374 mmol) was Boc-deprotected according to the general procedure. The crude product was reacted with acetic anhydride (175 µL, 1.87 mmol) and triethylamine (420 µL, 2.99 mmol) in dry CH$_2$Cl$_2$ (1 mL). The reaction was monitored by T.L.C., after completion, 1M HCl (1 mL) was added and the mixture was extracted twice with ethyl acetate (25 mL). The combined organic layers were dried and the solvent was removed *in vacuo*. After flash chromatography on silica gel (gradient of CH$_2$Cl$_2$:MeOH from 99:1 to 95:5) the acetylated dimethyl amide 16 (76 mg, 0.337 mmol, 90%) was isolated as a colorless oil.

^{1}H NMR (500 MHz, DMF-d$_7$, 22°C): δ (s-*trans*) = 4.38 (dd, J = 8.5 Hz, 6.6 Hz, 1H; Hα), 4.49 (ψq, J = 14.5 Hz, 7.1 Hz, 1H; Hγ), 4.09 (dd, J = 10.4 Hz, 7.1 Hz, 1H; Hδ), 3.41 (dd, J = 10.4 Hz, 7.3 Hz, 1H; Hδ), 3.10 (s, 3H; NCH$_3$), 2.86 (s, 3H; NCH$_3$), 2.74 (m, 1H; Hβ), 2.00 (s, 3H; acetyl-CH$_3$), 1.76 (dt, J = 12.9 Hz, 6.9 Hz, 1H; Hβ).

^{1}H NMR (500 MHz, DMF-d$_7$, 22°C): δ (s-*cis*) = 5.05 (dd, J = 9.0 Hz, 4.3 Hz, 1H; Hα), 4.36 (m, 1H; Hγ), 3.93 (dd, J = 12.3 Hz, 6.7 Hz, 1H; Hδ), 3.33 (dd, J = 12.3 Hz, 5.0 Hz, 1H; Hδ), 3.13 (s, 3H; NCH$_3$), 2.93 (s, 3H; NCH$_3$), 2.88 (m, 1H; Hβ), 1.97 (m, 1H; Hβ), 1.80 (s, 3H; acetyl-CH$_3$).

^{13}C NMR (125 MHz, DMF-d$_7$, 22°C): δ (s-*trans*) = 171.3, 168.5, 59.3, 55.6, 52.6, 36.8, 34.5, 34.7, 22.3.

^{13}C NMR (125 MHz, DMF-d$_7$, 22°C): δ (s-*cis*) = 171.1, 169.6, 58.1, 57.9, 51.3, 36.7, 36.6, 35.7, 21.7.

ESI-MS: *m/z*: calcd for C$_9$H$_{15}$N$_5$O$_2$ [*M*+Na]+ 248; found 248 (100%); [2*M*+Na]+ 473; found 473 (80%).

6.4.2.5 Acetyl-(4*S*)-azidoproline pyrrolidine amide **18**
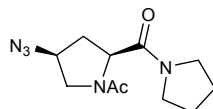
Boc-(4*S*)-azidoproline pyrrolidineamide (35 mg, 0.142 mmol) was Boc-deprotected following the general procedure. The crude product was reacted with acetic anhydride (67 µL, 0.71 mmol) and polyvinylpyridine (50 mg, ~ 0.71 mmol) as solid base in dry CH_2Cl_2 (1 mL). The reaction mixture was stirred over night at room temperature. The polyvinylpyridine was filtered off and washed with CH_2Cl_2 (3×3 mL). After removal of the solvent, the residual oil was purified by flash chromatography on silica gel (gradient of CH_2Cl_2:MeOH from 99:1 to 95:5) to yield the acetylated pyrrolidineamide **18** (31 mg, 0.125 mmol, 88%) as a colorless oil.

^{1}H NMR (400 MHz, DMF-d$_7$, 25°C): δ (major) = 4.59 (t, *J* = 7.7 Hz, 1H; Hα), 4.37 (m, 1H; Hγ), 4.08 (dd, *J* = 10.2 Hz, 7.1 Hz, 1H; Hδ), 3.67 (m, 2H; pyrrolidine), 3.48 (m, 2H; pyrrolidine), 3.39 (dd, *J* = 10.2 Hz, 7.7 Hz, 1H; Hδ), 2.73 (m, 1H; Hβ), 2.00 (s, 3H; C*H*$_3$), 1.93 (m, 2H; pyrrolidine), 1.81 (m, 1H; Hβ), 1.79 (m, 2H; pyrrolidine).

^{1}H NMR (400 MHz, DMF-d$_7$, 25°C): δ (major) = 4.83 (dd, *J* = 9.0 Hz, 4.7 Hz, 1H; Hα), 4.36 (m, 1H; Hγ), 3.94 (dd, *J* = 12.1 Hz, 6.8 Hz, 1H; Hδ), 3.36 (m, 2H; pyrrolidine), 3.31 (m, 1H; Hδ), 3.29 (m, 2H; pyrrolidine), 2.86 (ddd, *J* = 13.2 Hz, 9.0 Hz, 6.9 Hz, 1H; Hβ), 1.99 (m, 1H; Hβ), 1.82 (s, 3H; C*H*$_3$), 1.81 (m, 2H; pyrrolidine), 1.77 (m, 2H; pyrrolidine).

^{13}C NMR (125 MHz, CDCl$_3$, 22°C): δ = 169.1, 168.9, 58.4, 56.2, 52.0, 46.3, 46.0, 34.0, 26.1, 24.0, 22.3.

ESI-MS: *m/z*: calcd for $C_9H_{15}N_5O_2$ [*M*+Na]+ 274; found 274 (100%); [2*M*+Na]+ 525; found 525 (30%).

6.4.2.6 Acetyl-(4*R*)-azidoproline dimethyl amide **17**
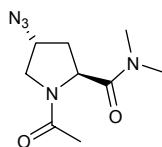
Acetyl-(4*R*)-azidoproline dimethyl amide **17** was synthesized in analogy to acetyl-(4*S*)-azidoproline dimethyl amide **16**.

^{1}H NMR (500 MHz, DMF-d$_7$, 22°C): δ (s-*trans*) = 4.91 (dd, *J* = 8.3 Hz, 6.1 Hz, 1H; Hα), 4.49 (ψq, *J* = 9.6 Hz, 5.5 Hz, 1H; Hγ), 3.84 (dd, *J* = 11.0 Hz, 5.5 Hz, 1H; Hδ), 3.64 (ddd, *J* = 11.0 Hz, 3.4 Hz, 1.1 Hz, 1H; Hδ'), 3.14 (s, 3H; NC*H*$_3$), 2.84 (s, 3H; NC*H*$_3$), 2.36 (dddd, *J* = 13.1 Hz, 8.3 Hz, 4.5 Hz, 1.2 Hz, 1H; Hβ), 2.14 (dt, *J* = 13.3 Hz, 6.0 Hz, 1H; Hβ'), 2.01 (s, 3H; acetyl-C*H*$_3$).

^{1}H NMR (500 MHz, DMF-d$_7$, 22°C): δ (s-*cis*) = 5.12 (dd, *J* = 8.5 Hz, 5.86 Hz, 1H; Hα), 4.37 (m, *J* = 9.4 Hz, 5.6 Hz, 3.9 Hz, 1H; Hγ), 3.68 (ddd, *J* = 12.3 Hz, 3.2 Hz, 1.4 Hz, 1H; Hδ), 3.55 (dd, *J* = 12.3Hz, 5.5Hz, 1H; Hδ), 3.16 (s, 3H; NC*H*$_3$), 2.93 (s, 3H; NC*H*$_3$), 2.65 (dddd, *J* = 13.0 Hz, 8.5Hz, 4.4 Hz, 1.5 Hz, 1H; Hβ), 2.42 (dt, *J* = 13.4 Hz, 5.9 Hz, 1H; Hβ), 1.82 (s, 3H; acetyl-C*H*$_3$).

^{13}C NMR (125 MHz, DMF-d$_7$, 22°C): δ (s-*trans*) = 171.5, 168.3, 60.5, 55.0, 53.1, 36.6, 34.9, 22.0.

^{13}C NMR (125 MHz, DMF-d$_7$, 22°C): δ (s-*cis*) = 171.3, 169.16, 58.9, 56.9, 51.4, 36.5, 36.3, 35.4, 21.3.

ESI-MS: *m/z*: calculated for C$_9$H$_{15}$N$_5$O$_2$ [*M*+Na]+ 248; found 248 (100%); [2*M*+Na]+ 473; found 473 (40%).

## 6.4.2.7 Acetyl-(4*S*)-azidoproline pyrrolidine amide **19**
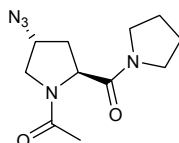
Acetyl-(4*S*)-azidoproline pyrrolidine amide **19** was synthesized in analogy to acetyl-(4*S*)-azidoproline pyrrolidine amide **18**.

^{1}H NMR (400 MHz, CDCl$_3$, 25°C): δ = 4.69 (dd, *J* = 7.9 Hz, 5.8 Hz, 1H; Hα), 4.46 (m, 1H; Hγ), 3.92 (m, 2H; 2Hδ), 3.32-3.56 (m, 4H, pyrrolidine H), 2.26 (m, 1H; Hβ), 2.16 (m, 1H; Hβ), 2.05 (s, 3H, C*H*$_3$) 1.78-2.02 (m, 4H, pyrrolidine H).

^{13}C NMR (100 MHz, CDCl$_3$, 25°C): δ = 169.7, 169.0, 59.8, 56.2, 52.8, 46.5, 46.0, 34.7, 26.0, 24.1, 22.3.

ESI-MS: *m/z*: calcd for C$_9$H$_{15}$N$_5$O$_2$ [*M*+Na]+ 274; found 274 (100%); [2*M*+Na]+ 525; found 525 (30%).

6.4.3 Synthesis of the dimeric methly ester derivatives

6.4.3.1 (4S)-azidoproline methyl ester hydrochloride **30**
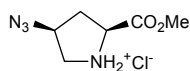
Boc-[Pro-(4S)-N$_3$]OCH$_3$ **24** (1.20 g, 4.44 mmol) was deprotected following the general protocol yielding the HCl-salt **30** (916 mg, 4.44 mmol, quant.).

^{1}H NMR (400 MHz, CD$_3$OD, 25°C): δ = 4.62 (dd, J = 9.9 Hz, 4.2 Hz, 1H; Hα), 4.58 (m, 1H; Hγ), 3.52 (dd, J = 12.5 Hz, 5.0 Hz, 1H; Hδ), 3.45 (dt, J = 12.5 Hz, 1.8 Hz, 1H; Hδ′), 2.65 (ddd, J = 14.4 Hz, 9.9 Hz, 5.6 Hz, 1H; Hβ), 2.43 (dddd, J = 14.4 Hz, 4.2 Hz, 2.5 Hz, 1.6 Hz, 1H; Hβ′).

^{13}C NMR (100.5 MHz, CD$_3$OD, 25°C): δ = 169, 59.6, 58.6, 53.2, 51.1, 34.2.

ESI-MS: m/z: calculated for C$_6$H$_{10}$N$_4$O$_2$ [M+H]+ 171; found 171 (100%).

6.4.3.2 Boc-di-(4*S*)-azidoproline methyl ester **31**
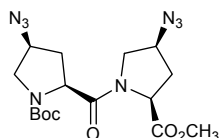
The Pfp-ester **27** (2.06 g, 4.88 mmol) and the HCl-salt **30** (916 mg, 4.44 mmol) were coupled following the general procedure. The crude product was purified by flash chromatography on silica gel (CH$_2$Cl$_2$:MeOH 100:1) yielding the dipeptide **31** (1.64 g, 4.02 mmol, 90%) as a colorless oil.

^{1}H and ^{13}C NMR show a double set of peaks ($\approx$ 2:1) due to the s-*trans* and s-*cis* conformers.

^{1}H NMR (500 MHz, CDCl$_3$, 25°C): δ (major) = 4.73 (dd, *J* = 4.6 Hz, 4.4 Hz, 1H; Hα), 4.48 (dd, *J* = 8.4 Hz, 6.8 Hz, 1H; Hα), 4.28 (m, 1H; Hγ), 4.07 (m, 2H; Hγ, Hδ), 3.82 (dd, *J* = 7.1 Hz, 10.9 Hz, 1H; Hδ), 3.72 (s, 3H; CH$_3$), 3.47 (ddd, *J* = 14.7 Hz, 4.3 Hz, 10.4 Hz, 1H; Hδ), 3.38 (dd, *J* = 10.9 Hz; 7.1 Hz 1H; Hδ), 2.61 (dt, *J* =13 Hz, 7.8 Hz, 1H; Hβ), 2.47 (ddd, *J* = 6 Hz, 9 Hz, 14.7 Hz, 1H; Hβ), 2.17 (dt, 13.5 Hz, 4.4 Hz, 1H; Hβ), 2.09 (m, 1H; Hβ), 1.4 (s, 3H; CH$_3$).

^{1}H NMR (500 MHz, CDCl$_3$, 25°C): δ (minor) = 4.69 (dd, *J* = 8.9 Hz, 4.4 Hz, 1H), 4.37 (t, *J* = 7.6), 4.27 (m, 1H), 4.08 (m, 1H), 3.88 (m, 2H), 3.74 (s, 3H), 3.48 (m, 1H), 3.39 (m, 1H), 2.61 (m, 1H), 2.41 (m, 1H), 2.22 (m, 1H), 2.07 (m, 1H), 1.37 (s, 3H).

^{13}C NMR (125 MHz, CDCl$_3$, 25°C): δ (major) = 171.2, 170.3, 154.2, 80.7, 59.7, 58.5, 57.5, 56.3, 52.7, 51.4, 51.1, 34.4, 34.1, 28.5.

^{13}C NMR (125 MHz, CDCl$_3$, 25°C): δ (minor) = 170.9, 170.4, 154.2, 80.6, 57.9, 57.6, 56.8, 52.8, 51.3, 50.8, 35.3, 28.4.

ESI-MS: *m/z*: calculated for C$_{16}$H$_{24}$N$_8$O$_5$ [*M*+Na]+ 431; found 431 (100%).

Elemental analysis calculated for C$_{16}$H$_{24}$N$_8$O$_5$ (408.19): C 47.05, H 5.92, N 27.44; found: C 47.20, H 5.89, N 27.31.

6.4.3.3 Acetyl-di-(4S)-azidoproline methyl ester 20
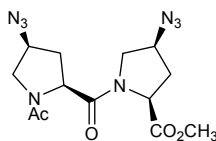
Boc-di-(4S)-azidoproline methyl ester (98 mg, 0.24 mmol) was Boc-deprotected following the general procedure. The HCl salt was reacted with acetic anhydride (62 μL, 0.66 mmol) and pyridine (197 μL, 1.32 mmol) in dry CH_2Cl_2 (1 mL) at room temperature for 30 min. The reaction mixture was diluted with CH_2Cl_2 (10 mL) and was extracted with 2N HCl. The aqueous layer was extracted two additional times with CH_2Cl_2 (10 mL). The combined organic layers were dried and the solvent was removed *in vacuo*. The crude product was purified by column chromatography (gradient CH_2Cl_2:MeOH 100:0 to 96:4), yielding **20** (77 mg, 0.034 mol 60%).

^{1}H NMR (500 MHz, CDCl$_3$, 25°C): δ = 4.68 (dd, *J* = 8.8 Hz, 4.6 Hz, 1H; Hα), 4.52 (dd, *J* = 7.9 Hz, 6.8 Hz, 1H; Hα), 4.29 (m, 1H; Hγ), 4.17 (dd, *J* = 10.4 Hz, 6.2 Hz, 1H; Hδ), 4.13 (m, 1H; Hγ), 3.84 (dd, *J* = 10.2 Hz, 7.2 Hz, 1H; Hδ), 3.72 (s, 3H; OC*H*$_3$), 3.50 (m, 1H; Hδ), 3.47 (dd, *J* = 10.4 Hz; 4.1 Hz 1H; Hδ), 2.61 (m, 1H; Hβ), 2.46 (ddd, *J* = 13.4 Hz, 8.8 Hz, 5.8 Hz, 1H; Hβ), 2.16 (m, 1H; Hβ), 2.12 (m, 1H; Hβ), 2.05 (s, 3H; Ac-C*H*$_3$).

^{13}C NMR (125 MHz, CDCl$_3$, 25°C): δ = 171.0, 169.6, 169.1, 59.4, 58.4, 57.2, 56.0, 52.5, 52.0, 51.4, 33.9, 33.8, 22.1.

ESI-MS: *m/z*: calcd for C$_{13}$H$_{18}$N$_8$O$_4$ [*M*+Na]+ 373; found 373 (60%); [2*M*+Na]+ 723; found 723 (100%).

6.4.3.4 Acetyl-di-(4*R*)-azidoproline methyl ester **21**
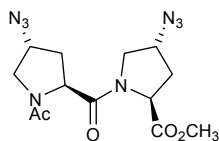
Acetyl-di-(4*R*)-azidoproline   methyl   ester   was   prepared   analogously   to
Acetyl-di-(4*S*)-azidoproline methyl ester **20**.

^{1}H NMR (500 MHz, CDCl$_3$, 25°C): δ = 4.65 (dd, *J* = 8.0 Hz, 5.9 Hz, 1H; Hα), 4.61 (dd, *J* = 8.1 Hz, 6.5 Hz, 1H; Hα), 4.45 (m, 1H; Hγ), 4.32 (m, 1H; Hγ), 4.07 (dd, *J* = 10.3 Hz, 4.4 Hz, 1H; Hδ), 3.88 (dd, *J* = 10.7 Hz, 5.8 Hz, 1H; Hδ), 3.85 (m, 1H; Hδ), 3.74 (s, 3H; OC*H*$_3$), 3.48 (dd, *J* = 10.7 Hz; 3.8 Hz 1H; Hδ), 2.31 (m, 2H; Hβ), 2.20 (m, 1H; Hβ), 2.06 (s, 3H; Ac-C*H*$_3$).

^{13}C NMR (125 MHz, CDCl$_3$, 25°C): δ = 172.0, 170.6, 169.3, 59.8, 59.5, 57.6, 56.0, 52.8, 52.5, 51.6, 34.5, 34.3, 22.1.

ESI-MS: *m/z*: calcd for C$_{13}$H$_{18}$N$_8$O$_4$ [*M*+Na]+ 373; found 373 (60%); [2*M*+Na]+ 723; found 723 (100%).

6.5 Synthesis of the cyclotriproline scaffold and derivatives

6.5.1 Boc-[Pro(4S)-N₃]₃-OCH₃ 35
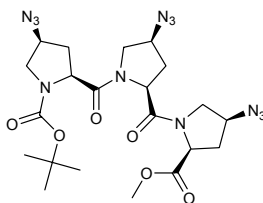
The methyl ester of the dipeptide **31** (504 mg, 1.224 mmol) was hydrolysed, converted into a Pfp-ester and coupled with the HCl salt **30** (253 mg, 1.224 mmol) following the general procedures. Purification by flash chromatography on silica gel (gradient of EtOAc:pentane from 1:1 to 3:1) yielded the tripeptide **35** (486 mg, 0.889 mmol, 73%) as a colorless oil.

^{1}H and ^{13}C NMR show multiple sets of peaks due to the s-*trans* and s-*cis* conformers. ^{1}H NMR (500 MHz, CDCl$_3$, 25°C): δ = 4.72-4.35 (m, 3H, Hα), 4.28 (m, 1H, Hγ), 4.15 (m, 3H, Hγ, Hδ), 4.03 (m, 1H, Hγ), 3.85-3.73 (m, 1H, Hδ), 3.72 (s, 3H, CH$_3$), 3.52-3-39 (m, 2H, Hδ), 3.35-3.28 (m, 1H, Hδ), 2.67-2.40 (m, 3H, Hβ), 2.22-1.98 (m, 3H, Hβ) 1.41-1.37 (2s, 9H, ^{t}bu).

^{13}C NMR (125 MHz, CDCl$_3$, 25°C): δ = 171.1, 170.5, 170.0, 169.7, 169.5, 154.1, 153.0, 80.6, 80.4, 59.7, 58.9, 58.5, 57.8, 57.4, 57.3, 56.7, 56.3, 51.6, 50.8, 35.0, 34.09, 34.07, 33.3, 28.4, 52.6, 51.6, 51.3, 51.1.

ESI-MS: *m/z*: calculated for C$_{21}$H$_{30}$N$_{12}$O$_6$ [*M*+Na]+ 569; found 569 (100%).

Elemental analysis calculated for C$_{21}$H$_{30}$N$_{12}$O$_6$ (546,54): C 46.15, H 5.53, N 30.75; found: C 46.10, H 5.58, N 30.65.

6.5.2   Boc[Pro-(4*S*)-N₃]₃-OH
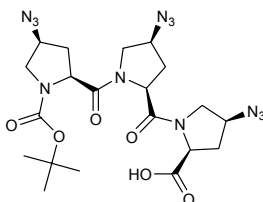
The methyl ester of the tripeptide **35** (465 mg, 0.851 mmol) was saponified, following the general procedure. Purification by flash chromatography on silica gel (gradient of CH₂Cl₂/AcOH/MeOH from 98.5/1/0.5 to 97/1/2) yielded the tripeptide (439 mg, 0.824 mmol, 97%) as a colorless oil.

^{1}H and ^{13}C NMR show multiple sets of peaks due to the s-*trans* and s-*cis* conformers. ^{1}H-NMR (500 MHz, CDCl₃, 25°C): δ = 4.72-4.45 (m, 3H, Hα), 4.42-4.17 (m, 2H, Hγ), 4.17-4.10 (m, 2H, Hδ), 4.10-3.98 (m, 1H, Hγ), 3.87-3.32 (m, 4H, Hδ), 2.67-2.01 (m, 6H, Hβ), 1.46-1.38 (2s, 9H, *t*bu)

^{13}C NMR (125 MHz, CDCl₃, 25°C): δ = 172.4, 172.3, 171.3, 170.3, 154.3, 153.1, 81.0, 80.7, 59.6, 58.9, 58.6, 58.3, 57.9, 56.9, 56.5, 52.2, 51.4, 51.2, 51.0, 35.0, 34.1, 33.4, 33.2, 28.5, 28.4

ESI-MS: *m/z*: calculated for C₂₀H₂₈N₁₂O₆ [*M*+Na]+ 555; found 555 (100%), 533 (40%, [*M*+H]+), 433 (25%, [*M*–Boc+H]+).

6.5.3   HCl•H-[(4S)-N$_3$-L-Pro]$_3$-OH 36
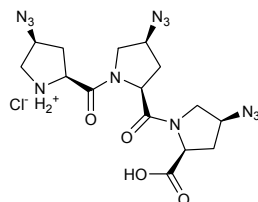
The Boc-protecting group of Boc[Pro-(4S)-N$_3$]$_3$-OH (498 mg, 0.935 mmol) was removed following the general procedure to yield the HCl-salt **36** (438 mg, 0.935 mmol, quant.) as a white solid that was used without further purification.

^{1}H and ^{13}C NMR show multiple sets of peaks due to the s-*trans* and s-*cis* conformers.

^{1}H NMR (500 MHz, CD$_3$OD, 25°C): δ = 4.82-4.58 (m, 3H, Hα), 4.58-4.30 (m, 3H, Hγ), 4.15-3.35 (m, 6H, Hδ), 2.95-1.95 (6H, Hβ);

^{13}C NMR (125 MHz, CDCl$_3$, 25°C): δ = 174.5, 173.7, 172.2, 171.0, 170.8, 168.2, 167.4, 61.0, 60.8, 60.5, 60.3, 60.0, 59.7, 59.5, 59.3, 59.1, 59.0, 58.9, 58.6, 58.5, 53.6, 53.5, 53.3, 52.7, 52.6, 52.3, 51.7, 37.4, 37.1, 36.9, 35.8, 35.6, 35.0, 34.9, 34.3.

ESI-MS: *m/z*: calculated for C$_{15}$H$_{20}$N$_{12}$O$_4$ [*M*+H]+ 433; found 433 (100%).

6.5.4   cyclo[Pro-(4*S*)-N₃]₃ 34
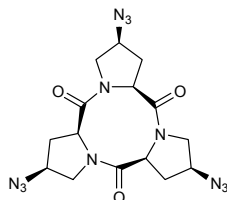
The HCl-salt **36** (438 mg, 0.935 mmol) was dissolved in anhydrous DMF (17 mL) and added within 1 h via syringe pump to a stirred solution of HATU (1.066 g, 2.805 mmol) and Hünig`s base (1.44 mL, 8.428 mmol) in anhydrous DMF (90 mL). The reaction mixture was stirred for an additional hour before removal of all volatiles at reduced pressure. The remaining oil was extracted with CH_2Cl_2 (100 mL) and 2M HCl (50 mL). The aqueous layers were extracted with CH_2Cl_2 (2×50 mL), the organic layers were washed with brine and dried over Na_2SO_4. Filtration and evaporation of the solvent at reduced pressure followed by flash chromatography on silica gel (EtOAc) yielded the cyclotripeptide **34** (284 mg, 0.685 mmol, 73%) as a white solid.

^{1}H NMR (500 MHz, CDCl3, 25°C); δ = 5.07 (dd, *J* = 8.1 Hz, 2.1 Hz, 3H; Hα), 4.52 (dd, *J* = 12.5 Hz, 8.1 Hz, 3H; Hδ), 4.04 (dtd, *J* = 9.9 Hz, 8.1 Hz, 5.3 Hz, 3H; Hγ), 3.14 (dd, *J* = 12.5 Hz, 8.2 Hz, 3H; Hδ), 2.64 (ddd, *J* = 13.9 Hz, 5.2 Hz, 2.1 Hz, 3H; Hβ), 2.54 (ddd, *J* = 13.8 Hz, 10.0 Hz, 8.2 Hz, 3H; Hβ).

^{13}C NMR (125 MHz, CDCl₃, 25°C): δ = 165.9, 56.3, 55.7, 49.3, 34.1.

FT-IR (NaCl, ν/cm-1): 2108, 1646, 1441, 1362, 1263, 1211.

ESI-MS: *m/z*: calculated for $C_{15}H_{18}N_{12}O_3$ [*M*+Na]+ 437; found 437 (100%).

Elemental analysis calculated for $C_{15}H_{18}N_{12}O_3$ (414.16): C 43.48, H 4.38, N 40.56, found: C 43.41, H 4.34, N 40.50.

6.5.5 cyclo[Pro(4*S*)NHAc]₃ 33
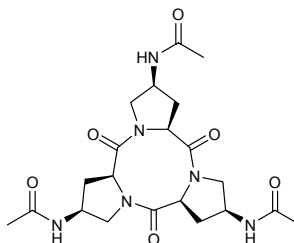
Palladium on carbon (10%, 3 mg) was added to the solution of the triazide **36** (10 mg, 24 µmol) in a 1:2 mixture of THF:MeOH (2 mL). The black suspension was evacuated, flushed with hydrogen and allowed to stir for 2 h at room temperature. After filtration over celite and removal of the solvent at reduced pressure, the residue was dissolved in THF, acetic anhydride (35 µL, 360 µmol) and polyvinylpyridine (10 mg) were added and the reaction mixture was stirred for 1 h. After filtration and removal of all volatiles at reduced pressure the residue was triturated with Et₂O (2×10 mL) to afford the acetylated cyclotriproline **33** (7 mg, 15 µmol, 63%) as a white solid.

^{1}H NMR (500 MHz, CDCl₃, 25°C): δ = 7.67 (d, *J* = 9.5 Hz, 3H; NH), 5.15 (d, *J* = 7.4 Hz, 3H; Hα), 4.93 (dq, *J* = 8.7 Hz, 4.1 Hz, 3H; Hγ), 4.37 (dd, *J* = 13.7 Hz, 8.7 Hz, 3H; Hδ), 3.04 (dd, *J* = 13.7 Hz, 4.1 Hz, 3H; Hδ'), 2.50 (m, 3H; Hβ), 2.18 (d, *J* = 14.0 Hz, 3H; Hβ'), 2.03 (s, 9H; AcC*H*₃).

^{13}C NMR (100.5 MHz, CDCl₃, 25°C): δ = 169.6, 167.1, 57.6, 53.7, 44.5, 36.5, 23.5.

ESI-MS: *m/z*: calculated for C₂₁H₃₀N₆O₆ [*M*+Na]+ 485; found 485 (100%).

6.5.6   cyclo[Pro-(4*R*)-N₃]₃ 40
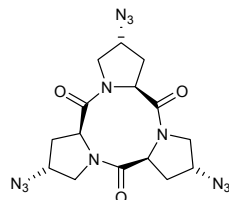
40 was prepared in analogy to **34** and isolated as a white solid in approximately 15% yield.

^{1}H NMR (500 MHz, CDCl$_3$, 25°C): δ = 5.15 (d, *J* = 6.9 Hz, 3H; Hα), 4.86 (qd, *J* = 7.4 Hz, 3.8 Hz, 3H; Hγ′), 3.87 (dd, *J* = 13.2 Hz, 3.8 Hz, 3H; Hδ′), 3.55 (dd, *J* = 13.2 Hz, 7.4 Hz, 3H; Hδ), 2.86 (ddd, *J* = 13.3 Hz, 7.5 Hz, 1.1 Hz, 3H; Hβ′), 2.06 (ddd, *J* = 13.4 Hz, 7.4 Hz, 6.9 Hz, 3H; Hβ).

^{13}C NMR (125 MHz, CDCl$_3$, 25°C): δ = 166.3, 58.7, 56.8, 51.1, 35.0.

FT-IR (KBr): ν = 3345, 2930, 2109, 1653, 1628, 1437, 1356, 1317, 1269.

ESI-MS: *m/z*: calculated for C$_{15}$H$_{18}$N$_{12}$O$_3$ [*M*+Na]+ 437; found 437 (100%).

Elemental analysis calculated for C$_{15}$H$_{18}$N$_{12}$O$_3$ (414.16): C 43.48, H 4.38, N 40.56, found: C 43.47, H 4.26, N 40.44.

6.5.7 cyclo[Pro-(4*R*)-NHAc]₃ 32
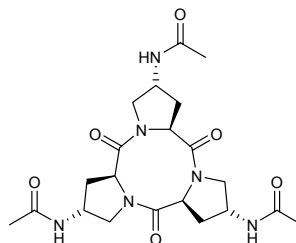
32 was prepared in analogy to **33** and isolated as a white solid in **64%** yield.

^{1}H NMR (400 MHz, CD$_3$OD, 25°C): δ = 5.55 (d, *J* = 7.2 Hz, 3H; Hα), 4.93 (dq, *J* = 5.1 Hz, 8.1 Hz, 3H; Hγ), 3.65 (dd, *J* = 12.9 Hz, 5.1 Hz, 3H; Hδ′), 3.57 (dd, *J* = 12.9 Hz, 8.5 Hz, 3H; Hδ), 2.68 (dd, *J* = 12.9 Hz, 8.1 Hz, 3H; Hβ′), 1.97 (dt, *J* = 12.9 Hz, 7.7 Hz, 3H; Hβ), 1.93 (s, 9H; CH$_3$).

^{13}C NMR (100.5 MHz, CD$_3$OD, 25°C): δ = 171.0, 167.1, 56.2, 50.3, 47.0, 34.6, 20.8.

ESI-MS: *m/z*: calculated for C$_{21}$H$_{30}$N$_6$O$_6$ [*M*+Na]+ 485; found 485 (100%).

6.6 Synthesis of the receptor prototype

6.6.1 Cyclotriproline-Tyr(DR)-Boc 42
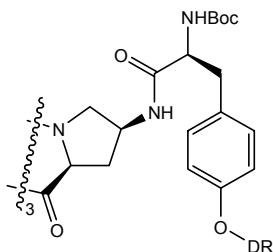
Cyclo[(4S)-N_3-L-Pro]$_3$ **34** (23 mg, 0.056 mmol) was suspended in dry THF (0.5 mL). 1 M trimethylphosphine in THF (0.27 mL, 0.27 mmol) was added and the reaction was stirred at room temperature. After 10 minutes H_2O (0.27 mL) were added. The reaction was stirred for 2 hours, then the solvent was removed and the residual solid was coevaporated with toluene (5×3 mL). The residual, off-white solid was reacted with Boc-Tyr(DR)-OH (146 mg, 0.252 mmol), HATU (128 mg, 0.337 mmol) and Hünig's base (172 μL, 1.0 mmol) in dry DMF (0.5 mL). After 2 hours the reaction mixture was diluted with CH_2Cl_2 (10 mL) and extracted with 1N HCl (5 mL). The aqueous layer was extracted again with CH_2Cl_2 (10 mL). The combined organic layers were dried and the solvent was removed *in vacuo*. The crude product was purified by column chromatography (gradient CH_2Cl_2:MeOH 100:0 to 90:10), and gel filtration (LH20, CH_2Cl_2:MeOH 90:10) yielding cyclotriproline-Tyr(DR)-Boc **42** (68 mg, 0.22 mol, 60%).

^{1}H NMR (500 MHz, CDCl$_3$, 25°C): δ = 8.28 (m, 2H; ar), 8.09 (d, J = 9.3 Hz, 1H; NH), 7.88 (m, 4H; ar), 7.08 (d, J = 8.5 Hz, 2H; ar), 6.78 (m, 4H; ar), 5.21 (d, J = 6.5 Hz, 1H; Pro-Hα), 4.95 (d, J = 7.1 Hz, 1H; NHcarb), 4.81 (m, 1H; Pro-Hγ), 4.31 (m, 2H; Tyr-Hα, Pro-Hδ), 4.12 (t, J = 5.7 Hz, 2H; CH$_2$), 3.57 (q, J = 7.1 Hz, 2H; *CH$_2$*CH$_3$), 3.04 (dd, J = 14.1 Hz, 5.5 Hz, 1H; Tyr-Hβ), 2.91 (m, 2H; Pro-Hδ, Tyr-Hβ), 2.42 (m, 1H; Pro-Hβ), 2.08 (d, J = 13.9 Hz, 1H; Pro-Hβ), 1.37 (s, 9H; ^{t}Bu), 1.25 (t, J = 7.1 Hz, 3H; CH$_2$*CH$_3$*).

^{13}C NMR (125 MHz, CDCl$_3$, 25°C): δ = 170.7, 167.1, 157.4, 156.7, 155.2, 151.2, 147.3, 143.6, 130.4, 129.0, 126.2, 124.6, 122.6, 114.5, 111.4, 79.9, 65.3, 57.5, 55.6, 53.4, 49.8, 46.1, 44.7, 37.5, 36.0, 29.6, 28.3, 12.2.

ESI-MS: *m/z*: calculated for C$_{105}$H$_{123}$N$_{21}$O$_{21}$ [*M*+Na]+ 2037; found 2037 (100%); [1/2*M*+Na]+ 1030, found 1030 (90%).

6.6.2 Cyclotriproline-Tyr(DR)-Asp(^{t}bu)-Fmoc 43
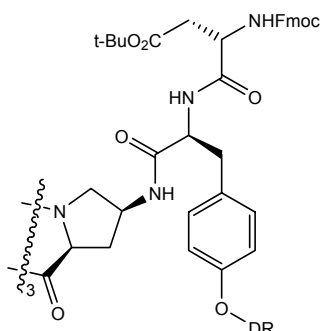
Cyclotriproline-Tyr(DR)-Boc (23 mg, 0.011 mmol) was Boc-deprotected using the general procedure. The hydrochloride salt was reacted with Fmoc-Asp(^{t}bu)-OH (27 mg, 0.066 mmol), EDC (13 mg, 0.069 mmol), and Hünig's base (13 μL, 0.077 mmol) in dry CH_2Cl_2 (0.25 mL). After 1 hour the reaction mixture was diluted with CH_2Cl_2 (5 mL) and extracted with 1N HCl (5 mL). The aqueous layer was extracted again with CH_2Cl_2 (5 mL). The combined organic layers were dried and the solvent was removed *in vacuo*. The crude product was purified by column chromatography (gradient CH_2Cl_2:MeOH 100:0 to 90:10), and gel filtration (LH20, CH_2Cl_2:MeOH 90:10) yielding **43** (29 mg, 0.01 mol, 91%) as pure product.

^{1}H NMR (500 MHz, CDCl$_3$, 25°C): δ = 8.30 (m, 2H; ar), 8.20 (d, *J* = 9 Hz, 1H; NH), 7.88 (m, 2H; ar), 7.83 (m, 2H; ar), 7.74 (m, 2H; ar), 7.57 (m, 2H; ar), 7.38 (m, 2H; ar), 7.29 (m, 2H; ar), 7.05 (m, 2H; ar), 6.88 (d, *J* = 7.7 Hz, 1H; NH), 6.69 (m, 4H; ar), 6.01 (d, *J* = 8.7 Hz, 1H; NH), 5.00 (d, *J* = 7.9 Hz, 1H; Pro-Hα), 4.77 (m, 1H; Pro-Hγ), 4.57 (m, 2H; Asp-Hα, Tyr-Hα), 4.40 (dd, *J* = 10.5 Hz, 6.9 Hz, 1H; *CH$_2$*Fmoc), 4.31 (m, 2H; Pro-Hδ, *CH$_2$*Fmoc), 4.18 (t, *J* = 7.1 Hz, 1H; *CH*Fmoc), 3.93 (m, 2H; *CH$_2$*dye), 3.67 (m, 2H; *CH$_2$*dye), 3.47 (q, *J* = 7.0 Hz, 2H; *CH$_2$*CH$_3$), 3.04 (m, 2H; Asp-Hβ), 2.89 (m, 2H; Pro-Hβ, Tyr-Hβ), 2.65 (m, 1H; Tyr-Hβ), 2.31 (m, 1H; Pro-Hβ), 2.00 (d, *J* = 13.9 Hz, 1H; Pro-Hβ), 1.40 (s, 9H; ^{t}Bu), 1.18 (t, *J* = 7.1 Hz, 3H; CH$_2$*CH$_3$*dye).

^{13}C NMR (125 MHz, CDCl$_3$, 25°C): δ = 171.4, 170.4, 169.6, 166.8, 157.4, 156.7, 156.1, 151.2, 147.3, 143.8, 143.6, 143.5, 141.2, 130.4, 127.8, 127.1, 126.2, 125.2, 125.0, 124.6, 122.6, 120.0, 114.4, 111.3, 81.7, 67.3, 65.1, 57.5, 54.5, 53.6, 51.1, 49.7, 47.0, 46.0, 44.6, 36.7, 36.5, 36.2, 28.0, 12.2.

ESI-MS: *m/z*: calculated for C$_{159}$H$_{168}$N$_{24}$O$_{30}$ [*M*+Na]+ 2915; found 2915 (100%).

6.6.3 Cyclotriproline-Tyr(DR)-Asp(*t*bu)-Asp(*t*bu)-Fmoc 44
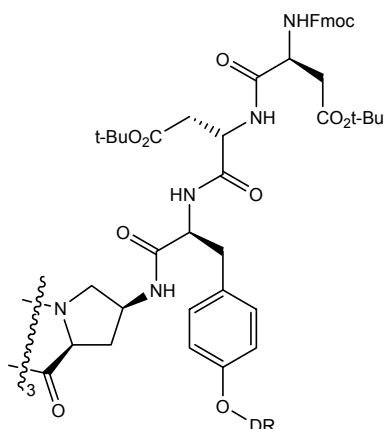
Cyclotriproline-Tyr(DR)-Asp-Fmoc (29 mg, 0.01 mmol) was Fmoc-deprotected following the general procedure. The free amine was reacted with Fmoc-Asp(*t*bu)-OH (25 mg, 0.06 mmol) and EDC (12 mg 0.063 mmol) in dry CH_2Cl_2 (0.25 mL). After 1 hour the reaction mixture was diluted with CH_2Cl_2 (5 mL) and extracted with 1N HCl (5 mL). The aqueous layer was extracted again with CH_2Cl_2 (5 mL). The combined organic layers were dried and the solvent was removed *in vacuo*. The crude product was purified by column chromatography (gradient CH_2Cl_2:MeOH 100:0 to 90:10), and gel filtration (LH20, CH_2Cl_2:MeOH 90:10) yielding **44** (21 mg, 0.061 mol 61%).

^{1}H NMR (500 MHz, CDCl$_3$, 25°C): δ = 8.30 (m, 2H; ar), 8.13 (d, *J* = 9.1 Hz, 1H; NH), 7.87 (m, 4H; ar), 7.74 (m, 2H; ar), 7.55 (m, 2H; ar), 7.38 (m, 2H; ar), 7.28 (m, 2H; ar), 7.18 (d, *J* = 7.7 Hz, 1H; NH), 7.08 (m, 2H; ar), 6.77 (m, 4H; ar), 5.86 (d, *J* = 8.2 Hz, 1H; NH), 4.98 (d, *J* = 7.6 Hz, 1H; Pro-Hα), 4.79 (m, 1H; Tyr-Hα), 4.72 (m, 1H; Pro-Hγ), 4.47 (m, 1H; Asp1-Hα), 4.43-4.28 (m, 4H; Pro-Hδ, Asp2-Hα, *CH$_2$*Fmoc), 4.20 (t, *J* = 7.1 Hz, 1H; *CH*Fmoc), 4.08 (m, 2H; *CH$_2$*dye), 3.76 (m, 2H; *CH$_2$*dye), 3.54 (q, *J* = 6.9 Hz, 2H; *CH$_2$*CH$_3$), 3.14 (dd, *J* = 14.0 Hz, 5.0 Hz, 2H; Asp1-Hβ), 3.00-2.78 (m, 4H; Pro-Hδ, Asp1-Hβ, Asp2-Hβ, Tyr-Hβ), 2.69 (m, 1H; Asp2-Hβ), 2.55 (m, 1H; Tyr-Hβ), 2.30 (m, 1H; Pro-Hβ), 2.01 (d, *J* = 14.0 Hz, 1H; Pro-Hβ), 1.43 (s, 9H; *t*Bu), 1.32 (s, 9H; *t*Bu), 1.22 (t, *J* = 6.9 Hz, 3H; CH$_2$*CH$_3$*dye).

^{13}C NMR (125 MHz, CDCl$_3$, 25°C): δ = 171.3, 171.1, 170.7, 170.3, 170.0, 167.0, 157.4, 156.9, 156.2, 151.4, 147.4, 143.8, 143.7, 141.4, 141.3, 130.4, 129.7, 128.0, 127.3, 127.2, 126.4, 125.2, 124.8, 122.7, 120.2, 114.6, 111.5, 82.2, 81.8, 67.2, 65.3, 57.6, 55.2, 51.8, 49.9, 49.7, 47.1, 46.2, 44.9, 36.3, 36.2, 29.8, 28.2, 28.1, 12.4.

ESI-MS: *m/z*: calculated for C$_{183}$H$_{207}$N$_{27}$O$_{39}$ [*M*+Na]+ 3429; found 3429 (100%).

6.6.4 Cyclotriproline-Tyr(DR)-Asp(^{t}bu)-Asp(^{t}bu)-Ac 45
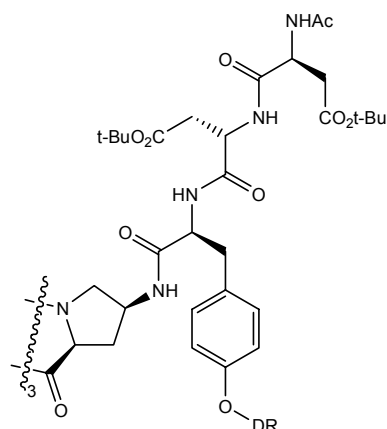
Cyclotriproline-Tyr(DR)-Asp-Fmoc (18 mg, 0.0053 mmol) was Fmoc-deprotected following the general procedure. The free amine was reacted with acetic acid (45 μL, 0.792 mmol), which had been preactivated by mixing with HCTU (393mg, 0.950 mmol) and Hünig's base (0.5 mL, 2.85 mmol) in dry DMF (0.3 mL). After 1 hour, the reaction mixture was diluted with CH_2Cl_2 (5 mL) and extracted with 1N HCl (5 mL). The aqueous layer was extracted again with CH_2Cl_2 (5 mL). The combined organic layers were dried and the solvent was removed *in vacuo*. The crude product was purified by column chromatography (gradient CH_2Cl_2:MeOH 100:0 to 90:10), and gel filtration (LH20, CH_2Cl_2:MeOH 90:10) yielding pure **45** (8 mg, 0.0027 mol, 50%).

^{1}H NMR (500 MHz, CDCl$_3$, 25°C): δ = 8.32 (m, 2H; ar), 8.13 (d, *J* = 9 Hz, 1H; NH), 7.90 (m, 4H; ar),7.43 (d, *J* = 8.3 Hz, 1H; NH), 7.12 (m, 2H; ar), 6.80 (m, 4H; ar), 6.73 (d, *J* = 7.9 Hz, 1H; NH), 5.06 (d, *J* = 7.3 Hz, 1H; Pro-Hα), 4.81-4.68 (m, 2H; Tyr-Hα, Pro-Hγ), 4.60 (m, 1H; Asp1-Hα), 4.42 (m, 1H; Asp2-Hα), 4.33 (dd, *J* = 13.5 Hz, 8.5 Hz, 1H; Pro-Hδ), 4.14 (t, *J* = 5.7 Hz, 2H; *CH$_2$*dye), 3.83 (t, *J* = 5.7 Hz, 2H; *CH$_2$*dye), 3.60 (q, *J* = 7.1 Hz, 2H; *CH$_2$*CH$_3$dye), 3.22 (dd, *J* = 14.2 Hz, 4.6 Hz, 1H; Asp2-Hβ), 2.95 (m, 2H; Asp2-Hβ, Pro-Hδ), 2.73 (m, 3H; Tyr-Hβ, 2xAsp1-Hβ), 2.56 (m, 1H; Tyr-Hβ), 2.39 (m, 1H; Pro-Hβ), 2.04 (d, *J* = 14.0 Hz, 1H; Pro-Hβ), 1.97 (s, 3H; Ac*CH$_3$*), 1.41 (s, 9H; ^{t}Bu), 1.33 (s, 9H; ^{t}Bu), 1.27 (t, *J* = 7.1 Hz, 3H; CH$_2$*CH$_3$*dye).

^{13}C NMR (125 MHz, CDCl$_3$, 25°C): δ = 171.1, 171.0, 170.5, 170.4, 170.3, 170.1, 167.0, 157.2, 156.8, 151.3, 147.3, 143.7, 130.2, 129.9, 126.3, 124.7, 122.6, 114.4, 111.4, 82.0, 81.6, 65.2, 57.5, 55.4, 53.0, 49.9, 49.6, 46.2, 44.9, 36.7, 36.1, 35.8, 29.7, 28.0, 27.9, 23.0, 12.3.

ESI-MS: *m/z*: calculated for $C_{144}H_{183}N_{27}O_{36}$ [*M*+Na]+ 2889; found 2889 (100%).

Cyclotriproline-Tyr(DR)-Asp-Asp-Ac 46
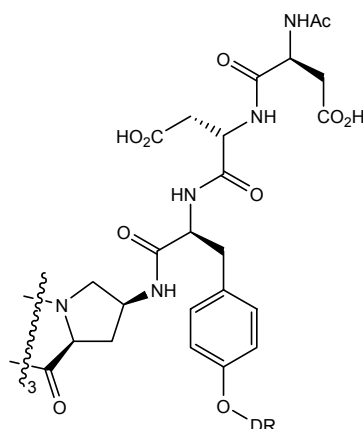
Cyclotriproline-Tyr(DR)-Asp(^{t}bu)-Asp(^{t}bu)-Ac **45** (6 mg, 0.002 mmol) was treated with 50% TFA in CH_2Cl_2 (2 mL) for 30 minutes at room temperature. After removal of all volatiles, the residual oil was triturated with pentanes to yield the deprotected receptor **46** (2.6 mg, 0.001 mmol, 50%).

^{1}H NMR (500 MHz, CDCl$_3$, 25°C): δ = 7.99 (m, 2H; ar), 7.57 (m, 4H; ar), 6.82 (m, 2H; ar),6.52 (m, 4H; ar), 5.08 (d, J = 8.0 Hz, 1H; Pro-Hα), 4.51 (t, J = 6.0 Hz, 1H; Tyr-Hα), 4.31 (m, 1H; Asp1-Hα), 4.25 (m, 1H; Pro-Hδ), 4.10 (dd, J = 8.7 Hz, 5.3 Hz, 1H; Asp2-Hα), 4.00 (dd, J = 13.0 Hz, 8.2 Hz, 1H; Pro-Hδ), 3.84 (t, J = 5.4 Hz, 2H; *CH$_2$*dye), 3.53 (t, J = 5.4 Hz, 2H; *CH$_2$*dye), 3.30 (q, J = 7.1 Hz, 1H; *CH$_2$*CH$_3$dye), 2.83 (dd, J = 14.0 Hz, 5.8 Hz, 1H; Asp2-Hβ; Pro-Hδ), 2.67 (m, 1H; Asp2-Hβ), 2.59 (dd, J = 13.4 Hz, 4.4 Hz, 1H; Pro-Hδ), 2.50 (m, 2H; Tyr-Hβ, Asp1-Hβ), 2.39 (m, 2H; Tyr-Hβ, Asp1-Hβ), 2.11 (m, 1H; Pro-Hβ), 1.78 (d, J = 13.4 Hz, 1H; Pro-Hβ), 1.62 (s, 3H; Ac*CH$_3$*), 0.56 (t, J = 7.1 Hz, 3H; CH$_2$*CH$_3$*dye).

^{13}C NMR (125 MHz, CDCl$_3$, 25°C): δ = 173.6, 172.6, 172.0, 171.6, 168.7, 158.1, 157.3, 152.3, 147.8, 144.1, 130.8, 130.1, 127.0, 125.2, 123.0, 115.0, 112.2, 66.1, 57.8, 56.3, 50.5, 50.4, 40.5, 49.3, 49.2, 49.0, 48.8, 48.7, 48.5, 36.2, 35.9, 35.5, 30.1, 22.6, 12.5.

ESI-MS: *m/z*: calculated for $C_{120}H_{135}N_{27}O_{36}$ [*M*-3H]- 824; found 824 (100%).

7 References and Appendices

7.1 References

1. D. H. Williams, *Nat. Prod. Rep.* **1996**, *13*, 469-477.

2. M. Schäfer, T. R. Schneider, G. M. Sheldrick, *Structure*, **1996**, *4*, 1509-1515.

3. J. Liu, K. J. Volk, M. S. Lee, M. Pucci, S. Handwerger, *Anal. chem.* **1994**, *66*, 2412-2416.

4. For a review see: R. W. Hoffmann, *Angew. Chem. Int. Ed.* **2000**, *39*, 2054-2070.

5. a) W. C. Still, P. Hauck, D. Kempf, *Tetrahedron Lett.* **1987**, *28*, 2817-2820; b) P. K. Somers, T. J. Wandless, S. L. Schreiber, *J. Am. Chem. Soc.* **1991**, *113*, 8045-8056.

6. D. A. Evans, R. P. Polniaszek, K. M. DeVries, D. E. Guinn, D. J. Mathre, *J. Am. Chem. Soc.* **1991**, *113*, 7613-7630.

7. a) U. Gräfe, W. Schade, M. Roth, L. Radics, M. Incze, K. Ujszaszy, *J. Antibiot.* **1984**, *37*, 836-846; b) L. Radics, *J. Chem. Soc. Chem. Commun.* **1984**, 599-601.

8. H. A. Brooks, D. Gardner, J. P. Pyser, T. J. King, *J. Antibiot.* **1984**, *37*, 1501-1504.

9. R.W. Hoffmann, *Angew. Chem.* **1992**, *104*, 1147-1157; *Angew. Chem. Int. Ed. Engl.* **1992**, *31*, 1124-1134.

10. a) W. Adam, T. Wirth, *Acc. Chem. Res.* **1999**, *32*, 703-710; b) B. Giese, W. Damm, R. Batra, *Chemtracts: Organic Chemistry*, **1994**, *7*, 355-370; c) R.W. Hoffmann, *Chem. Rev.* **1989**, *89*, 1841-1860; d) S. Hanessian, V. Mascitti, S. Giroux, *Proc. Nat. Am. Sci.* **2004**, *101*, 11996-12001; e) U. Schopfer, M. Stahl, T. Brandl, R. W. Hoffmann, *Angew. Chem.* **1997**, *109*, 1805-1807; *Angew. Chem. Int. Ed. Engl.* **1997**, *36*, 1745-1747.

11. a) S. Tang, W.C. Still, *Tetrahedron Lett.* **1993**, *34*, 6701-6704; b) S.S. Yoon, T. M. Georgiadis, W.C. Still, *Tetrahedron Lett.* **1993**, *34*, 6697-6700; c) G. Li, W.C. Still, *J. Am. Chem. Soc.* **1993**, *115*, 3804-3805; d) G. Li, W.C. Still, *Tetrahedron Lett.* **1993**, *34*, 919-922; e) G. Li, W.C. Still, *Bioorg. Med. Chem. Lett.* **1992**, *2*, 731-734; f) X. Wang, S. D. Erickson, T. Iimori, W.C. Still, *J. Am. Chem. Soc.* **1992**, *114*, 4128-4137; g) S. D.. Erickson, W.C. Still, *Tetrahedron Lett.* **1990**, *31*, 4253-4256; h) T. Iimori, S. D.. Erickson, A. L. Rheingold, W.C. Still, *Tetrahedron Lett.* **1989**, *30*, 6947-6950.

12. G. Quinkert, E. Egert, C. Griesinger, *Aspekte der Organischen Chemie : Struktur*, Verl. Helvetica Chemica Acta, Basel, **1995**.

13. E.S. Eberhardt, N. Panasik, R. T. Raines, *J. Am. Chem. Soc.* **1996**, *118*, 12261-12266.

14. a) D. E. Stewart, A Sarkar,. J. E. Wampler, *J. Mol. Biol.* **1990**, *214*, 253-260. (b) M. S. Weiss, A. Jabs, R. Hilgenfeld, *Nat. Struct. Biol.* **1998**, *5*, 676.

15. C. Nathaniel, L. A. Wallace, J. Burke, H. W. Dir, *Biochem. J.* **2003**, *372*, 241–246.

16. T. C. Evans Jr., G. L. Nelsestuen, *Biochemistry* **1996,** *35,* 8210-8215.

17. K. Lang, F. X. Schmid, G. Fischer, *Nature* **1987**, *329*, 268-270.

18. For an overview of the biochemistry of PPIases see: A. Galat, S. M. Metcalfe, *Proc. Biophys. molec. Biol.* **1995**, *63*, 67-118.

19. A. B. Mauger, *J. Nat. Prod.* **1996**, *59,* 1205-1211.

20. E. Fischer, *Ber. Dtsch. Chem. Ges.* **1902**, *35*, 2660-2665.

21. M. R. Stetten, *J. Biol. Chem.* **1949**, *181*, 31-37.

22. F. Irreverre, K. Morita, A. V. Robertson, B. Witkop, *J. Am. Chem. Soc.* **1963**, *85*, 2824-2831.

23. M.-T. Weiss, M. Weninger, J. Hausler, G. Lubec, *Padiatrie Padagogie* **1988**, *23,* 9-14.

24. G. Lancini, F. Parenti, *Antibiotics – An Integrated View*, Springer-Verlag, New York, **1982**.

25. H. Brockmann, G. Pampus, J. H. Manegold, *Chem. Ber.* **1959**, *92,* 1294- 1302.

26. H. Brockmann, J. H. Manegold, *Z. Physiol. Chem.* **1965**, *343*, 86-100.

27. H. Brockmann, E. A. Stähler, *Tetrahedron Lett.* **1973**, 2567-2570.

28. E. Katz, K. T. Mason, A. B. Mauger, *Biochem. Biophys. Res. Commun.* **1975**, *63*, 502-508.

29. A. B. Mauger, O. A. Stuart, E. Katz, K. T. Mason, *J. Org. Chem.* **1977**, *42*, 1000-1005.

30. E. Katz, K. T. Mason, A. B. Mauger, *Biochem. Biophys. Res. Commun.* **1973**, *52,* 819-826.

31. S. Nakamura, T. Chikaike, H. Yonehara, H. Umezawa, *Chem. Pharm. Bull.* **1965**, *13*, 599-602.

32. G. W. Engstrom, J. V. DeLance, J. L. Richard, A. L. Baetz, *J. Agric. Food Chem.* **1975**, *23,* 244-253.

33. J. P. Springer, R. J. Cole, J. W. Dorner, R. H. Cox, J. L. Richard, C. L. Barnes, D. van der Helm, *J. Am. Chem. Soc.* **1984**, *106,* 2388-2392.

34. L. Fowden, A. Smith, D. S. Millington, R. C. Sheppard, *Phytochemistry* **1969**, *8*, 437-443.

35. S. Murakami, T. Takemoto, Z. Shimizu, K. Daigo, *Jpn. J. Pharm. Chem*. **1953**, *25*, 571-574.

36. J. V. Nadler, *Life Sci.* **1979**, *24*, 289-300.

37. G. A. R. Johnston, D. R. Curtis, J. Davies, R. M. McCulloch, *Nature (London)* **1974**, *248*, 804-805.

38. J. T. Coyle, R. Schwarcz, *Nature (London)* **1976**, *263*, 244-246.

39. V. W. Magaard, R. M. Sanchez, J. W. Bean, M. L. Moore, *Tetrahedron Lett.* **1993**, *34*, 381-384.

40. Bonnett, R.; Clark, V. M.; Giddey, A.; Todd, S. A. *J. Chem. Soc.* **1959**, 2087-2093.

41. S. S. A. An, C. C. Lester, J.-L. Peng, Y.-J. Li, D. M. Rothwarf, E. Welker, T. W. Thannhauser, L. S. Zhang, J. P. Tam, H. A. Scheraga, *J. Am. Chem. Soc.* **1999,** *121,* 11558-11566.

42. a) T. Haack, M. Mutter, *Tetrahedron Lett.* **1992**, *33*, 1589-1592; (b) T. Wöhr, M. Mutter, *Tetrahedron Lett.* **1995**, *36*, 3847-3848; (c) M. Mutter, A. Nefzi, T. Sato, X. Sun, F. Wahl, T. Wöhr, *Peptide Res.* **1995**, *8*, 145-153.

43. T. Wöhr, F. Wahl, A. Nefzi, B. Rohwedder, T. Sato, X. Sun, M. Mutter, *J. Am. Chem. Soc.* **1996,** *118,* 9218-9227.

44. M. Keller, C. Sager, P. Dumy, M. Schutkowski, G. S. Fischer, M. Mutter, *J. Am. Chem. Soc.* **1998,** *120,* 2714-2720.

45. J. A. Hodges, R. T. Raines, *J. Am. Chem. Soc.* **2003**, *125*, 9262-9263.

46. a) E. S. Eberhardt, N. Panasik, R. T. Raines, *J. Am. Chem. Soc.* **1996,** *118,* 12261-12266. b) S. K. Holmgren, K. M. Taylor, L. E. Bretscher, R. T. Raines *Nature* **1998**, *392*, 666-667.

47. M. L. DeRider, S. J. Wilkens, M. J. Waddell, L. E. Bretscher, F. Weinhold, R. T. Raines, J. L. Markley, *J. Am. Chem. Soc* **2002**, *124*, 2497-2505.

48. M. C. Conza, M. Nold, P. Krattiger, H. Wennemers, unpublished results.

49. Matthias Nold, Ph.D. Thesis.

50. H. Wennemers, M. Conza, M. Nold, P. Krattiger, *Chem. Eur. J.* **2001**, *7*, 3342-3347.

51. H. Wennemers, M. C. Nold, M. M. Conza, K. J. Kulicke, M. Neuburger, *Chem. Eur. J.* **2003**, *9*, 442-448.

52. D. F. DeTar, N. P. Luthra, *J. Am. Chem. Soc* **1977**, *99*, 1232-1244.

53. M. Karplus, *J. Phys. Chem.,* **1959**, *30*, 11-15.

54. G.C.K. Roberts, *NMR of Macromolecules – A Practical Approach*, Oxford University Press, p. 362.

55. C.M. Derber, D.A. Torchia, E.R. Blout, *J. Am. Chem. Soc.*, **1971**, *93*, 4893-4897.

56. S. Wolfe, *Acc. Chem. Res.* **1972**, *5*, 102-111.

57. (a) H. B. Bürgi, J. D. Dunitz, E. Shefter, *J. Am. Chem. Soc.* **1973**, *95*, 5065-5067; (b) H. B. Bürgi, J. D. Dunitz, J. M. Lehn, G. Wipff, *Tetrahedron* **1974**, *30*, 1563-1572; (c) H. B. Bürgi, J. M. Lehn, G. Wipff, *J. Am. Chem. Soc.* **1974**, *96*, 1965-1966; (d) H. B. Bürgi, J. D. Dunitz, E. Shefter, *Acta Crystallogr. Sect. B* **1974**, *30*, 1517-1527.

58. L.E. Bretscher, C.L. Jenkins, K.M. Taylor, M.L. DeRider, R.T. Raines, J. *Am. Chem. Soc.* **2001**, *123*, 77-778.

59. J. A. Hodges, R.T. Raines, *J. Am. Chem. Soc.* **2003**, *125*, 9262-9263.

60. The higher mesomeric stabilization of the amide versus the ester is a well-established fact; it is also used to explain the lower reactivity of amides in nucleophilic substitution reactions. See: R. Brückner, *Reactionsmechanismen: Organische Reaktionen, Stereochemie, moderne Synthesemethoden*, Spectrum, Akad. Verlag, **1996**, p. 205.

61. Collaboration with Dipl. Chem. Sabine Schweizer and Prof. Dr. Christian Ochsenfeld at the Univeristy of Tübingen, Germany.

62. Spartan'02 Wavefunction, Inc., Irvine, CA.

63. J. Kong, C. A. White, A. I. Krylov, C. D. Sherrill, R. D. Adamson, T. R. Furlani, M. S. Lee, A. M. Lee, S. R. Gwaltney, T. R. Adams, H. Daschel, W. Zhang, P. P. Korambath, C. Ochsenfeld, A. T. B. Gilbert, G. S. Keziora , D. R. Maurice, N. Nair, Y. Shao, N. A. Besley, P. E. Maslen, J. P. Dombroski, J. Baker, E. F. C. Byrd, T. v. Voorhis, M. Oumi, S. Hirata, C.-P. Hsu, N. Ishikawa, J. Florian, A. Warshel, B. G. Johnson, P. M. W. Gill, M. Head-Gordon, J. A. Pople, *J. Computational Chem.,* **2000***, 21,* 1532.

64. R. Ahlrichs, M. Bär, M. Häser, H. Horn, C. Kölmel, *Chem. Phys. Lett.*, **1989**, *162*, 165.

65. a) L. Radom, W. A. Lathan, W. J. Hehre, J. A. Pople, *J. Am. Chem. Soc.* **1973**, *95*, 693-698; b) T. K. Brunck, F. Weinhold, *J. Am. Chem. Soc.* **1979**, *101*, 1700-1709; c) P. R. Rablen, R. W. Hoffmann, D. A. Hrovat, W. T. Borden, *J. Chem. Soc., Perkin Trans. 2*: **1999**, *8*, 1719-1726; d) K. B. Wiberg, M. A. Murcko, K. E. Laidig, P. J. MacDougall, *J. Phys. Chem.* **1990**, *94*, 6956-6959; e) K. B. Wiberg, *Acc. Chem. Res.* **1996**, *29*, 229-234; f) C. Trindle, P. Crum, K. Douglass, *J. Phys. Chem. A* **2003**, *107*, 6236-6242; g) V. G. S. Box, L. L. Box, *J. Mol. Struct.* **2003**, *649*, 117-132; h) K.-H. Chen, G. A. Walker, N. L. Allinger, *THEOCHEM* **1999**, *490,* 87-107; i) O. Engkvist, G. Karlstroem, P.-O. Widmark, *Chem. Phys. Lett.* **1997**, *265,* 19-23; j) S. Papasavva, K. H. Illinger, J. E. Kenny, *J. Phys. Chem.* **1996**, *100*, 10100-10110; k) J. M. Martell, R. J. Boyd, Z. Shi, *J. Phys. Chem.* **1993**, *97*, 7208-7215; l) I. A. Topol, S. K. Burt, *Chem. Phys. Lett.* **1993**, *204,* 611-616; m) D. A. Dixon, N. Matsuzawa, S. C. Walker, *J. Phys. Chem.* **1992**, *96,* 10740-10746; n) D. A. Dixon, B. E. Smart, *J. Phys. Chem.* **1988**, *92*, 2729-2733; m) K. B. Wiberg, M. A. Murcko, *J. Phys. Chem.* **1987**, *91*, 3616-3620; o) T. Miyajima, Y. Kurita, T. Hirano, *J. Phys. Chem.* **1987**, *91*, 3954-3959; p) G. F. Smits, M. C. Krol, P. N. Van Kampen, Cs. Altona, *THEOCHEM* **1986**, *32*, 247-253; q) L. Radom, J. Baker, P. M. W. Gill, R. H. Nobes, N. V. Riggs, *J. Mol. Struct.* **1985**, *126*, 271-290.

66. a) J. R. Durig, J. Liu, T. S. Little, V. F. Kalasinsky, *J. Phys. Chem.* **1992**, *96*, 8224-8233; b) N. C. Craig, A. Chen, K. H. Suh, S. Klee, G. C. Mellau, B. P. Winnewisser, M. Winnewisser, *J. Phys. Chem. A* **1997**, *101*, 9302-9308; c) L. Fernholt, K. Kveseth, *Acta Chem. Scand., A: Phys. Inorg. Chem.* **1980**, *A34*, 163-170; d) H. Takeo, C. Matsumura, Y. Morino, *J. Chem. Phys.* **1986**, *84*, 4205-4210.

67. D. O'Hagan, C. Bilton, J. A. K. Howard, L. Knight and D. J. Tozer, *J. Chem. Soc.*, *Perkin Trans. 2* **2000**, 605–607.

68. C. Perrin, T. Dwyer, *Chem. Rev.* **1990**, *90*, 935-967.

69. M. Conza, H. Wennemers, *J. Org. Chem.* **2002**, *67*, 2696-2698.

70. P. Krattiger, H. Wennemers, *Synlett* **2005**, 4, 706-708.

71. F. Mohamadi, N. G. J. Richards, W. C. Guida, R. Liskamp, M. Lipton, C. Caufield, G. Chang, T. Hendrickson, W. C. Still, *J. Comput. Chem.* **1990**, *11*, 440-467.

72. Calculations were performed by Dipl. Chem. Stanislav Ivan of the group of Prof. Dr. Bernd Giese, University of Basel.

73. W. L. Jorgensen, D. S. Maxwell, J. Tirado-Rives, *J. Am. Chem. Soc.* **1996**, *118*, 11225 -11236.

74. D. Qiu, P.S. Shenkin, F.P. Hollinger, W. C. Still, *J. Phys. Chem. A* **1997**, *101*, 3005-3014.

75. M. Rothe, K.-D. Steffen, I. Rothe, *Angew. Chem.* **1965**, *77*, 347-348.

76. M. H. J. Ohlmeyer, R. N. Swanson, L. W. Dillard, J. C. Reader, G. Asouline, R. Kobayashi, M. Wigler, W. C. Still, *Proc. Natl. Acad. Sci. USA* **1993**, *90,* 10922.

77. H. P. Nestler, P. A. Bartlet, W. C. Still, *J. Org. Chem.* **1994**, *59*, 4723.

78. A. Furka, F. Sebestyén, M. Asgedom, G. Dibo, *Int. J. Pept. Protein Res.* **1991**, *37*, 487.

79. K. S. Lam, S. E. Salmon, E. M. Hersh, V. J. Hruby, W. M. Kazmierski, R. J. Knapp, *Nature* **1991**, *354*, 82.

80. M. Nold, H. Wennemers, *Chem. Commun.* **2004**, *16,* 1800-1801.

81. This assumption is supported by studies of diketopiperazine-based receptors with acid-rich side-chains, which bound similar peptides as receptor **46**. In ITC measurements with Ac-Arg-Ser-Arg-NH-propyl and Ac-Arg-Arg-Ser-NH-propyl, sequences also found in the combinatorial screening, lower binding affinities were found. PhD thesis, Philipp Krattiger.

82. The titrations were analyzed using a least squares curve-fitting procedure (Origin$^{®}$ implemented with the calorimetric setup provided by Microcal).

83. J. Jeener, B.H. Meier, P. Bachmann, R.R. Ernst, *J. Chem. Phys.* **1979**, *71*,4546-4553.

84. R. Wagner, S. Berger, *J. Magn. Reson.* **1996**, *123 A*, 119-121.

7.2   Appendix A: List of Sequences found in the combinatorial screenings

Sequences found in on-bead combinatorials screenings:

0,01M NaHCO3 pH 8,5

Position

3.	2.	1.
D-Ala	D-Arg	D-Arg
D-Ala	D-Arg	L-Arg
D-Ala	L-Arg	L-Pro
D-Arg	D-Arg	D-Arg
D-Arg	D-Arg	D-Lys
D-Arg	D-Arg	D-Phe
D-Arg	D-Arg	D-Val
D-Arg	D-Pro	D-Arg
D-Arg	D-Thr	D-Arg
D-Arg	Gly	D-Arg
D-Arg	Gly (?)	L-Arg
D-Arg	L-Arg	D-Val
D-Arg	L-Asn	D-Arg
D-Arg	L-Glu	L-Arg
D-Arg	L-His	D-Arg
D-Asn	D-Arg	D-Arg
D-Asn	D-Arg	L-Arg
D-Asn	L-Arg	L-Arg
D-Lys	L-Arg	L-Ser/L-Lys
D-Pro	D-Arg	L-Pro
D-Thr	D-Arg	L-Arg
D-Thr	L-Arg	L-Arg
L-Arg	D-Arg	?
L-Arg	D-Arg	D-Arg
L-Arg	D-Arg	D-Arg
L-Arg	D-Arg	D-Arg
L-Arg	D-Arg	D-Thr
L-Arg	D-Asn	D-Arg
L-Arg	D-Asn	L-Arg
L-Arg	D-Gln	L-Arg
L-Arg	D-Ser	D-Arg
L-Arg	D-Ser	D-Arg
L-Arg	D-Ser	D-Arg
L-Arg	D-Thr	L-Arg
L-Arg	D-Thr (?)	D-Arg
L-Arg	Gly	D-Arg
L-Arg	L-Arg	L-Arg
L-Gln	D-Arg	L-Arg
L-Gln	L-Arg	L-Pro
L-His	D-Arg	D-Arg
L-His	L-Arg	D-Arg

L-Pro	L-Arg	D-Arg
L-Val	L-Arg	D-Arg

0,01M NaOH pH 12.0
Position

3.	2.	1.
D-Arg	?	?
D-Arg	D-Arg	D-Thr
D-Arg	D-Arg	D-Val
D-Arg	D-Arg	L-Ala
D-Arg	D-Arg	L-Thr
D-Arg	D-Arg	L-Val
D-Arg	D-Arg	D-Phe
D-Arg	Gly	D-Arg
D-Arg	L-Arg	L-Phe
D-Arg	L-Arg	L-Phe
D-Arg	L-Glu	D-Arg
D-Arg	L-Ser	L-Arg
D-Lys	L-Arg	L-Pro(?)
D-Pro	D-Arg	D-Arg
D-Thr	L-Arg	L-Arg
D-Val	L-Arg	L-Arg
L-Ala	D-Arg	L-Arg
L-Arg	D-Arg	D-Leu
L-Arg	D-Arg	D-Ser
L-Arg	D-Arg	D-Thr
L-Arg	D-Arg	D-Val
L-Arg	D-Arg	L-Thr
L-Arg	D-Arg(?)	L-Ala(?)
L-Arg	D-Ser	L-Arg
L-Arg	L-Ala	D-Arg(?)
L-Arg	L-Arg	D-Arg
L-Arg	L-Arg	D-Val
L-Arg	L-Arg	D-Val
L-Arg	L-Arg	L-Ala
L-Arg	L-Ser	D-Ser(?)
L-Arg	L-Ser	L-Arg(?)
L-Arg (?)	D-Ser	L-Arg(?)
L-Leu	L-Arg	L-Arg
L-Thr	L-Arg	D-Arg

7.3 Appendix B: Crystallographic data

Table 1: Crystal data for **15**

formula	$C_8H_{12}N_4O_3$
formula weight	212.21
Z, calculated density	4, 1.392 Mg m^{-3}
F(000)	448
description and size of crystal: colorless plate,	$0.10 \cdot 0.22 \cdot 0.23$ mm^3
absorption coefficient	0.109 mm^{-1}
min/max transmission	0.98 / 0.99
temperature	173K
radiation(wavelength)	Mo K_α ($\lambda = 0.71073$ Å)
Crystal system, space group	monoclinic, P 1 2$_1$ 1
a	9.2443(2) Å
b	12.7360(2) Å
c	9.4877(2) Å
α	90°
β	115.0156(8)°
γ	90°
V	1012.25(4) Å^3
min/max Θ	2.369° / 27.870°
number of collected reflections	7874
number of independent refections	2524 (merging r = 0.077)
number of observed reflections	2226 (I>0.50σ(I))
number of refined parameters	271
r	0.0390
Rw	0.0495
goodness of fit	0.9367

Bond distances		Å
C1	C2	1.541(3)
C1	C7	1.515(3)
C1	N1	1.460(3)
C1	H11	0.984
C2	C3	1.527(3)
C2	H21	0.986
C2	H22	0.985
C3	C4	1.521(3)
C3	N2	1.495(3)
C3	H31	0.995
C4	N1	1.471(3)
C4	H42	0.992
C4	H41	1.023
C5	C6	1.498(3)
C5	N1	1.349(3)
C5	O1	1.235(3)
C6	H61	1.020
C6	H63	0.985
C6	H64	0.978
C7	O2	1.330(3)
C7	O3	1.204(3)
C8	O2	1.447(3)
C8	H81	0.995
C8	H82	0.990
C8	H83	0.989
C9	C10	1.540(3)
C9	C15	1.522(3)
C9	N5	1.457(3)
C9	H91	0.980
C10	C11	1.527(3)
C10	H101	0.971
C10	H102	0.987
C11	C12	1.524(4)
C11	N6	1.485(3)
C11	H111	0.990
C12	N5	1.458(3)
C12	H121	0.992
C12	H122	0.962
C13	C14	1.504(3)
C13	N5	1.350(3)
C13	O4	1.229(3)
C14	H141	0.990
C14	H142	0.996
C14	H143	0.972
C15	O5	1.198(3)
C15	O6	1.329(3)
C16	O6	1.446(3)
C16	H161	1.000
C16	H162	1.000
C16	H163	1.000

N2	N3	1.226(3)
N3	N4	1.133(3)
N6	N7	1.223(3)
N7	N8	1.127(3)

Bond angles			Deg
C2	C1	C7	110.52(18)
C2	C1	N1	103.09(16)
C7	C1	N1	110.72(18)
C2	C1	H11	111.864
C7	C1	H11	108.237
N1	C1	H11	112.383
C1	C2	C3	104.55(18)
C1	C2	H21	108.752
C3	C2	H21	109.838
C1	C2	H22	110.284
C3	C2	H22	115.580
H21	C2	H22	107.675
C2	C3	C4	103.4(2)
C2	C3	N2	113.9(2)
C4	C3	N2	106.16(19)
C2	C3	H31	112.796
C4	C3	H31	111.378
N2	C3	H31	108.893
C3	C4	N1	102.62(19)
C3	C4	H42	110.883
N1	C4	H42	109.975
C3	C4	H41	110.575
N1	C4	H41	110.564
H42	C4	H41	111.860
C6	C5	N1	117.04(19)
C6	C5	O1	122.7(2)
N1	C5	O1	120.3(2)
C5	C6	H61	114.639
C5	C6	H63	107.135
H61	C6	H63	108.710
C5	C6	H64	110.704
H61	C6	H64	109.025
H63	C6	H64	106.265
C1	C7	O2	111.08(18)
C1	C7	O3	124.5(2)
O2	C7	O3	124.3(2)
O2	C8	H81	115.739
O2	C8	H82	111.988
H81	C8	H82	102.563
O2	C8	H83	116.392
H81	C8	H83	104.276
H82	C8	H83	104.349
C10	C9	C15	111.59(19)
C10	C9	N5	102.86(17)
C15	C9	N5	112.33(17)
C10	C9	H91	108.961

C15	C9	H91	110.259
N5	C9	H91	110.600
C9	C10	C11	103.18(17)
C9	C10	H101	110.494
C11	C10	H101	111.221
C9	C10	H102	109.786
C11	C10	H102	112.520
H101	C10	H102	109.495
C10	C11	C12	103.98(18)
C10	C11	N6	110.60(19)
C12	C11	N6	110.0(2)
C10	C11	H111	110.471
C12	C11	H111	109.718
N6	C11	H111	111.774
C11	C12	N5	104.69(18)
C11	C12	H121	110.612
N5	C12	H121	109.686
C11	C12	H122	113.210
N5	C12	H122	109.947
H121	C12	H122	108.627
C14	C13	N5	117.3(2)
C14	C13	O4	122.0(2)
N5	C13	O4	120.7(2)
C13	C14	H141	111.735
C13	C14	H142	109.221
H141	C14	H142	106.937
C13	C14	H143	108.710
H141	C14	H143	110.339
H142	C14	H143	109.876
C9	C15	O5	125.5(2)
C9	C15	O6	109.73(18)
O5	C15	O6	124.8(2)
O6	C16	H161	109.501
O6	C16	H162	109.485
H161	C16	H162	109.476
O6	C16	H163	109.413
H161	C16	H163	109.476
H162	C16	H163	109.476
C4	N1	C1	113.12(18)
C4	N1	C5	127.15(19)
C1	N1	C5	119.71(17)
C3	N2	N3	115.3(2)
N2	N3	N4	173.5(3)
C12	N5	C9	112.36(18)
C12	N5	C13	120.0(2)
C9	N5	C13	127.50(18)
C11	N6	N7	115.5(2)
N6	N7	N8	172.3(3)
C8	O2	C7	116.02(18)
C16	O6	C15	116.79(18)

Table 2: Crystal data for **34**

formula	$C_{15}H_{18}N_{12}O_3$
formula weight	414.39
Z, calculated density	4, 1.453 Mg · m^{-3}
F(000)	864.300
description and size of crystal	colorless plate , 0.10 0.22 0.50 mm^3
absorption coefficient	0.109 mm^{-1}
min/max transmission	0.98 / 0.99
temperature	293K
radiation(wavelength)	Mo K_α (λ = 0.71073 Å)
Crystal system, space group	orthorhombic , P 2_1 2_1 2_1
a	10.842(1) Å
b	11.840(5) Å
c	14.757(7) Å
α	90°
β	90°
γ	90°
V	1894.3 Å^3
min/max Θ	4.13° / 27.57°
number of collected reflections	13264
number of independent refections	4271 (merging r = 0.12)
number of observed reflections	2914 (>2.00σ(I))
number of refined parameters	272
r	0.0449
rW	0.0480
goodness of fit	1.0616

Bond distances		Å
O1	C1	1.222(3)
O2	C6	1.213(3)
O3	C11	1.217(3)
N1	C1	1.342(3)
N1	C2	1.463(3)
N1	C5	1.470(3)
N2	C6	1.345(3)
N2	C7	1.463(3)
N2	C10	1.465(3)
N3	C11	1.332(3)
N3	C12	1.456(3)
N3	C15	1.472(3)
N4	N5	1.202(4)
N4	C3	1.483(4)
N5	N6	1.128(4)
N7	N8	1.212(4)
N7	C8	1.466(4)
N8	N9	1.132(4)
N10	N11	1.231(4)
N10	C13	1.468(3)
N11	N12	1.123(4)
C1	C15	1.535(3)
C2	C3	1.519(5)
C2	H21	1.000
C2	H22	1.000
C3	C4	1.514(5)
C3	H31	1.000
C4	C5	1.533(3)
C4	H41	1.000
C4	H42	1.000
C5	C6	1.532(3)
C5	H51	1.000
C7	C8	1.512(4)
C7	H71	1.000
C7	H72	1.000
C8	C9	1.542(4)
C8	H81	1.000
C9	C10	1.522(3)
C9	H91	1.000
C9	H92	1.000
C10	C11	1.527(3)
C10	H101	1.000
C12	C13	1.514(3)
C12	H121	1.000
C12	H122	1.000
C13	C14	1.532(4)
C13	H131	1.000
C14	C15	1.532(3)
C14	H141	1.000
C14	H142	1.000
C15	H151	1.000

Bond Angles			Deg
C1	N1	C2	121.4(2)
C1	N1	C5	127.6(2)
C2	N1	C5	108.0(2)
C6	N2	C7	122.0(2)
C6	N2	C10	127.68(19)
C7	N2	C10	110.03(18)
C11	N3	C12	122.87(18)
C11	N3	C15	128.14(18)
C12	N3	C15	108.67(16)
N5	N4	C3	115.2(3)
N4	N5	N6	173.0(4)
N8	N7	C8	116.1(2)
N7	N8	N9	173.9(3)
N11	N10	C13	116.0(2)
N10	N11	N12	172.2(3)
O1	C1	N1	121.9(2)
O1	C1	C15	120.0(2)
N1	C1	C15	117.9(2)
N1	C2	C3	100.9(2)
N1	C2	H21	111.58(15)
C3	C2	H21	111.57(15)
N1	C2	H22	111.58(13)
C3	C2	H22	111.59(16)
H21	C2	H22	109.467
N4	C3	C2	113.1(3)
N4	C3	C4	109.1(3)
C2	C3	C4	104.5(2)
N4	C3	H31	105.76(18)
C2	C3	H31	110.29(15)
C4	C3	H31	114.31(18)
C3	C4	C5	105.6(2)
C3	C4	H41	110.44(15)
C5	C4	H41	110.44(15)
C3	C4	H42	110.44(18)
C5	C4	H42	110.43(16)
H41	C4	H42	109.467
N1	C5	C4	104.1(2)
N1	C5	C6	109.66(19)
C4	C5	C6	110.8(2)
N1	C5	H51	113.25(12)
C4	C5	H51	112.19(16)
C6	C5	H51	106.88(12)
O2	C6	N2	121.2(2)
O2	C6	C5	121.5(2)
N2	C6	C5	117.36(19)
N2	C7	C8	103.9(2)
N2	C7	H71	110.83(14)
C8	C7	H71	110.82(15)
N2	C7	H72	110.85(13)
C8	C7	H72	110.87(14)

H71	C7	H72	109.467
N7	C8	C7	108.5(2)
N7	C8	C9	113.3(2)
C7	C8	C9	106.19(18)
N7	C8	H81	106.55(13)
C7	C8	H81	113.60(15)
C9	C8	H81	108.84(13)
C8	C9	C10	106.59(19)
C8	C9	H91	110.18(14)
C10	C9	H91	110.18(13)
C8	C9	H92	110.20(13)
C10	C9	H92	110.18(13)
H91	C9	H92	109.467
N2	C10	C9	103.39(18)
N2	C10	C11	108.11(17)
C9	C10	C11	111.87(18)
N2	C10	H101	115.03(12)
C9	C10	H101	111.46(13)
C11	C10	H101	107.02(11)
O3	C11	N3	121.3(2)
O3	C11	C10	119.7(2)
N3	C11	C10	118.95(18)
N3	C12	C13	102.53(19)
N3	C12	H121	111.16(11)
C13	C12	H121	111.16(13)
N3	C12	H122	111.20(11)
C13	C12	H122	111.19(13)
H121	C12	H122	109.467
N10	C13	C12	114.0(2)
N10	C13	C14	115.7(2)
C12	C13	C14	105.71(18)
N10	C13	H131	100.44(14)
C12	C13	H131	111.46(13)
C14	C13	H131	109.60(13)
C13	C14	C15	106.2(2)
C13	C14	H141	110.28(14)
C15	C14	H141	110.28(13)
C13	C14	H142	110.27(13)
C15	C14	H142	110.27(14)
H141	C14	H142	109.467
N3	C15	C1	107.72(18)
N3	C15	C14	102.85(18)
C1	C15	C14	111.74(19)
N3	C15	H151	115.54(11)
C1	C15	H151	107.21(14)
C14	C15	H151	111.77(15)

8   Curriculum Vitae

Louis-Sebastian Sonntag

Date of Birth: 9th of August 1976
Place of Birth: Frankfurt (Main), Germany

Academic record:

Since July 2005	Post-doctoral research in the group of Prof. David A. Evans, Harvard University, Cambridge, U.S.A.
April 2001-May 2005	PhD studies in the group of Prof. Helma Wennemers, University of Basel, Switzerland
Febuary 2000	Graduation as "Diplom-Chemiker"
July 2000-February 2001	Diploma work in the group of Prof. Christian Griesinger, University of Frankfurt, Germany
June 2000	Final exams (Hauptexamen)
April 1998	Mid-study exams (Vordiplom)
April 1996	Enrollment at the Johann-Wolfgang Goethe University in Frankfurt (Main), Germany
July 1995	Graduation from Schutz American School, in Alexandria, Egypt

Publications and poster presentations:

L.-S. Sonntag, S. Schweizer, C. Ochsenfeld, H. Wennemers, "The Azide Gauche Effect and its Influence on the Conformation of 4-Azidoproline", *in preparation*.

L.-S. Sonntag, S. Ivan, M. Langer, M. Conza, H. Wennemers, „Functionalised Cyclotriproline – A Bowl-shaped Tripodal Scaffold", *Synlett* **2004**, *7*, 1270-1272.

L.-S. Sonntag, M. Conza, M. Langer, H. Wennemers, „From Diketopiperazines to Cyclotriprolines: Development of a Novel Class of Three-Armed Receptors", American Chemical Society, National Meeting, Boston, M.A., August 2002.

L.-S. Sonntag, M. Conza, M. Langer, H. Wennemers, „From Diketopiperazines to Cyclotriprolines: Development of a Novel Class of Three-Armed Receptors", 6th German Peptide Symposium, Berlin, 23.-26.3.2003.

The following Professors contributed to my education:

B. Brutschy, E. Constable, E. Egert, J. Engels, H. Fasold, B. Giese, M. Göbel, C. Griesinger, S. Hashmi, K. Hensen, B. Ludwig, A. Pfaltz, T. Priesner, G. Quinkert, D. Rehm, F. Schüth, U. Séquin, M. Wagner, H. Wennemers, W. Woggon.